Development of a micro burner for the experimental determination of the net calorific value at constant pressure of pulverised coal

AJ Storm

Orcid.org 0000-0003-3281-7800

Thesis accepted in fulfilment of the requirements for the degree *Doctor of Philosophy in Mechanical Engineering* at the North-West University

Promoter:	Prof J Markgraaff
Co-promoter:	Prof CP Storm

Graduation:	May 2020
Student number:	20968892

DECLARATION

I, André Johan Storm, hereby declare that this is my own work and that no plagiarism was committed.

A.J. Storm

25 November 2019

Date

SUMMARY

Coal combustion remains the major resource of power generation internationally. Coal consists of different substances, which influence its quality and properties. One such property is the calorific value (CV), which specifies the amount of energy per mass contained in a substance after it is released in the form of heat after complete combustion.

There are basically two types of CV, the gross calorific value at constant volume (GCVv), and the net calorific value at constant pressure (NCVp). These values differ owing to the different processes that are followed to determine the CV. When considering the method of determining the overall efficiency of a power station, the CV of coal is the greatest contributor to inaccuracy; therefore, it is very important to determine the correct CV of coal.

The Bomb calorimeter is the norm used to determine the CV on power stations in South Africa. The Bomb calorimeter utilises a direct method to determine the GCVv. However, the GCVv does not represent an accurate CV on a power station. The constant volume process followed by the Bomb calorimeter enables it to recover latent heat formed during the combustion process. This latent heat is, however, not recovered in the constant pressure process by a burner on a power station. Therefore, the NCVp is a more representative CV, since it utilises the same process as on a power station.

The only method currently used to determine the NCVp of a solid fuel such as coal is from derived calculations. Different methods exist to determine the NCVp by derived calculations; however, no international standard is available for these derived calculations and these calculations differ to some degree. This is still a theoretical approach that does not include losses. The development of a direct method was thus required to determine the NCVp of one type of coal as a proof of concept.

The literature survey indicated that the NCVp coal analyser must be based on the principle of a flow calorimeter that is used to determine the NCVp of gaseous fuels on a mass-energy balance. To develop this device, it was necessary to design a burner and combustion chamber, as well as to select and size associated auxiliaries. The burner was designed by using cold flow computational fluid dynamics (CFD) modelling in conjunction with burner and combustion principles to attain a self-sustained coal flame on a laboratory-sized scale.

The device was then commissioned by assembling the different components and by doing preliminary tests, such as liquid petroleum gas (LPG) combustion, pulverised coal settling flow and calibration. The calibration test showed that the NCVp coal analyser's result differed by 1.4% from the known NCVp of LPG. After the commissioning of the device had been completed, one type of coal was tested to attain a self-sustaining flame, and to determine the NCVp.

The test was deemed successful, since a self-sustaining flame was indeed achieved, and the NCVp of the tested coal was determined. The burner achieved 99.78% combustion efficiency based on unburnt carbon content in ash. The profile of the self-sustaining flame correlated well with the cold flow CFD streamlines used to design the burner. The NCVp of the tested coal determined by the NCVp coal analyser differed to some extent from that of the different calculated NCVp of different methods. However, since the calibration showed difference of a mere 1.4% of LPG, the NCVp of the tested coal is considered acceptable.

KEYWORDS

Aerodynamic flame profile
Burner
Coal
Combustion
Computational Fluid Dynamics
Heat rate
Net calorific value at constant pressure
Pulverised coal

DEDICATION

This thesis is dedicated to my loving wife Jana, my father Chris and my mother Annamie, who supported me throughout the completion of my study.

_____

ACKNOWLEDGEMENTS

Herewith I would like to thank the following persons and parties for the aid given with this project:

- Prof. Johan Markgraaff: *Supervisor*
- Prof. C. P. Storm: *Co-supervisor*
- Mr Sarel Naude, Mr Willem van Tonder and Mr Bethuel Diobe: *Mechanical Engineering laboratory*
- Prof. Fika van Rensburg and Prof. Lucas Venter*: Project funding*
- Mr Bartlo van der Merwe and André Fourie of the Mechanical Workshop: *Manufacturing*
- Prof. C. G. Du Toit and Mrs. Francina Jacobs: *Financial support*
- Mr Thys Taljaard and the staff of the Instrument Makers Workshop at NWU: *Manufacturing*
- Rickus Senekal, Easy Way Gadgets: *Manufacturing*
- Dr C. van Alphen, Chief Advisor – Fuel, Plant Performance & Optimisation, Research, Testing & Development, Eskom: *Project funding and support*
- Mr Bonny Nyangwa, Pilot Scale Test Burner, Rosherville, Testing & Development, Eskom
- Mrs Barbara Bradley: Proofreading: *Project funding and support*

TABLE OF CONTENTS

LIST OF TABLES

LIST OF FIGURES

NOMENCLATURE

A	Ash
A: F	Air-to-fuel ratio
AD	Air dried
AR	As received
C	Carbon
C_3H_8	Propane
CA	Core air
Cd Factor	Coefficient of discharge
CFD	Computational Fluid Dynamics
C_{FIXED}	Fixed carbon
Cl	Chloride
F	Fluoride
CO	Carbon monoxide
CO_2	Carbon dioxide
cp	Specific heat capacity at constant pressure
C_{TOTAL}	Total Carbon
CV	Calorific value
DB	Dry basis
DNS	Direct Numerical Simulation
DPM	Discrete Phase Method
DTF	Drop tube furnace
GCVv	Gross Calorific value at constant volume
H_2	Hydrogen
H_2O	Water/moisture
LES	Large Eddy Simulation
LPG	Liquid Petroleum Gas
$M_{ATMOSPHERIC\ AIR,\ ACTUAL}$	Mass atmospheric air, actual

$M_{DRY\ AIR\ ACTUAL}$	Mass dry air actual
Mi	Inherent moisture
Ms	Surface moisture
Mt	Total moisture
$M_{WATER\ VAPOUR\ ACTUAL}$	Mass water vapour actual
N_2	Nitrogen
N_20	Nitrous Oxide
NCVp	Net calorific value at constant pressure
NOx	Nitrogen oxides
O_2	Oxygen
OH	Hydroxide
PA	Primary air
PC	Pulverised coal
PID	Proportional Integral Derivative
R	Ideal gas constant
RANS	Reynold averaged Navier-Stokes
RSM	Reynolds Stress Model
RT&D	Research, Testing & Development
S	Sulphur
SA	Secondary air
SO_2	Sulphur dioxide
SS	Stainless steel
STP	Standard temperature and pressure
TA	Tertiary air
UBC	Unburnt carbon
USO	Electric units sent out
VM	Volatile matter
VSD	Variable Speed Drive

LIST OF SYMBOLS

$\dot{m}$	mass flow	[kg/s]
$\dot{Q}$	heat rate	[kW]
cp	specific heat capacity at constant pressure	[kJ/kg-K]
$\eta_{overall}$	overall plant efficiency	[-]
C	velocity	[m/s]
Cd	coefficient of discharge	[-]
k	thermal conductivity coefficient	[W/m-K]
P	pressure	[kPa]
T	temperature	[^{o}C]/[K]
ε	emissivity	[-]
ρ	density	[kg/m^{3}]
σ	Stefan Boltzmann constant	[-]
D	diameter	[m]
t	thickness	[mm]
L	length	[m]

1 INTRODUCTION

1.1 BACKGROUND

Coal remains the leading source of energy for electricity generation across the world, serving as primary energy source for about 40% of the world's electricity generation. Especially in South Africa, more than 85% of electricity is generated using coal since it is comparatively cheap and is available in great quantity. It is therefore important to conduct further coal research since coal is projected to be the main source of supply for electricity generation for the next three decades (World Energy Council, 2016).

As stated by Falcon (2013), coal is mainly composed of substances such as fixed carbon (C), volatile matter (VM), moisture and minerals which affect the properties and quality of coal. The quality and properties of coal need to be understood since these affect combustibility and heat release and, therefore determine the application of coal in industry (Wang *et. al*, 2011).

Although the origin and mineralogical composition of coal determine the characteristics in its application as primary energy source, the properties influencing combustion are of concern regarding the coal as an already unchangeable substance. According to Kitto and Stultz (2005), one of the most important properties of coal is the calorific value (CV). The CV specifies the amount of energy per mass contained in a substance after it has been released in the form of heat after complete combustion.

CV is also the most frequently used classification criterion to relate similarities of nearly limitless types of coal (Smoot & Pratt, 1979). Consequently, coal can be categorised into peat, lignite, sub-bituminous, bituminous and anthracite. Peat is the first product produced during the formation of coal. It has a very high moisture content of 70% and has the lowest CV of approximately 6.9 MJ/kg. Lignite is coal that is geologically young and has a CV of up to 19 MJ/kg. It consists of 30% moisture and needs to be dried in order to combust, but has a high VM content which promotes ignition. Lignite and peat have a brown appearance, since they both have a relatively low fixed C content. Sub-bituminous coal contains a relatively high amount of VM and fixed C, with a moisture content of 15 – 30% and a CV of 19 – 26 MJ/kg. The coal mostly used for power generation is bituminous coal. Bituminous coal has a high fixed C content of up to 86%, lower moisture and VM content than sub-bituminous coal and has a CV of 24 – 32 MJ/kg. Because of the relatively high VM content and fixed C, sub-bituminous and bituminous coal ignite easily. The highest rank of coal is anthracite, with a CV of up to 34 MJ/kg. It consists of 86-98% fixed C which is the highest amount of any coal, but also has the lowest amount of moisture and VM. Because of the low VM, it is a slow-burning fuel and is difficult to ignite. Sub- bituminous, bituminous and anthracite coal appear black because of the high fixed C content (Kitto & Stultz, 2005).

Even though coal is ranked by means of CV, within an equivalent rank, different coals with similar CV may differ regarding varying quantities of constituents. These differences in coal types make it difficult to create exact models for coal combustion. According to Wróblewska *et al*. (1977), a specific aerodynamic flow field exists for a specific coal to obtain optimum combustion.

According to Storm (1998), the overall efficiency of a power station is calculated by using the electric units sent out (USO), divided by the mass flow of coal and the CV of coal. The instrumentation used to measure the USO and mass flow of coal is adequately accurate, however, the greatest contributor to inaccuracy in respect of this equation is the CV. Regarding the procurement of coal, it should be borne in mind that the payment is for mass, although, the commodity bought is actually energy. It is therefore very important to have a representative CV to calculate a power station's efficiency accurately.

The method used at power stations and mines to determine the CV of coal is the experimental method of a Bomb calorimeter. According to Basu (2013), the Bomb calorimeter consists of the Bomb, which is a constant volume, high quality pressurised oxygen (O_2), closed environment as well as a water bath surrounding the Bomb. A certain amount of fuel is ignited inside the Bomb by the spark of an electrically

infused wire, to promote complete combustion of the fuel. Thereafter, the energy is measured by means of the water bath when the water temperature has stabilised.

During the combustion process of a hydro -carbon fuel, moisture forms by the reaction of hydrogen (H_2) and O_2; however, some fuels like coal also contain a certain amount of moisture. The moisture absorbs some of the heat released by the combustion process in order to vaporise. If the vapour is allowed to condense in a constant volume, latent energy is released to form a liquid. If the latent heat is included in the measurement of heat released by combustion, the gross calorific value at constant volume (GCVv) is obtained (Rajoo, 2010). Thus, since the Bomb calorimeter method is a constant volume process, the vapour can condensate to release latent heat and it measures the GCVv (Kitto & Stultz, 2005).

However, according to Storm (1998), the Bomb calorimeter poses a problem for the CV determination of coal when comparing it to the actual combustion process on a power station. On a power station, combustion takes place by using a burner, which is a constant pressure device. The latent heat is not recovered inside the furnace during this process since the vapour condensates in the atmosphere. This is due to the flue gas still being at a sufficiently high temperature while exiting the furnace. As stated by Obert (1973), if combustion takes place in a constant pressure environment and the vapour is not allowed to condensate and to release its latent heat in the measuring method, the heat measured does not include the latent heat of moisture and the net calorific value at constant pressure (NCVp) is obtained. It is therefore necessary to determine the NCVp for coal on a power station.

Another method used to determine the CV at power stations is the well-known Dulong method. Lowry (1945) reports that the Dulong method is an empirical calculation that utilises a weighted average by using the CVs of combustible elements contained in the fuel. The combustible elements contained in coal are mostly C, H_2 and sulphur (S). Although the Dulong method can be used to calculate the GCVv, it can only be regarded as a theoretical approach since it does not account for losses, and the values obtained are usually higher than those obtained from the Bomb.

Currently, the only method available to determine the NCVp for coal is by calculation, as reported by Kitto and Stultz (2005). Depending on the referenced GCVv from either the Bomb or the Dulong method, the NCVp is determined by subtracting the calculated latent heat from the GCVv. Calculated values of South African coal used on power stations suggest that the difference of GCVv between the Dulong and Bomb amounts to 8%, where the Dulong value is always the greater of the two. The GCVv and its derived NCVp show a difference of 5% for South African coal. However, the difference between GCVv and calculated NCVp can be up to 25% in countries such as India, which commonly utilises lignite and peat coal that consists of more volatiles and moisture compared to sub-bituminous and bituminous coal (Priyadarshi, 2012).

Even though Kitto and Stultz (2005) suggest that the difference between NCVp and GCVv is insignificant, the difference becomes very significant when considering the method of determining the efficiency of a power station. According to Langenhoven (2019), power utilities such as Eskom consume an amount of 120 million tons of coal annually. Implementing the 5% difference between the calculated NCVp and the Bomb GCVv, implies that the deficit in coal planned or budgeted for, amounts to 6 million tons per annum. Conversely, the above-mentioned difference between the GCVv and NCVp with coal mass flow kept constant, results in an overall efficiency difference of 1.75%. This can imply a significant misjudgement of a plant's performance.

As stated by Kitto and Stultz (2005), a direct method to determine the CV of coal is most appropriate. Furthermore, no international standards exist to verify the calculation of NCVp from the directly determined GCVv. It can be argued that if the calculated GCVv from the Dulong method differs by 8% from the direct method by the Bomb, the calculated NCVp from the Bomb can also differ from the true NCVp even though the Bomb is partially an actual process. This highlights the importance of the NCVp for coal being determined by means of a direct method.

Although the actual combustion process in a power station encompasses all the conditions to determine the NCVp of coal, practical problems exist to perform this on a routine basis. One unit on a power station normally contains 24 – 36 burners. These burners are usually 50 – 80 MW each in capacity, and can be relatively expensive. During combustion on a power station there are a large number of unaccounted losses and unknowns. To remove the problem of unaccounted losses, a single burner needs to be isolated. However, to isolate such a burner is nearly impossible owing to daily energy demand.

Single isolated and smaller scale test burners must be considered for low-cost NCVp routine testing and to reduce losses. The only small scale test burner available in South Africa is the 1MW Pilot scale test burner at Eskom Research, Testing and Development (RT&D) at Rosherville, Gauteng. However, in order to do NCVp testing, this test facility needs to be retrofitted to measure NCVp. Making these required additions to the existing test burner will also be costly and therefore alternative options should be investigated. Moreover, the pilot scale test burner needs to procure a minimum of 3 tons of coal per test involving three days of testing.

1.2 PROBLEM STATEMENT

There is a need to determine the actual CV of coal that represents the combustion process more accurately on a power station at relatively low cost.

- For the sake of convenience, the only device currently enabling the direct determination of CV for coal on utilities, is the Bomb calorimeter. However, it unfortunately provides the GCVv which is not representative of the process in an actual burner.
- The deriving of the required NCVp of coal, has inconsistent variances between the different methods, i.e. by means of pure calculation with the Dulong method or derived from the direct Bomb calorimeter value with the British Standard calculation.
- No international standard exists for the verification of the calculated NCVp of coal.
- Currently, no device exists for the direct determination of NCVp of coal.

1.3 AIM

- To review and investigate different methods of CV determination for different fuels.
- Thereafter, a method should be derived to more specifically determine the NCVp for coal directly.
- Since the CV of any fuel is related to its specific combustion parameters, these should be investigated and determined for a range of coal qualities as solid fuel.
- To develop a device that will serve as an experimental model that can comply with these requirements and findings for the direct determination of NCVp for coal.

1.4 OBJECTIVES

- As for gaseous fuels, it has been decided that the NCVp analyser for coal should also be a type of flow calorimeter.
- The flow calorimeter to be developed for the determination of the NCVp of coal, needs to be based on a similar principle to that of a mass-energy balance as used for gas.
- To achieve this, the primary components that need to be developed, are a burner and a combustion chamber.
- The burner and combustion chamber should achieve a combustion efficiency that is as high as possible.
- Auxiliaries in support of the functionality for this flow calorimeter needs to be selected and sized.
- The operation and characteristics of this NCVp analyser for coal, should be similar to that of a full-scale burner used on large boilers.
- The main goal to achieve, is to produce such a device, but a laboratory size, scaled-down version at relatively low cost.

1.5 SCOPE AND LIMITS

- Although the device should be designed to be adjustable to accommodate a range of coal qualities, only one type of coal will be tested to demonstrate proof of concept.
- Only cold flow computational fluid dynamics (CFD) modelling will be used as a process-designing tool.
- Intensive CFD combustion modelling will not be part of this study.
- The intention of this study is not to indulge in an intensive CFD study: the endeavour is rather to produce a physical, functional product.

1.6 RESEARCH METHODOLOGY

The research methodology will entail the following:

- Literature survey;
- Concept design;
- Detail design;
    - Thermal sizing of NCVp analyser for coal regarding the envelope of coal qualities to be accommodated;
    - Burner design utilising cold flow CFD analysis as process-designing tool;
    - Combustion chamber design;
    - Material selection for the design;
- Auxiliaries selection and sizing;
- Manufacturing of designed components;
- Assembly of device;
- Commissioning, calibration and testing;
- Determination of the NCVp of coal;
- Analysis of results;
- Conclusion and recommendations.

1.7 POSSIBLE CONTRIBUTIONS

This research can provide much insight and understanding of the usage of coal in industry. If the NCVp can be directly determined, the following can be established on power stations globally:

- the overall efficiency;
- mass flow of coal required for steam generation;
- Boiler sizing and design

1.8 THESIS STRUCTURE

This thesis consists of the following seven chapters, augmented by references, bibliography and appendices, as documented below:

CHAPTER 1: Introduction

CHAPTER 2: Literature review and existing technology

CHAPTER 3: Concept design for the net calorific value at constant pressure analyser of coal

CHAPTER 4: Detail design

CHAPTER 5: Commissioning and testing

CHAPTER 6: Calculations and interpretations of results

CHAPTER 7: Conclusion and recommendations

REFERENCES

BIBLIOGRAPHY

APPENDICES

2 LITERATURE REVIEW AND EXISTING TECHNOLOGY

The concepts at stake in this study were identified and arranged in a logical order:

- Coal quality and characteristics, methods for determining the CV of coal;
- Fundamental combustion and burner principles;
- Combustion and burner principles of coal;
- Methods for determining the CV of coal
- Computational combustion modelling;
- Conclusions and design considerations resulting from literature review.

2.1 COAL QUALITY AND CHARACTERISTICS

Coal is essentially burnable rock which is derived from the compaction of different plant material. Coal is composed of fixed carbon, volatile matter, ash (minerals) and moisture (Falcon, 2013). These constituents are used to categorise coal by its rank, where fixed carbon and volatile matter are the most important (Kitto & Stultz, 2005).

Falcon (2013) suggests that the constituents of coal are analysed and quantified by a proximate analysis to determine the rank of coal. A proximate analysis procedure is determined by using different thermal amounts of heat to determine the amount of moisture, VM, fixed C and ash for a specific coal sample.

According to Rajoo (2010), coal can also be viewed as comprising different chemical elements. These elements can be identified and the amounts (in terms of weight) of the elements can be quantified by means of a chemical analysis called an ultimate or elemental analysis.

Another property in terms of coal quality is the heating value or CV, which is measured in MJ/kg. The CV of coal or any substance specifies the amount of combustion energy that exists in that substance. There are two processes of determining CV, the GCVv process and the NCVp process (Kitto & Stultz, 2005). Obert (1973) states that the difference between the two methods is that the GCVv includes the latent heat of water vapour and the NCVp does not. During the combustion process, moisture is a product that is formed by the reaction of H_2 and O_2, which are constituents of coal. Coal also consists of moisture that resides in the crystal structure of coal. The moisture absorbs some heat of combustion and forms a vapour. With a constant volume process, the vapour is allowed to condensate and the latent heat is recovered. During a constant pressure process, the latent heat is not recovered, since it condensates in the atmosphere and not in the measuring device.

2.2 FUNDAMENTAL COMBUSTION AND BURNER PRINCIPLES

Since combustion is the basis of determining the CV of coal, basic combustion principles need to be investigated.

2.2.1 COMBUSTION FUNDAMENTALS

According to El-Mahallaway and Habik (2002), combustion is a fast chemical exothermic reaction between an oxidiser and fuel which generates heat and is able to propagate through an appropriate medium. The heat that is generated by the chemical reaction emits light of a certain colour that is also

known as a flame. The colour of the flame depends on the type of material that's combusted and the temperature. The flame is the hottest part of the heat released. Heat released from a combustion process can be controlled by using a burner that controls the mixing of an oxidiser and fuel (Worgas, 2011).

El-Mahallaway and Habik (2002) also stated the following:

- A flame can only be present where the burner presents a mixture of fuel and air in stoichiometric conditions. Basically, two types of flames exist, namely premixed and diffusion flames. Premixed flames exist where the oxidant and fuel are mixed before they enter the flame area. A premixed flame can only exist if a composition limit of air and fuel for combustion exists. A diffusion flame is established when the mixing of oxidant and fuel takes place after the two streams exit the burner tubes. These two types of flames also differ physically. The premixed flame has a defined burning velocity and adiabatic flame temperature, whereas the diffusion flame does not possess such properties.
- It is safer and provides more stability for flames when a diffusion flame is used, splitting the combustion air in separate streams for coaxial jets such as a primary and secondary air stream.
- When considering a diffusion flame that is situated on the border of atmospheric air and fuel, the flue gas formed is transported in two directions, to the incoming air and fuel, and away from the flame. The products moving toward the reactants must heat and diffuse these in order to mix and react.

Two different types of diffusion flames can form namely, laminar and turbulent flames. To explain the two different types, consider Figure 2.1:

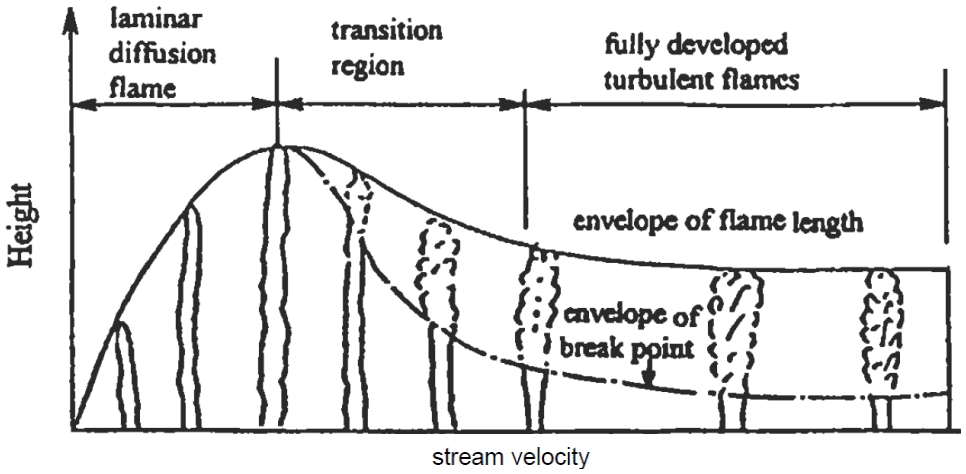

FIGURE 2.1: REPRESENTATION OF THE TRANSITIONING FROM A LAMINAR TO A TURBULENT FLAME (MODIFIED FROM EL-MAHALLAWAY & HABIK, 2002)

- If a flame is situated vertically in surrounding air, and the fuel is supplied by a tube, the flame length will increase as the velocity of the fuel increases. Continuing to increase the velocity of fuel, will keep increasing the flame length until it reaches a maximum. However, before the maximum length is reached, the flame starts to flicker, at which point it enters the transition zone. This is the separation of laminar to transition type diffusion flames. When the flow is increased further, the flickering propagates downwards until it stops a few diameters from the nozzle, where a small length is free of fluctuations. At this stage the flame length is independent of the flow rate or velocity of the fuel and switches over from transition to a turbulent diffusion flame. With a further increase in the velocity and flow rate the flame's breakpoint will maintain a certain distance from the nozzle rim and the flame length will show little change with the increase in turbulence and mixing rate until blow-off.

- Laminar diffusion flames have to mix by molecular diffusion, whereas turbulent diffusion flames accelerate the molecular diffusion process by a coarse mixture of a large-scale transport process rate. Therefore, a turbulent flame may be taken as an array of laminar flamelets. It is desirable to have as much turbulence as possible for enhanced mixing of fuel and air as well as transport.
- Turbulence can increase with air or fuel velocity increase, however, when turbulence is so severe it can strain the flame so that the chemical reaction rate is slower than the mixing rate, which can cause quenching of the flame before blow-off occurs.

2.2.2 FLAME STABILISATION

For continuous ignition and propagation of a flame, the broad consensus is that a chain reaction needs to be created. Chain reactions consist of chain carriers which are usually free radicals. A rise in temperature provides adequate chain carriers to the unburned fuel at the start of the chemical reaction process. Heat loss and chain carrier loss are lower when the flame is further from the burner, which creates higher burning velocity since the flow velocity is lower. At a certain point the flow velocity and the burning velocity are equal, which indicates equilibrium (El-Mahallaway & Habik, 2002)

As adapted from El-Mahallaway and Habik (2002), if the flow velocity is smaller than the burning velocity, flash-back (when the flame propagates into the burner) occurs. Increasing the flow velocity moves the equilibrium point downstream from the burner rim. When the equilibrium point is increasingly moved downstream, the burnable gas mixture is increasingly diluted by inter-diffusion with the atmosphere or flue gas, which in turn causes a decrease in the burning velocity. Thus, an optimum equilibrium position exists where the dilution of combustible gas is balanced by an increase in burning velocity. When the flow velocity exceeds the burning velocity, the flame is balanced by the boundary layer gradient, which consists of lower velocity streamlines than the burning velocity. This explains why combustion can be sustained even if the mean velocity exiting the burner mouth is higher than the burning velocity. If the boundary velocity gradient is so high that the combustion wave is driven beyond this position, the flow velocity exceeds the burning velocity in every streamline and then blow-off occurs.

To avoid blow-off in high-velocity burners, the flame needs to be stabilised owing to the high velocity streams that can be higher than the laminar flame velocity. In such burners the flame stabiliser plays the most important role. Air-to-fuel ratio, distribution of average velocity, distribution of burning velocity and swirl intensity are all parameters that play a role in flame stability and are thus important for burner design (El-Mahallaway & Habik, 2002).

According to Lieuwen (2014), one of the ways to stabilise the flame is using a recirculation zone, which transfers mass and energy from burned gases to unburned gases. This way the recirculated flue gas acts as if using a pilot flame that can work as a constant ignition source. The other reason a recirculation zone is good for stabilisation is that within a recirculation zone, two stagnation points exists, which will allow the flow velocity to be slower than the burning velocity. This is illustrated in Figure 2.2:

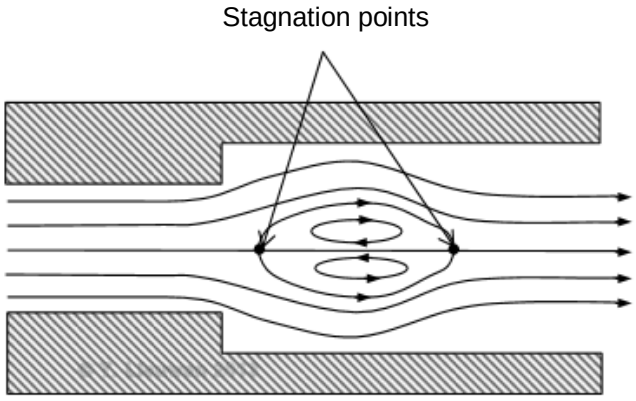

FIGURE 2.2: STAGNATION POINTS FORMED BY A RECIRCULATION ZONE (MODIFIED FROM LIEUWEN, 2014)

Flame stabilisation by non-streamlined or bluff bodies:

According to El-Mahallaway and Habik (2002), a bluff body is used in industrial multi-concentric diffusion burners to create turbulence, increase mixing, improve flame stability and control a flame more easily. The bluff body is non-streamlined, which creates low static pressure downstream of the flow (the wake) when a medium flows over it. The fluid then flows from a high-pressure region to the low pressure in the wake in an opposite direction as opposed to the incoming direction, to create the recirculating zone. The recirculating flow is determined by the geometry of the bluff body. The wake of the bluff body creates a low-velocity area that allows the flame to stabilise because the velocity at which the flame propagates and the flow velocity are in equilibrium. This is illustrated in Figure 2.3:

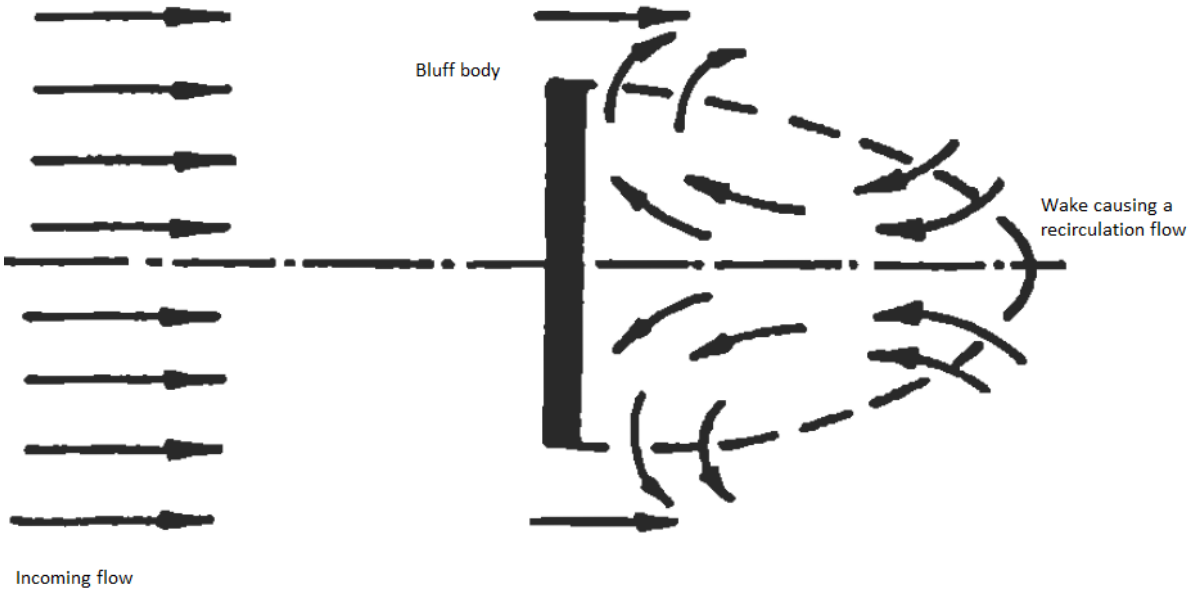

FIGURE 2.3: REPRESENTATION OF THE RECIRCULATION ZONE FORMED IN THE WAKE OF A BLUFF BODY (MODIFIED FROM EL-MAHALLAWAY & HABIK, 2002)

El-Mahallaway and Habik (2002) illustrate the effects of a bluff body on a burner, as shown in Figure 2.4. The burner consists of two concentric tubes, a fuel tube and a combustion air tube. When fuel enters the combustion zone at low velocity (top drawing in Figure 2.4), the recirculating flue gas formed by the previous combustion products, behind the bluff body, entrains the fuel and is transported radially outward to mix with combustion air. The flue gas being transported in a reversed direction acts as a pilot flame for constant ignition. This creates an intense flame with rapid mixing. As the fuel velocity is increased, it starts to penetrate the recirculation zone, but only partially, as it is entrained by the combustion air. When the fuel velocity is increased further (bottom drawing in Figure 2.4), it is able to penetrate the recirculation zone entirely, leaving a small annular region of reverse flow between the fuel and air. Some of the fuel is entrained in the reversed flow together with some hot combustion gases to create the primary combustion zone which is anchored to the burner mouth and stabilises the flame. The rest of the fuel cannot ignite because of low O_2 content and is only pre-heated at this stage. It then burns downstream in the secondary combustion zone where it mixes with the rest of the air and produces a long diffusion flame with a neck-like shape.

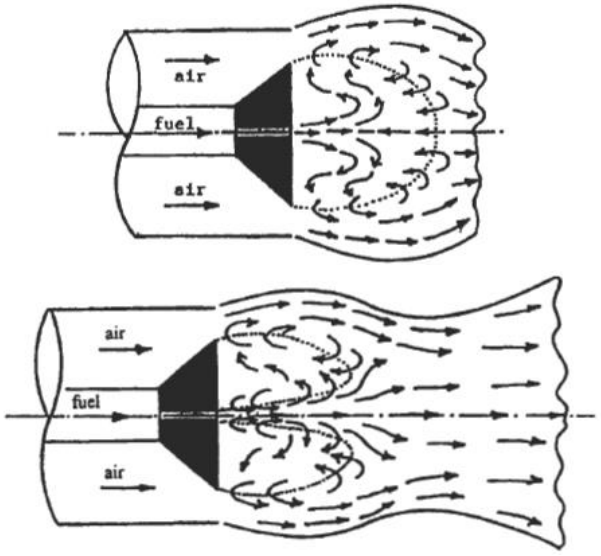

FIGURE 2.4: INFLUENCE OF A BLUFF BODY ON A BURNER WITH AND WITHOUT PENETRATION OF RECIRCULATION ZONE (MODIFIED FROM EL-MAHALLAWAY & HABIK, 2002)

Flame stabilisation by swirl

Cushman-Roisin (2015) suggests that swirl is a rotating or spiral movement pattern of a fluid. When a fluid is swirling, it has an axial and radial component. Recirculation zones can also be formed by swirling flow, if the opposing axial pressure gradient is larger than the kinetic energy of fluid particles entering the flow field (El-Mahallaway & Habik, 2002). As illustrated in Figure 2.5, the recirculation zone formed by swirling jets is called an internal recirculation zone. When flow is entrained from outside the jet, another recirculation zone is formed, which is called the external recirculation zone. The factors that affect the recirculation zone are the strength of swirl, the angle of the swirler and the chamber-to-burner diameter. Flame stability and combustion efficiency depend on the size and strength of the recirculation vortex. This creates a higher burning velocity and blow-off velocity.

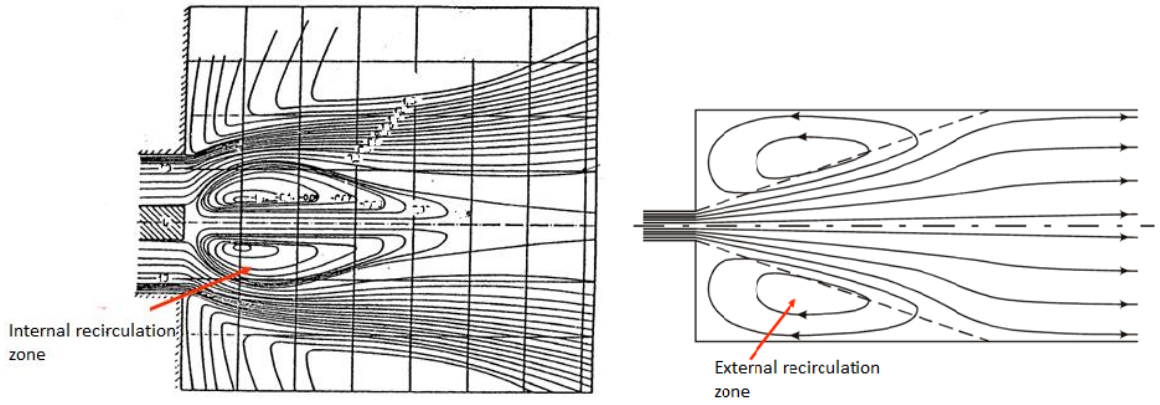

FIGURE 2.5: ILLUSTRATION OF INTERNAL AND EXTERNAL RECIRCULATION ZONES (MODIFIED AFTER CUSHMAN-ROISIN, 2015)

According to El-Mahallaway and Habik (2002), swirl can be created by three methods:

- Tangential and axial entry;
- Guided vanes;
- Direct rotation by a rotating pipe.

For tangential and axial entry, the amount of swirl can be controlled by adjusting either the tangential or axial entry. To achieve the specific swirl, the pressure requirement is relatively high and commercial systems often opt for guided vanes. A guided vane swirler is placed in an axial pipe flow, where the flow is deflected by the vanes that are situated at a certain angle. The direct rotation is created by rotating a pipe that causes frictional drag with the axial fluid moving through it causing it to swirl (El-Mahallaway & Habik, 2002).

Swirl allows an increase in nominal burner load without jeopardising ignition. In a study done by El-Mahallaway and Habik (2002) on different fuels, all the fuels indicated that when the flow and velocity of fuel increase, the chance of blow-off increases. However, when swirl is applied, the chance for blow off decreases. With weak swirl the volatility of the fuel had a large effect on flame stability. With high swirl, the recirculation has a greater effect on the flame stability compared to the volatility.

Different types of flames influenced by swirl

Heap *et al*. (1976) explain that different flames form with different amounts of swirl. As mentioned before, swirlers and bluff bodies increase mixing at the boundaries of the recirculation zone and near the burner. As a result, the flame length is reduced and the flame intensity (in terms of flame volume) is increased. The types of flames can be defined in terms of flame intensity:

1) Low-intensity jet flames

These are flames with no or too low swirl to form a recirculation zone. Stabilisation devices of these flames are pilot flames or bluff bodies. These flames are long and have a slow increase in axial temperature, as illustrated in Figure 2.6:

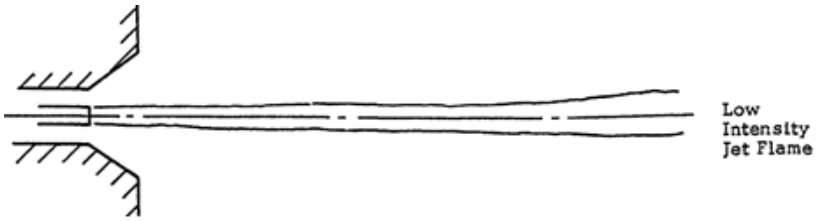

FIGURE 2.6: REPRESENTATION OF A LOW INTENSITY FLAME (MODIFIED AFTER HEAP *ET AL.*, 1976)

2) High intensity type 1 flames

When increasing the swirl intensity beyond a critical amount of swirl, an internal recirculation zone forms. If the fuel's momentum is large enough, the fuel will penetrate the recirculation zone and two internal recirculation zones will form. This flame will then have two sections: a short bulbous zone close to the burner mouth, and a long tail section. The two sections may merge or split, as can be seen in Figure 2.7:

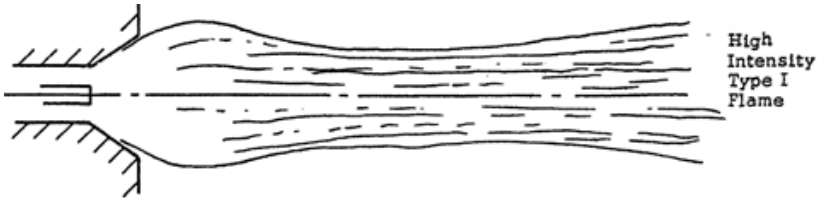

FIGURE 2.7: REPRESENTATION OF A HIGH-INTENSITY TYPE 1 FLAME (MODIFIED AFTER HEAP *ET AL.*, 1976)

3) High-intensity type 2 flames

As shown in Figure 2.8, these flames have an internal recirculation zone on the flame axis, which can be created by the following fuel injection methods:

- Wide-angle divergent fuel injection at zero or low swirl. For no swirl, the recirculation is caused by the blockage of the fuel injector;
- Divergent, annular or low-momentum axial fuel injection at medium swirl;
- High-momentum axial fuel injection at high swirl angles.

These flames are of higher intensity than the type 1 flames. These flames' fuel momentum is not high enough to penetrate the recirculation zone.

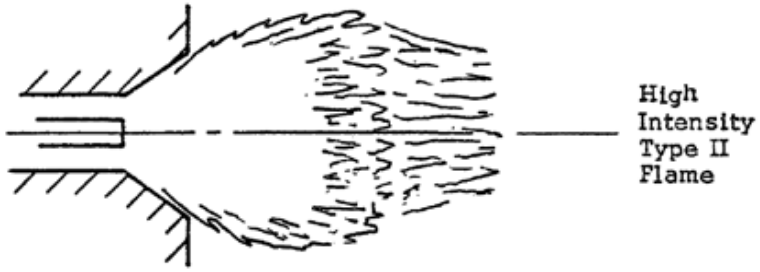

FIGURE 2.8: REPRESENTATION OF A HIGH-INTENSITY TYPE 2 FLAME (MODIFIED AFTER HEAP *ET AL.*, 1976)

4) High-intensity type 3 flames

These types of flames are a combination of high intensity flame types 1 and 2. The flame has a bulbous base, but the tail is reduced. This type of flame is characterised by low annular air velocities and with fuel injection from an axial direction. When the air velocity increases, there is an immediate change from a high-intensity type 1 flame to a high-intensity type 3 flame. The fuel only partially penetrates the recirculation zone and stagnates. This is illustrated in Figure 2.9:

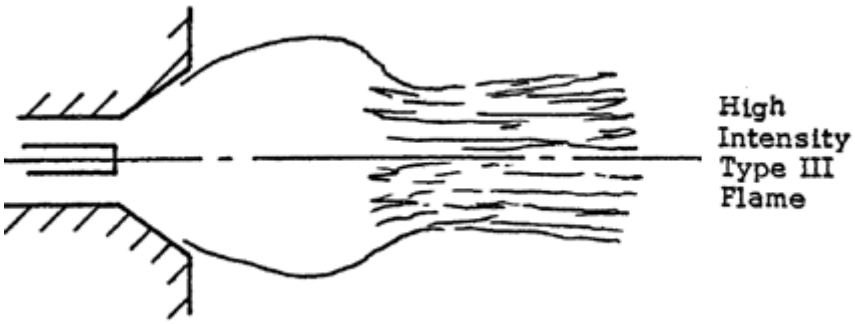

FIGURE 2.9: REPRESENTATION OF A HIGH-INTENSITY TYPE 3 FLAME (MODIFIED AFTER HEAP *ET AL.*, 1976)

5) Lifted flames

As illustrated in Figure 2.10, these flames find stability at some distance downstream of the fuel injector. The flame can be stabilised by enhancing the swirl or increasing the environmental temperature.

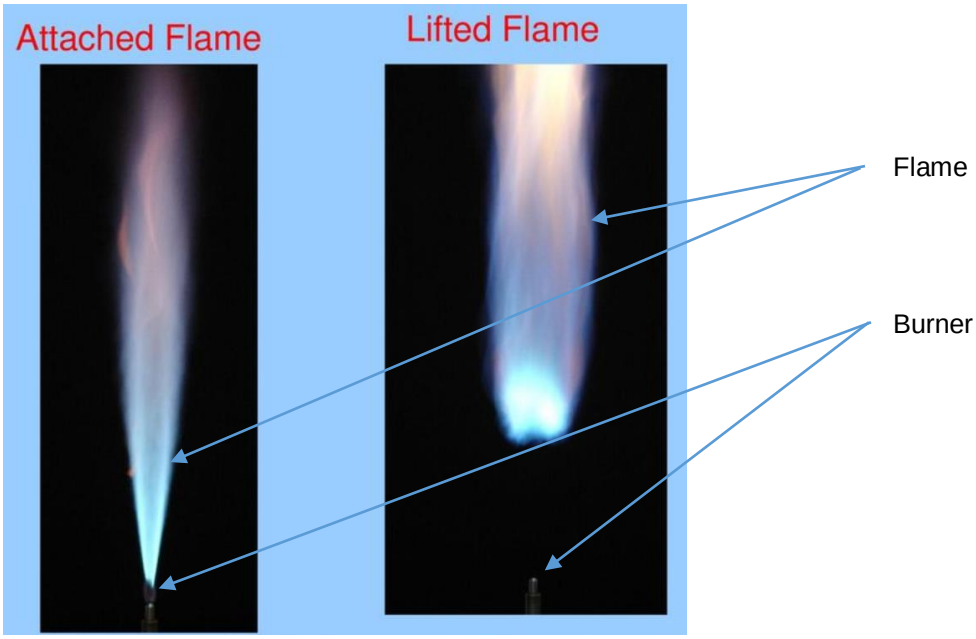

FIGURE 2.10: REPRESENTATION OF A LIFTED FLAME (MODIFIED AFTER WU *ET AL*., 2009)

2.2.3 OTHER AERODYNAMIC FACTORS INFLUENCING COMBUSTION

Certain factors exist that can affect combustion by altering the aerodynamics other than swirl and bluff bodies. These factors will now be explained:

Time, temperature and turbulence

According to El-Mahallaway and Habik (2002), to obtain good combustion, the three T's of time, turbulence and temperature are important. High temperature increases the number of chain carriers for sustained continuous combustion, the time a fuel particle spends in a flame allows for better burnout and the turbulence increases the mixing rate of fuel and oxidiser. The three T's make it possible to achieve shorter flames and higher temperatures, to reduce furnace volumes and lengths and in turn to make the application smaller. Turbulence plays a role in the two zones, namely the zone where fuel and air are mixed and the one where combustion takes place.

Jets

Cushman-Roisin (2015) suggests that a jet is formed when a fluid exits a nozzle and interacts with its surroundings. Downstream near the nozzle, a region called the potential core exists where the velocity and concentration of the fluid is unchanged, as it was inside the nozzle. Outside the potential core a free boundary layer develops where mass and momentum are transferred perpendicular to the flow. After the potential core comes the transition region, followed by the fully developed region. El-Mahallaway and Habik (2002) also state that the potential core and transition region has a length of about 4-5 and 8-10 diameters of the nozzle respectively. The fully developed regions of turbulent jets are similar regarding velocity and concentration distributions. This is illustrated in Figure 2.11:

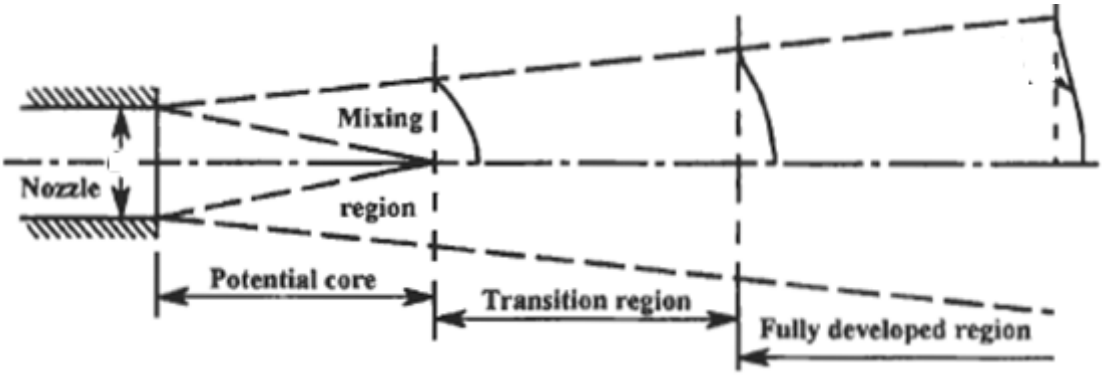

FIGURE 2.11: ILLUSTRATION OF A JET THAT IS FORMED BY A FLUID (MODIFIED FROM EL-MAHALLAWAY & HABIK, 2002)

Entrainment

According to El-Mahallaway and Habik (2002), since there is a momentum exchange between the jet and the surroundings, fluid is entrained from the surroundings across the boundaries of the jet. The amount of fluid a turbulent jet can entrain is equal to the amount of mass flow rate inside the nozzle, every three nozzle diameters downstream on the jet centreline. If fluids exit from two concentric tubes, the fluid with the largest momentum will entrain the other fluid. This is shown in Figure 2.12:

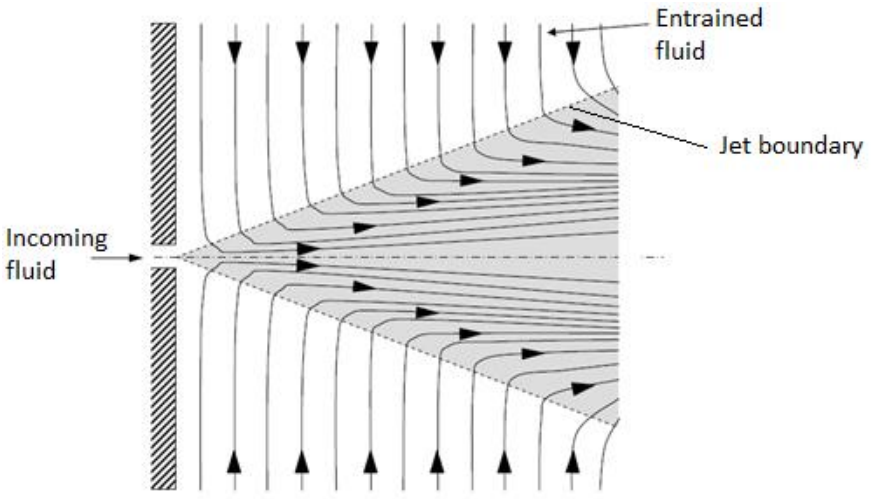

FIGURE 2.12: ENTRAINMENT EFFECT OF A JET (MODIFIED AFTER COLLINS, 2016)

Quarl

A quarl is a diverging exit of a tube. When confining a swirling flow to a quarl, it greatly affects the recirculating zone. Experiments were carried out by El-Mahallaway and Habik (2002) on short diverging, long diverging and converging diverging nozzles for swirling flow. It was concluded that when the swirl is increased, the spread angle of the jet increases, and correspondingly, the maximum values of axial, tangential and radial components of velocity decay more quickly along the length of the jet.

2.3 COMBUSTION AND BURNER PRINCIPLES OF COAL

Since there are a many different coal types, there are no exact models when dealing with coal combustion. According to Wróblewska *et al*. (1977), it has been found that a unique aerodynamic flow

field exists for each type of coal for optimum combustion. Therefore, coal combustion principles need to be investigated.

2.3.1 FUNDAMENTALS OF PULVERISED COAL COMBUSTION IN A BURNER

Coal combustion by means of a burner, requires the coal to be pulverised in order to be transported through the burner. The combustibility of pulverised coal (PC) has been a topic of research for many years. The major areas of interest include heat release, burning velocity and flammability limits for different types of coal (Slezak *et al*., 1985).

For PC to combust, an exothermic chemical reaction of the combustible elements of PC must take place in order to release heat. High combustion efficiency requires that most of the combustible matter be oxidised, thus releasing the highest amount of available energy in the coal (Kitto & Stultz, 2005).

According to Kitto and Stultz, (2005), during the combustion process of coal, heterogeneous and homogeneous combustion processes take place. A homogeneous combustion process is a chemical reaction of only gas elements that release heat and form flue gas. Yang, (1993) defines a heterogeneous combustion process as a reaction between different phases such as solid and gas to release heat and form products. PC undergoes heterogeneous and homogeneous combustion processes.

When a PC particle enters the combustion zone, the particle is heated by means of radiation and convection, and the particle is dried of any moisture in about 5 milliseconds (Cloke *et al*.,1997). When the particle reaches a temperature of more or less 400^{o}C, devolitilisation takes place. This is where the coal bond structure breaks up to yield carbon monoxide (CO), H_2 and hydrocarbons. The volatiles that are released and formed burn in a gas phase. The devolitilisation process takes approximately 100 milliseconds for the spectrum of the very fine PC particles utilised. The rate of burning depends on two factors: the rate at which the volatiles are mixed with air after being emitted from the coal particles, and the rate of the chemical reaction. Thereafter, the residual char or fixed C (which remains after complete devolatilisation) is combusted, leaving only ash. Char burning takes up approximately 70 to 80% of the total burning time, which is approximately 2 seconds (Kim *et al*., 2014).

According to Kitto and Stultz, (2005), a specific coal ignites at a specific temperature. Factors such as pressure, velocity, ignition source, and air-fuel mixture distribution greatly influence the ignition temperature. For instance, high pressure will lower the ignition temperature, whereas moisture will increase it. It is approximated that coal has the same ignition temperature as that of the fixed C content (400^{o}C), and the volatile content released does not ignite before this temperature is reached.

Figure 2.13 illustrates the combustion process of a coal particle.

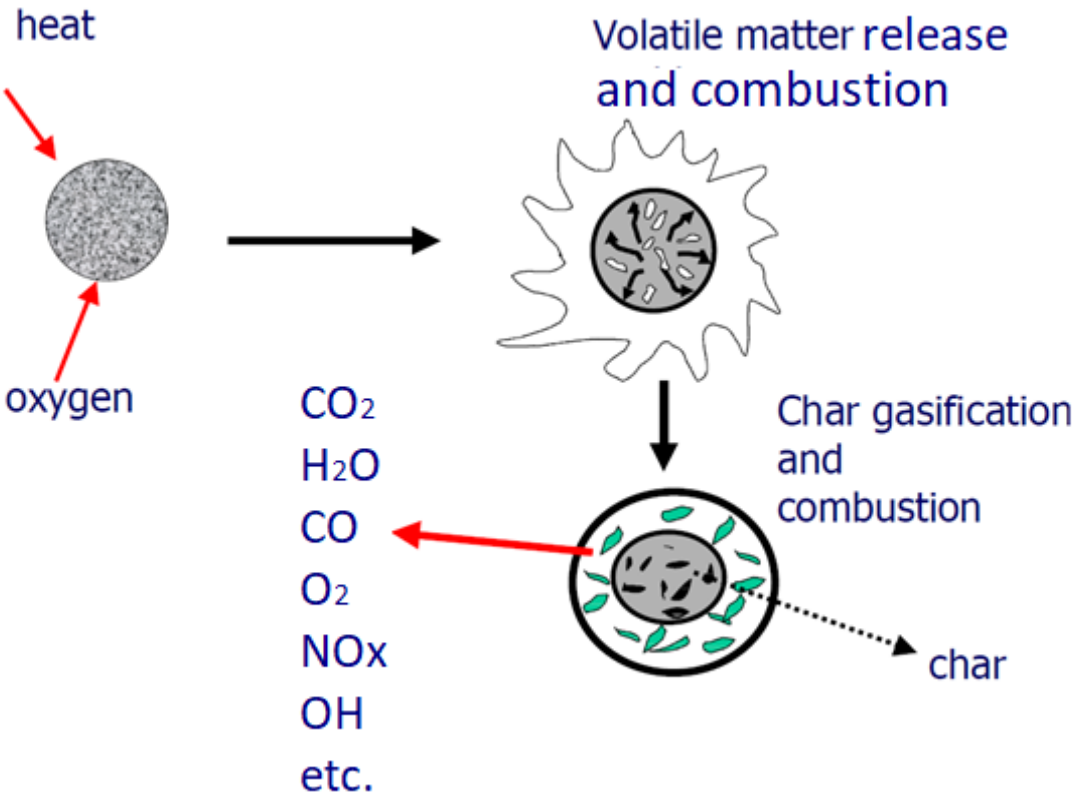

FIGURE 2.13: COMBUSTION PROCESS OF A COAL PARTICLE (MODIFIED AFTER PRADEEP, 2013)

According to Kitto and Stultz (2005), stoichiometric air is the theoretical amount of air required for complete combustion for a certain type of fuel. This means that theoretically, all the O_2 contained in the air will be used to form products and nothing will be left in excess. When coal is burned the major products formed are carbon dioxide (CO_2), water (H_2O) and sulphur dioxide (SO_2), whereas the other products are minute.

The main chemical reactions of combustible elements that take place during coal combustion are as follows:

$$2C + O_2 = 2CO \quad (1)$$

$$C + O_2 = CO_2 \quad (2)$$

$$2CO + O_2 = 2CO_2 \quad (3)$$

$$2H_2 + O_2 = 2H_2O \quad (4)$$

$$S + O_2 = SO_2 \quad (5)$$

These chemical reactions are also used to calculate the stoichiometric amount of combustion air for coal.

Sub-stoichiometric air is an insufficient amount of air provided for combustion. Although this method is used in certain applications, it is not desired for coal combustion since it leads to low combustion efficiency as well as the occurrence of flame-outs (Kitto & Stultz, 2005).

Hyper-stoichiometric air is an excess amount of air provided for combustion. This method is most often used in industry to guarantee high combustion efficiency, since air and PC are mixed better. The amount of excess air should not be disproportionate, since a stage can be reached where too much excess air will start to cool down the flame. The optimum amount of excess air varies for different applications of coal combustion, but a general guideline for PC is 10 – 20% excess air, which will result in an O_2 content in flue gas of 2 – 3.5%.

2.3.2 FACTORS AFFECTING COMBUSTION OF PULVERISED COAL

The most important factors influencing PC will now be discussed:

PC fineness

The fineness of the PC is very important for complete combustion as well as the rate of combustion. The finer the PC, the greater the surface area per mass available for heat transfer (Xiumin *et al*., 2001). According to Storm (1998), the PC fineness can be analysed by using a plotted Rosin-Rammler graph. The PC is sampled iso-kinetically, from a burner pipe exiting a mill. After being dried in an oven the PC is placed into a specified shaker with different size sieves that range from 75 - 300 µm. Thereafter, the mass percentages of PC on each sieve is plotted on the graph, as seen in Figure 2.14. As required for adequate combustion, this graph is primarily utilised to evaluate mill performance. The generally accepted criterion is that at least 70% of the sample must pass through the 75 µm sieve into the pan and not more than 1% must remain on the 300 µm sieve, with a reasonably linear connection passing through the sieve sizes in between.

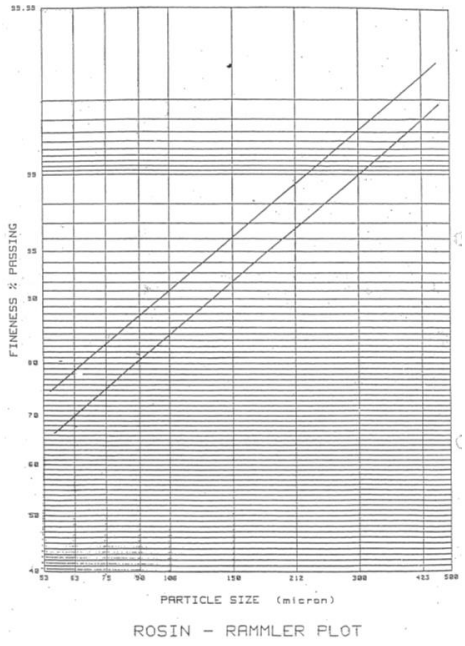

FIGURE 2.14: STANDARD TEMPLATE OF A ROSIN–RAMMLER PLOT FOR PF FINENESS CRITERIA (STORM, 1998)

Combustion rate

According to Makino and Law (2009), because of the fineness of PC, complete combustion of a 150 μm particle occurs at about 2 seconds. However, burnout time also depends on the coal's VM content. An increase in VM decreases the burnout time. Howard and Essenhigh (1966) state that VM also plays an important role in flame stability and ignition. Low-volatility coal can produce longer flames. To compensate for this, higher furnace temperatures, longer furnaces to increase residence time and recirculation of hot flue gas can be considered (Kitto & Stultz, 2005).

Moisture

According to Kitto and Stultz (2005), moisture is a serious problem for coal combustion, since it absorbs heat in order to vaporise. This in turn reduces the absorption of heat of coal particles to initiate combustion. Although drying of particles is applied before these enter the flame, the moisture is carried along to the furnace.

Ash

PC contains a certain amount of minerals, which are substances that do not participate in the exothermic chemical reactions of combustion to produce heat. These minerals, however do absorb some of the heat during the combustion process in order to oxidise and form ash constituents afterwards. This also extracts heat from the flame. Some of the minerals contain crystalline water, which also contributes to the cooling of the flame. At high enough temperatures, the ash will melt and thereafter solidify on the heat transfer areas, which can be problematic for the furnace.

Aerodynamics of coal combustion

The most important factor that affects the aerodynamic flow field of a coal burner is swirl. By using swirl, the following parameters are affected:

- The mixing of PC and air, flame length and location the flame (Khanafer & Aithal, 2011);
- Flame temperature (Xue *et al*., 2009);
- Flame stability, flame speed as well as residence time (Nettleton, 2004);
- Size and intensity of the recirculation zone (Gu *et al*., 2005);
- Burnout time of PC and combustion efficiency (Rajoo, 2010).

Generally speaking, an increase in swirl will:

- Increase the mixing of PC and air;
- Increase flame temperature;
- Increase flame stability;
- Increase flame propagation velocity;
- Increase residence time of a coal particle;
- Increase the recirculation zone size and intensity;
- Increase combustion efficiency;
- Decrease burnout time;
- Decrease flame length.

However, an excessive amount of swirl can:

- Divert PC particles away from the recirculation zone due to overwhelming centrifugal force;
- Decrease flame stability;
- Cause excessive diverging flow that can dilute the concentration of air and fuel.

2.3.3 PULVERISED COAL BURNER CHARACTERISTICS

Burner design plays a significant role in PC combustion according to Basu *et al*. (2000). It influences the aerodynamics, flame and ignition conditions. Kitto and Stultz (2005) state that a PC burner usually consists of an igniter to light natural gas, primary air (PA) and secondary air (SA) concentric tubes. The PA is used to convey the PC to the burner mouth pneumatically and is usually preheated to 66^{o}C to evaporate the surface moisture on the coal particles. The PA quantity is low enough to prevent combustion and this is therefore a safe mixture of fuel and air. The velocity of PA is very important in order to prevent PC settling inside the PA tube. The minimum velocity inside the PA tube needs to be 20 m/s. A severe case of PC settling is shown in Figure 2.15. After the PA and PC mixture exits the burner, it is mixed with the SA. The SA is used to provide the PC with a sufficient amount of air for complete combustion purposes. The SA is heated to 316^{o}C and is introduced to the burner by a force draft fan into an air box that encloses the SA tube. When the combustion temperature is too high, the flame can produce NOx which is a non-combustible and hazardous gas. To reduce NOx, the SA can be divided into two groups namely SA and tertiary air (TA). When staging the combustion air, the flame is stretched out and is cooler owing to delayed combustion. However, low NOx burners tend to produce lower combustion efficiency.

FIGURE 2.15: PRESENTATION OF SEVERE PC SETTLING INSIDE A PA TUBE (MODIFIED AFTER VAN DER MERWE, 2014)

Basu *et al*. (2012) suggest that there are mainly two types of PC burners: swirl type and parallel/direct type burners. A swirl PC burner uses guide vanes to initialise a swirling motion in the fluid and creates a recirculation zone downstream. In direct burners the fuel and combustion air flows are parallel to each other and do not create a recirculation zone. Mostly, direct burners are used in tangential or corner-fired boilers. These burners operate in collaboration with other burners to create a swirling motion in the furnace and are difficult to operate on their own. The swirl burner is mostly used in front or opposite wall furnaces and has been designed to achieve a certain flame shape and aerodynamics; it can operate on its own.

The basic requirements for a burner are the following:

- Proper aerodynamics at the outlet to ensure good ignition and a stable flame;
- Proper load control;
- Safety.

An axial swirler is designed to allow air to flow parallel to the concentric burner tubes into a set of axial fixed vanes which is situated in the burner tube. The axial vanes are set at a specific angle and when the air exits the swirler, it has a tangential velocity component, as well as an axial component depending on the swirl angle. These tangential and axial components create the swirling effect. Axial swirlers are shown in Figure 2.16:

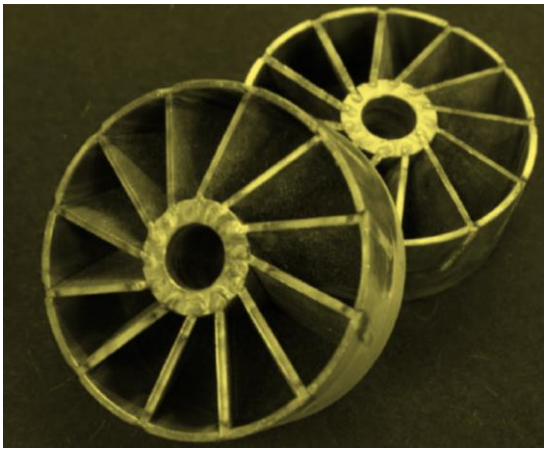

FIGURE 2.16: EXAMPLE OF AXIAL SWIRLERS (MODIFIED AFTER HALL AND POVEY, 2015)

A conical axial vane swirler can be used to create variable swirl. Unlike the normal axial vane swirler, which is situated inside a constant diameter concentric tube, the conical axial vane swirler is situated inside a conical tube. When the conical swirler is positioned against the conical tube, maximal swirl can be achieved, which is dictated by the fixed vanes' angle, since the total flow has to move through the vanes. By moving the conical swirler away from the maximum position, an annular passage is formed between the conical swirler and the conical tube. This allows some of the air to move over the conical swirler and some air to move through the conical swirler. At the exit of the swirler, the two streams mix and the resultant swirl is less. This is illustrated in Figure 2.17:

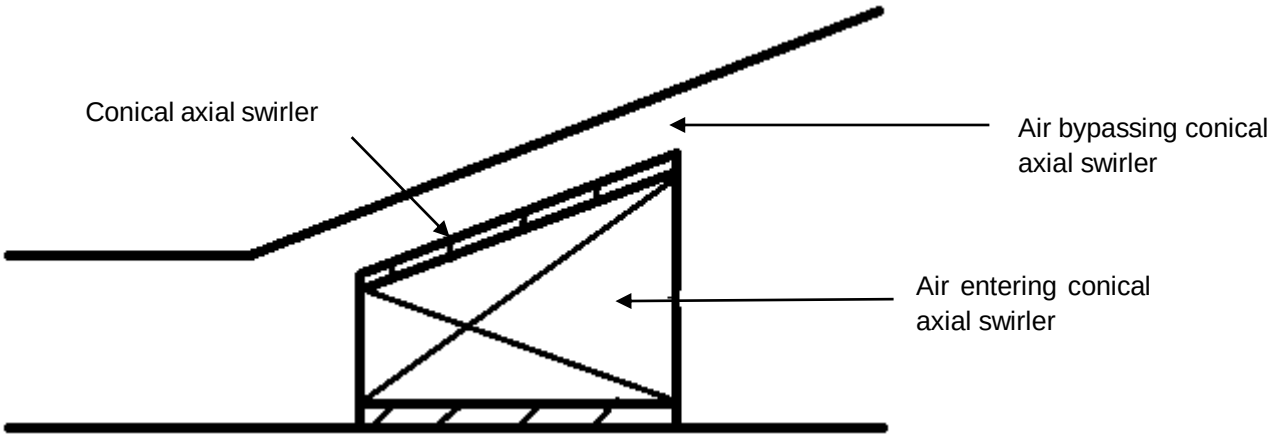

FIGURE 2.17: ILLUSTRATION OF FLOW BYPASSING A CONICAL SWIRL TO CREATE LESS SWIRL (MODIFIED AFTER BASU *ET. AL*, 2012)

A combustion efficiency of 97% and greater for an actual coal burner is generally considered good burner performance (Sharifi & Scaroni, 1996). Combustion efficiency is defined as the ratio of heat released by fuel to the actual heat potential of the fuel (Miller, 2017). The measurable indicator for combustion efficiency is the amount of unburned carbon (UBC) remaining in ash. A typically acceptable amount of UBC in ash is approximately 2 - 3% (Wang *et al*., 2017).

2.4 METHODS FOR DETERMINING THE CALORIFIC VALUE OF COAL

It is of great importance to be able to calculate the CV of coal accurately according to the process of combustion. According to Storm (1998), the CV of coal has a significant effect on the calculation of overall efficiency for power stations. This can be explained more clearly when considering the following formula used by Storm (1998):

$$\eta_{overall} = \frac{USO}{\dot{m}_{coal} * CV} \quad (6)$$

where:

$\eta_{overall}$ - Overall plant efficiency [-]

$\dot{m}_{coal}$ - Mass flow of coal used for combustion [kg/s]

USO - Electric units sent out [MW].

The instrumentation used to measure the USO and $\dot{m}_{coal}$ is adequately accurate; however, the greatest contributor to error concerning equation (6) is the CV. It is therefore very important to have the correct CV to calculate a power station's efficiency.

2.4.1 METHODS TO DETERMINE THE GCV_V AND NCV_P OF COAL

As mentioned in Section 2.1, two forms of CV exist, GCVv and NCVp. The methods used to determine these values for coal will now be explained:

The manner of calculating the GCV of coal has always been a topic of disagreement and there are two methods of doing so. The first method is empirically calculated. As stated by Lowry (1945), the original and most commonly used formula for calculating GCVv is the so called Dulong (1820) equation, which uses a weighted average of predetermined CVs of the combustible elements contained in the coal:

$$GCVv = (34.7\ x\ C) + (148.2\ x\ H) - (18.5\ x\ O) + (10.7\ x\ S) \quad (7)$$

where C, H, O and S are the weighted percentage amounts of C, H_2, O_2 and S respectively for the coal sample. The GCVv is measured in MJ/kg.

The second method to determine GCVv, is using a Bomb calorimeter. This method is a direct or experimental technique used mostly for liquid and solid fuels (Kitto & Stultz, 2005). According to Basu (2013), the procedure is to insert a specific amount of fuel into the Bomb (which has a constant volume) and to pressurise the Bomb with 3-5 MPa of sufficient O_2 to ensure complete combustion. The Bomb is then placed inside a water container. The water's temperature is constantly monitored and it is continuously stirred. The fuel is then ignited by an electrical wire and combustion of the fuel starts. A sharp increase in water temperature occurs since it absorbs the heat released by the fuel. The water temperature continues to rise until stability is reached. By knowing the heat capacities of the Bomb material and water, the amount of heat released by combustion of the fuel can be calculated by a mass-energy balance.

According to Kitto and Stultz (2005), the only way of determining the NCVp is empirical calculation since, direct determination is extremely difficult. This method uses either the calculated GCVv or directly determined GCVv and subtracts the latent heat of the moisture at constant pressure. As stated by the British Standards Institution (2009), the equation is as follows:

$$NCVp = [GCVv - (0.212x\ H) - 0.8(O + N)]\ x\ (1 - 0.01M) - 24.43M \qquad (8)$$

where H, O, N and M are the weighted percentage amounts of hydrogen, oxygen, nitrogen and moisture respectively for the coal sample. The NCVp is measured in J/kg.

2.4.2 PROBLEMS OF CURRENT METHODS TO DETERMINE CV ON POWER STATIONS

The problem of using current methods for determining the CV of coal on power stations is mostly that they do not represent the correct process of measurement.

According to Storm (1998), on a power station combustion of coal occurs by means of a burner. In a burner, ignition and combustion take place by continuous exothermic heat transfer. Some of the heat produced is absorbed by the boiler to create steam. However, the remaining heat, in the form of flue gas, is released into the atmosphere at a temperature that is higher than that required for condensation purposes of moisture. Therefore, the moisture in the flue gas condensates and releases latent heat into the atmosphere and not into the boiler. As stated in Section 2.1, this is a constant pressure process and requires the NCVp to be measured.

The Bomb calorimeter method poses some problems for determining an accurate CV of coal that represents an actual combustion process on a power station. In a Bomb calorimeter, the fuel is ignited by an induced electric spark from a fuse wire. Conditions during combustion in the Bomb are different from those in a burner. The Bomb has a high pressure environment of O_2 at a pressure of 3-5 MPa whereas a burner has air supply and atmospheric pressure. Calibration of the Bomb is also problematic, since it is calibrated by a benzoic tablet that has a CV double that of most coal in South Africa. Most importantly, the Bomb calorimeter is a constant volume process that includes latent heat of moisture and not a constant pressure process that excludes latent heat of moisture which represents a burner more accurately. Occasionally, three different value of the same sample are obtained from three different Bomb calorimeters.

Although, according to Kitto and Stultz (2005), the NCVp can be calculated from the GCVv by subtracting the latent heat of moisture, there is no exact standard available to determine the NCVp from GCVv since the references of constants used for heats of combustion and the temperature at which the latent heat of moisture is calculated differ. It is also important to note that, determining the CV by using a direct method is more accurate than when using a calculated method since the calculated method does not take into account losses and can be taken as a theoretical guideline.

Even though the difference between GCVv and NCVp may be small (about 5%), when one considers the fact that 3024 t/day coal can be combusted, the difference becomes very significant in terms of the calculation of $\eta_{overall}$.

In conclusion, the most accurate manner to determine the NCVp for coal directly is using a process that represents the combustion process of a burner, but does not include the latent heat from moisture since it is a constant pressure process.

2.4.3 DIRECT METHODS TO DETERMINE NCV_P FOR GASEOUS FUELS

The direct method to determine the NCVp is using a flow calorimeter, as stated by Obert (1973). This method is mostly used for gaseous fuels. A flow calorimeter basically consists of a water-cooled combustion chamber, a burner and measuring apparatuses. Sustainable combustion is initiated by inserting a measured amount of air and fuel through the burner and igniting it with a spark. The furnace is cooled by means of a mass measured amount of water flowing on the outside of the furnace, of which the temperature is measured constantly. As combustion occurs inside the furnace, the water starts to absorb some of the heat through the furnace walls. After the water temperature has been stabilised and steady state conditions have been reached, the heat absorbed by the water is calculated. The heat is calculated by the measurement of water temperature at the inlet and outlet as well as the mass flow of water. These measurements are used in a mass-energy balance. However, not all of the heat is absorbed by the water through the furnace walls; instead the remaining heat exits the furnace to the atmosphere. This remaining heat is then also calculated by measuring the mass and temperature of the fuel and air entering the furnace, as well as the temperature of the flue gas exiting the furnace. The mass of the flue gas is equal to the sum of air and fuel. These measurements are once again used in the mass-energy balance.

If the combustion gases are allowed to exit the furnace at a sufficient higher temperature than the condensation temperature of water, then vapour cannot condensate to release latent heat.

According to Dryjanska *et al.* (2006), the most frequently used flow calorimeter is the Junkers calorimeter. This method is based on the measurement of water temperature increase of a certain mass flow, which flows around the calorimeter. The combustion of gas inside the calorimeter heats the water in a sustained manner.

The Junkers calorimeter consists of a burner, combustion chamber with a double walled water jacket, an exhaust system and a housing to reduce radiation heat transfer to the surroundings. The process will subsequently be explained:

- An overflow vessel is used to supply constant pressure, and therefore a constant mass flow of water to the water jacket. This water enters the water jacket at the inlet and its temperature is measured. When the water exits the water jacket, it enters a second over flow vessel. The temperature is measured again at the outlet, since it absorbed the heat released by a certain amount of fuel burned inside the calorimeter. The amount of water is also measured in the process.
- A water temperature difference of 6 – 12^{o}C is desirable. The burner' outlet is situated inside the combustion chamber. The combustion air and gas are also delivered at a constant rate; quantities are determined by an air-to-fuel ratio (A: F) to enable complete combustion. The flue gas will then exit the chamber at atmospheric conditions.

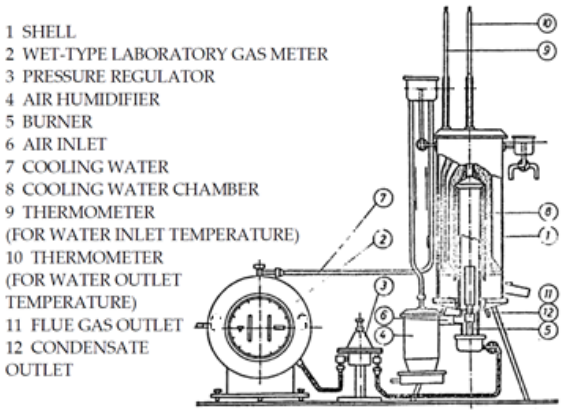

FIGURE 2.18: ILLUSTRATION OF A TYPICAL JUNKERS FLOW CALORIMETER (MODIFIED ACCORDING TO BUDAPEST UNIVERSITY OF TECHNOLOGY AND ECONOMICS, S.A.)

Based on the points mentioned, to determine the NCVp of a fuel via a flow calorimeter, it is very important that the burner achieves combustion efficiency that is as high as possible.

2.5 COMPUTATIONAL COMBUSTION MODELLING

Computer technology has evolved in such a way that it makes numerical modelling much more feasible to perform on large and complicated problems. A numerical method is defined as solving a mathematical depiction of a physical procedure by using a numerical approach. A numerical approach is usually more applicable if an analytical approach is not available. Computers are mostly used in numerical modelling, since high computing power is needed for complex systems (Kitto & Stultz: 2005).

As Versteeg and Malalasekera (2007) state, a very common numerical method used on computers is CFD. CFD is the analysis of systems concerning fluid flow, heat transfer and other phenomena by making use of data tables and numerical techniques.

According to Ranade and Gupta (2015), because of the development of advanced fluid physics and numerical techniques, CFD is a very important tool to be used in the optimisation of boiler performance on parameters such as reduced emissions and boiler and plant efficiency.

Using CFD has many benefits, such as:

- Reduced cost and time in the design phase;
- Increased understanding of a physical process;
- Exploration of unfamiliar conditions;
- Troubleshooting problems on existing systems;
- Design validation or examination of different components' interactions.

Although the field and understanding of CFD on coal combustion is increasingly being developed, it is computationally very expensive and time-consuming owing to the complexity of the problem. It is therefore necessary to adapt and simplify CFD techniques by applying certain fundamentals when modelling combustion numerically.

One of the techniques used to reduce computation time and to predict combustion is the simulation of the flow field in cold flow conditions. According to El-Mahallaway and Habik (2002), a diffusion flame process depends only on the mixing rates, since the chemical process is very rapid. The rate of mixing is determined by the aerodynamic flow field and turbulent transport process of mass, momentum and heat. Because of the complexity of measurements in flames, a lot of valuable data on mixing and basic

flow can be acquired with cold flow tests without chemical reactions. Cold flow experiments compared to actual combustion experiments show that the cold flow tests have similar general shapes of the radial distribution of axial and tangential velocities to those of combustion tests. However, cold flow tests are only an approximation of the flow and mixing.

According to Versteeg and Malalasekera (2007), CFD is primarily focused on the conservation laws of mass, momentum and energy. However, to use these conservation laws in flow dynamics, the Navier-Stokes differential equations are needed. The Navier-Stokes equations describe the flow of fluids. When linking the Navier-Stokes and conservation laws, a mathematical model can be established to form governing equations in order to solve fluid flow problems. When CFD solves a fluid flow problem, the flow domain is discretised by substituting the differential equations and solving these numerically by algebraic equations. The most commonly used discretised method is the finite volume method.

According to Ranade and Gupta (2015), to use the finite volume method, the flow domain needs to be divided into a grid or mesh of nodes. The volume that surrounds the nodes is called a cell and is of finite volume. The solution involves solving a cell numerically by using the algebraic equations and then carrying over the result to the next cell. The next cell is then solved by using the results of the previous cell as inputs. This process continues until the fluid domain is solved to an acceptable error. Versteeg and Malalasekera (2007) report that there are commercial packages available that use the finite volume discretisation method. The most common codes available are FLUENT, STAR CD and PHOENICS.

Since turbulence is prominent on burners, it is necessary to include its effects in CFD modelling. The biggest problem when dealing with turbulence is the fluctuations of velocity in turbulent flow. The most common method to approach turbulence modelling is eliminating the fluctuations in turbulent flow, and replacing these with a time averaging model called the Reynolds averaged Navier-Stokes (RANS) model. RANS is based on the Reynolds decomposition of average and fluctuating flows. This turbulence model is the least computational and time-consuming. The governing equations are solved by focusing on the mean effects of flow and mean properties. Another method used to model turbulence is the large Eddy simulation (LES). This method solves only the large fluctuations or large eddies of turbulence directly, but ignores the smaller eddies. The resolved flow involves mean flow as well as large eddies. The LES turbulence is much more time-consuming than the RANS model. The direct numerical simulation model solves all the velocity fluctuations, as well as the average flow. To solve the equations related to all the velocity fluctuations, this model utilises a spatial grid that is fine enough and has enough time steps. This method is, however, very time-expensive and is rarely used (Versteeg & Malalasekera: 2007).

Because of the relatively inexpensive computation time of RANS based turbulent models, these models are mostly used for turbulent and combustion modelling (Ranade & Gupta: 2015). According to Versteeg and Malalasekera (2007), when Reynolds decomposition is applied to the Navier-Stokes equations, an additional term known as the Reynolds stress term is added. The method to solve the Reynolds stress term can be divided into two methods, namely: the k-ε model and the Reynolds stress model (RSM). The k-ε model is based on solving two variables: k (turbulent kinetic energy) and ε (rate of dissipation of kinetic energy). The RSM model is based on solving six representative turbulent stresses.

As stated by Ranade and Gupta (2015), for turbulent modelling, the mesh type and cell type also play a role. There are two types of meshes, namely a structured and an unstructured mesh. A structured mesh is a consistent arrangement of cells that enables gridlines of a cell to cross neighbouring cells' gridlines only once. This allows for passing information from one cell to another more easily. The main disadvantage of the structured mesh is that it does not fit well for very complex geometries. An unstructured mesh is very useful when dealing with complex geometries and can be used for almost any geometry owing to its flexibility. The disadvantage of this mesh is that the retrieval of information is more difficult than with a structured mesh. Although different types of cells exist, the most commonly used types of cells for turbulent modelling are the hexahedral and polyhedral cells.

2.6 CONCLUSIONS AND DESIGN CONSIDERATIONS RESULTING FROM LITERATURE REVIEW

In order to develop an NCVp analyser for coal, the following conclusions and considerations are relevant:

2.6.1 MEASUREMENT OF CV FOR COAL

- NCVp is the representative method to determine the CV of coal on a power station.
- NCVp is obtained if moisture cannot condensate inside the measuring apparatus.
- NCVp must be determined directly.
- Small scale testing is necessary for low costs.
- The flow calorimeter is the direct method used to determine the NCVp of gaseous fuels.
- No flow calorimeters for coal are available on the market.
- A flow calorimeter consists mainly of a combustion chamber, burner, water jacket and measuring apparatus.
- The Junkers flow calorimeter is the most popular flow calorimeter.
- The procedure of using a flow calorimeter is basically the following:
    - The burner is used to combust fuel inside the water-cooled furnace.
    - The fuel gives off heat; some of this heat is absorbed by the water-cooled furnace walls and some of the heat exits the furnace to the atmosphere.
    - The NCVp is determined from a mass-energy balance, which depends on the measurements of:
        - inlet and outlet water temperature;
        - mass flow of water;
        - inlet temperature of fuel;
        - mass flow of fuel;
        - inlet temperature of combustion air;
        - mass flow of combustion air;
        - outlet temperature of flue gas.
- Mass flow of flue gas is calculated by using the conservation law of mass for combustion air and fuel.
- It is important that the fuel is completely combusted.
- The test duration must be sufficient to allow a stable water temperature to be reached.
- The flue gas must be at a sufficient temperature to prevent condensation inside the furnace.
- The burner is a critical part of a flow calorimeter.
- No coal burners are available to buy on small scale.

2.6.2 FUNDAMENTAL COMBUSTION AND BURNER PRINCIPLES

- Combustion is an exothermic chemical reaction between a fuel and oxidiser, which releases heat and light. The light released can be of a certain colour that is also known as a flame. The flame is the hottest part of the heat released.
- A manner of controlling combustion is using a burner.
- Chain carriers in the form of free radicals create chain reactions that sustain continuous combustion in a burner. Chain carriers are created by increasing temperature.
- Diffusion flames are a safer method of combustion, since they prevent combustion inside the fuel tube. A diffusion flame is established when the mixing of oxidant and fuel takes place after the two streams exit the burner tubes.
- Turbulent and laminar flames depend on the velocity at which the fuel and oxidiser exit the burner tubes.
- Turbulent flames combust faster and reduce the size of the burner.
- Turbulent flames mix by coarse mixture of large-scale transport process rate.
- An increase in turbulence increases the mixing of fuel and air.

- Too much turbulence can cause flame outs when the chemical reaction rate is slower than the mixing rate.
- For a continuous flame, the flame propagation velocity and flow velocity must be in equilibrium.
- Since high velocity streams (of fuel and air) are necessary to create high turbulence, a flame stabiliser is necessary to create an equilibrium point to prevent flame-outs in high-velocity streams.
- A recirculation zone is one flame stabiliser technique. The recirculation zone creates stagnation points, which allows the flow velocity to be slower than the flame propagation velocity.
- Bluff bodies are used to create a recirculation zone by creating a wake or low pressure-zone behind the bluff body. Flow moves from high pressure to a low pressure and recirculates.
- A recirculation zone can be penetrated by a fluid to form a neck-like flow shape.
- Swirlers can also be used to create a recirculation zone.
- Two types of recirculation zones exist: internal and external.
- Swirl can be created by using a tangential fluid entry or by using a conical axial swirler. The conical axial swirler is the most commonly used.
- Different intensity types of flames are created, depending on the amount of swirl.
- An internal recirculation zone is critical for flame stability. It creates a constant ignition zone close to the burner mouth.
- Using time, temperature and turbulence makes it possible to have shorter flames, higher temperatures and shorter furnaces.
- Entrainment affects fluid flow and aerodynamics. A jet of fluid can entrain surrounding fluid to create an external recirculation zone. If fluids exit from two concentric tubes, the fluid with the largest momentum will entrain the other fluid.
- A quarl is used to enlarge the internal recirculation zone.

2.6.3 COMBUSTION AND BURNER PRINCIPLES OF COAL

- No exact models are available to predict coal combustion.
- Each type of coal has a specific aerodynamic flow field for optimum combustion. Therefore, a burner needs to be adaptable in order to create different aerodynamic flow fields that are applicable to a certain type of coal.
- Coal needs to be pulverised in order to be conveyed and to enhance the combustion rate.
- The particle sizes of coal allow 70% to pass through a 75 μm sieve; 1% is larger than a 300μm sieve.
- Good burner performance for coal burners is estimated at 97% combustion efficiency.
- The coarsest coal particle takes about 5 seconds to combust completely.
- Unburned C and CO indicate incomplete combustion.
- Chemical equations are used to determine the A: F.
- A hyper-stoichiometric A: F is used to burn coal.
- 13-20% excess air is used for coal combustion.
- An increase in VM increases the combustion rate. Low volatility coal requires longer and hotter furnaces.
- Moisture influences combustion negatively. Therefore, PC needs to be dried before entering the flame.
- Mineral deposits in coal form ash during combustion.
- Direct and swirl burners are used for pulverised coal combustion.
    - Swirl burners can operate on their own much more easily compared to direct burners,
- Swirl is used to create recirculation zones for coal burners.
- Swirl has the following effects on coal combustion:
    - Increases the mixing of PC and air;
    - Increases flame temperature;
    - Increases flame stability;
    - Increases flame propagation velocity;
    - Increases residence time of a coal particle;

  - Increases recirculation zone size and intensity;
  - Increases combustion efficiency;
  - Decreases burnout time;
  - Decreases flame length;
- However, an excess amount of swirl can:
  - Divert PC particles away from the recirculation zone due to an overwhelming centrifugal force;
  - Decrease flame stability;
  - Have excessive diverging flow that can dilute the concentration of air and fuel.
- A pulverised coal burner consists of a PA and a SA tube, as well as a gas igniter.
- The PA is used to convey PC to the burner mouth. The velocity of the PA needs to be high enough to prevent PC settling and it is pre-heated to dry PC.
- SA is the amount left to enable complete combustion by using the calculated A: F and is pre-heated to about 316^{o}C for enhanced combustion.
- Low NOx PC burners often yield lower combustion efficiencies.

2.6.4 COAL COMBUSTION MODELLING

- CFD is the most frequently used combustion modelling tool.
- CFD uses the finite volume method and is used by commercial codes such as FLUENT.
- Computation time can be reduced by using cold flow models to model the aerodynamic flow field and coupling it with burner fundamentals.
- The RANS turbulence model is computationally the least expensive and is mostly used in combustion modelling.
- Under the RANS turbulence model, the k-epsilon and RSM methods are most common.
- Mesh-dependent studies are done to see if a mesh is fine enough.
- An unstructured mesh is used for complex geometries.
- Hexahedral and polyhedral cells are appropriate to use when modelling burners and turbulence.

3 CONCEPT DESIGN FOR THE NET CALORIFIC VALUE AT CONSTANT PRESSURE COAL ANALYSER

The following section explains the process followed and concepts used to develop the concept design for the NCVp coal analyser. Principles obtained in the literature review were used to establish the concept design, converting it to establish an NCVp for coal, then establishing the components needed to realise the NCVP analyser.

3.1 CONCEPT OF THE NET CALORIFIC VALUE AT CONSTANT PRESSURE COAL ANALYSER

Since the literature review states that the direct method to determine the NCVp of a fuel is using a flow calorimeter, the NCVp coal analyser was based on the principle of a flow calorimeter. As discussed earlier in Section 2.4, the basic components of a flow calorimeter are a burner, a fluid-cooled combustion chamber and measuring apparatus. When the fuel combusts inside the combustion chamber, some of the combustion heat is lost owing to the cooling of the combustion chamber walls, while the rest exits to the atmosphere in the form of flue gas. In order to determine the amount of heat the fuel releases during combustion, the heat lost through the combustion chamber walls and the heat that exits to the atmosphere need to be measured. The heat is calculated by using a mass-energy balance of the measured temperature and mass flow of:

- the fuel and air entering the burner;
- the fluid used to cool the combustion chamber;
- the flue gas exiting to the combustion chamber.

The principle of the mass-energy balance used to determine the NCVp of coal is explained by the following figure and equations (9) – (11) thereafter:

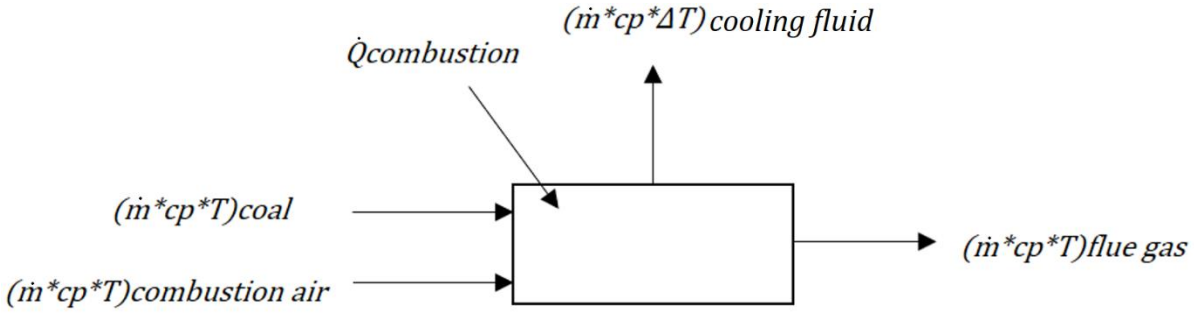

FIGURE 3.1: ILLUSTRATION OF THE MASS-ENERGY BALANCE PRINCIPLE USED IN THE NCV_P COAL ANALYSER

$$\dot{Q}_{in} = \dot{Q}_{out} \tag{9}$$

$$(\dot{m} * cp * T)_{coal} + (\dot{m} * cp * T)_{combustion\ air} + \dot{Q}_{combustion} = (\dot{m} * cp * \Delta T)_{cooling\ fluid} + (\dot{m} * cp * T)_{flue\ gas} \tag{10}$$

$$NCVp = \frac{\dot{Q}_{combustion}}{\dot{m}_{coal}} \tag{11}$$

where:

- $\dot{Q}$ is the heat rate [kW]
- $\dot{m}$ is mass flow [kg/s]
- T is temperature [K]
- cp is the specific heat capacity at constant pressure [kJ/kg-K]
- $NCVp$ is the heat content in the coal

According to the law of heat conservation, the heat entering the burner must be equal to the heat exiting the combustion chamber. The heat entering consists of coal, combustion air and combustion. The heat exiting consists of flue gas and the heat absorbed by the cooling fluid. The equation is used to determine $\dot{Q}_{combustion}$ and $\dot{m}_{coal}$ is then used to determine the NCVp.

The concept design of the NCVp coal analyser can be examined in Figure 3.2:

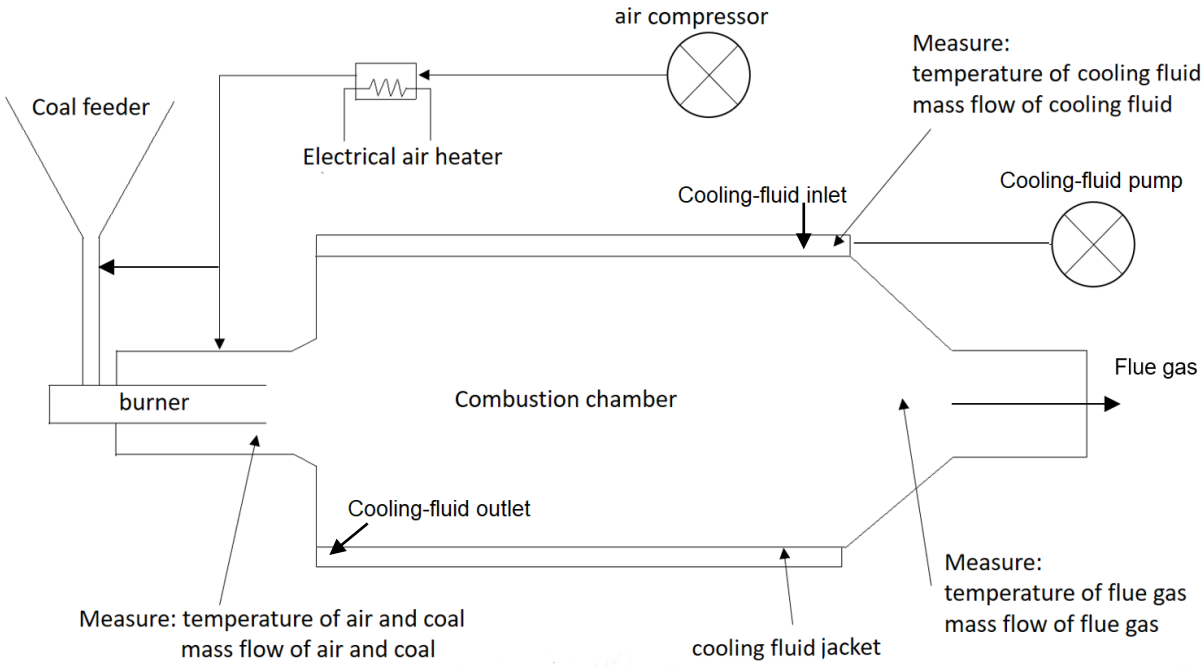

FIGURE 3.2: ILLUSTRATION OF THE COMPONENT CONFIGURATION USED IN THE NCV_P COAL ANALYSER

The essence of the NCVp coal analyser consists of the PC burner, which is used to combust PC by using combustion air, and a fluid-cooled combustion chamber in which combustion can take place. However, for the NCVp coal analyser to be functional, the following auxiliaries are required: a compressor that supplies combustion air, electrical air heaters that pre-heat the combustion air, a PC feeder to supply PC at various mass flows, a cooling-fluid pump for the combustion chamber cooling, and measuring apparatus. Each of these components will be discussed below.

3.2 CONCEPT DESIGN FOR THE PULVERISED COAL BURNER

The PC burner is the most crucial part of the NCVp coal analyser, since it is required to achieve maximum combustion efficiency of PC.

3.2.1 BURNER THERMAL SIZING

The thermal sizing of the PC burner is determined by the CV of the PC, as well as the mass flow of the PC, and is shown in the following equation:

$$\dot{Q}_{thermal} = CV_{coal} * \dot{m}_{coal} \quad (12)$$

The design of the NCVp coal analyser, has to accommodate a range of coal qualities regarding CV. A general guideline for an envelope of coal CVs used internationally in power stations, range between 13 – 26 MJ/kg (Storm, 1998). However, the design of this NCVp coal analyser should be able to cater for coals outside this envelope as well, within reasonable limits. A nominal CV rating was also needed for the PC burner design. A nominal CV of 21 MJ/kg was selected, since the majority of power stations in South Africa are fuelled with coal within the region of this CV. Therefore, calculations were made for thermal rating, A: Fs and PC and combustion air mass flows, utilising the minimum, nominal and maximum values. Coal analyses of actual coals, as close as possible to these minimum, nominal and maximum CVs, were used for the design calculations.

For laboratory-scale testing, a PC feeder (which is discussed in Section 3.5) was chosen to deliver a PC feed rate of 1.5 g/s – 6.2 g/s. In the design philosophy shown in Section 4.1.2, it was decided to maintain a constant mass flow of combustion air for a certain thermal load and rather to vary the PC mass flow instead (for different coal CVs, requiring different A: Fs). This is simply due to the fact that the PC feed rate can be varied and not the diameter of PC burner tubes, which influences velocities, swirl and turbulence.

The minimum thermal load of the burner was calculated by using equation (12). Therefore, the coal with the highest CV (26 MJ/kg) determined the minimum thermal amount and was calculated to be 40 kW at 1.5 g/s. Although this is the minimum thermal rating of the burner, the design point will be at a maximum of approximately 80 kW, since the PC burner needs to be adaptable, because of the unknown optimum velocity and turbulence required for optimal coal combustion. Since no PC burners of this small thermal magnitude are available, the PC burner needs to be designed and manufactured. A self-sustained PC flame (without any gas support) is required when calculating the NCVp of coal, since the NCVp of gas does not need to be taken into consideration.

3.2.2 FLOW CHARACTERISTICS FOR COMBUSTION

In designing the PC burner, principles established in the literature review that affect coal combustion were applied. The aerodynamic flow field that the burner produces plays a key part in the flame shape and intensity. A unique aerodynamic flow field exists for the optimum combustion of each coal type (Wróblewska *et al*., 1977). Therefore, the burner needs to be adaptable not only in terms of thermal load. It also needs to be able to produce different flow fields which are unknown beforehand. As shown in the literature review, swirl burners will be used rather than direct burners, since swirl burners have more flame stability when operated on their own. In this regard, combustion efficiency is very important and low-NOx burners will be avoided, as they tend to decrease efficiency.

It is desired that the PC burner achieves the following for the purpose of NVCp determination:

- High intensity flame for good burnout and flame stability;
- High residence time to allow complete particle burnout;

- Constant ignition zone close to PC burner mouth;
- High combustion efficiency.

To achieve the above-mentioned points, the PC burner's aerodynamic flow field needs to be designed using the effects of swirl angle, entrainment, turbulence and a quarl. These effects will create an internal recirculation zone and enhance the mixing of fuel and air.

3.2.3 BURNER LAYOUT

The PC burner needs to consist of concentric tubes, namely a gas tube, core air (CA) tube, PC/PA tube and SA tube, to produce a turbulent diffusion flame. The gas lance is to convey liquid petroleum gas (LPG) to the burner mouth. The LPG is used to ignite the PC and to pre-heat the combustion chamber to a pre-determined minimum temperature to promote spontaneous ignition of coal. The CA supplies the required combustion air for the LPG. The PC/PA tube will convey the PC to the burner mouth by using PA. After the LPG is turned off, the CA is to be used for the cooling of tubes and combustion purposes. The SA supplies the remainder of the combustion air for optimal combustion of coal.

Figure 3.3 shows the concept of the PC burner based on the desired points mentioned above.

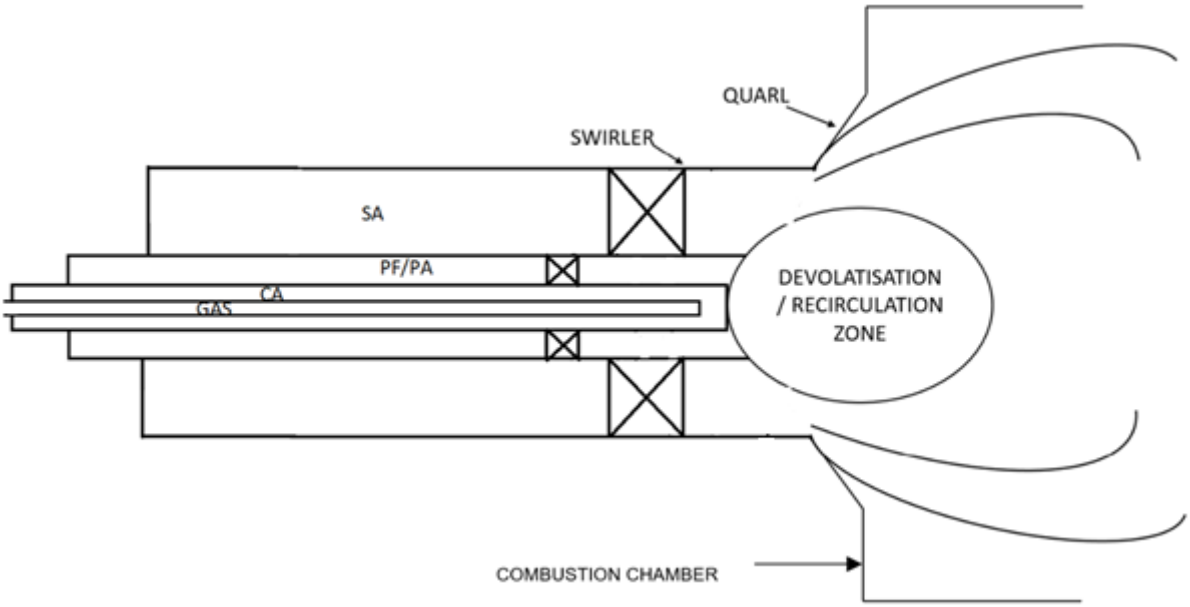

FIGURE 3.3: CONCEPT OF PC BURNER INVOLVING PHYSICAL LAYOUT AND AERODYNAMICS

3.2.4 CFD MODELLING

CFD needs to be used as a designing tool to design the aerodynamic flow field by using the software of ANSYS FLUENT. Actual combustion simulation per se was not used since it is time-consuming and arduous. Therefore, cold flow models were used in conjunction with burner principles such as swirl and recirculation to predict coal flame structure and shape.

3.2.5 CRITERIA FOR COMBUSTION AIRFLOW DETERMINATION

By using the results of an ultimate analysis of the specific coal to be tested, chemical reaction equations were used to determine an appropriate hyper-stoichiometric A: F for coal. The known chemical composition of LPG was used to calculate an A: F thereof. The A: F inside the PC/PA tube is required to be low enough to prevent combustion and explosions inside the PC bunker. The velocity of PA must be a minimum of 20 m/s to avoid PC settling, while the velocity of CA and SA was chosen to be high enough to create sufficient turbulence. The temperatures of CA, PA and SA were chosen to be 150^{o}C, 150^{o}C and 280^{o}C respectively. These temperatures are chosen to allow drying of PC and not to exceed the operating temperature of the swirler materials. The operating temperature of the swirlers will be discussed in further detail in Section 4.3.2.

3.3 CONCEPT DESIGN OF COMBUSTION CHAMBER

The combustion chamber needs to provide an environment in which combustion can take place and needs to be used to measure the heat loss of the flame via the cooling-fluid jacket through the walls. However, if the amount of heat loss through the walls can be minimised, the environment inside the combustion chamber increases and promotes combustion. After combustion has taken place, the flue gas needs to be allowed to exit to the atmosphere through a chimney. When exiting the combustion chamber, the flue gas temperature needs to be maintained above the dew point temperature of water vapour at the measuring point. Because of the specific requirements the combustion chamber was custom-built.

Since the combustion chamber will experience temperatures of up to 1600 ^{o}C, insulation materials are necessary. The volume of the combustion chamber must be sufficient to allow for proper PC residence time for proper burnout of PC particles.

3.4 AUXILIARIES OF NET CALORIFIC VALUE COAL ANALYSER

The auxiliaries described below were used to enable the NCVp coal analyser to be functional.

3.4.1 PC FEEDER

For combustion and conveying purposes to the burner via combustion air, coal needs to be pulverised and comply with the Rosin-Rammler standard. Since a pulveriser and its integrated controls over-complicate the NCVp coal analyser, it was decided that PC was to be tested. The PC feeder regulates the combustion rate of the burner by controlling the feed rate of PC. The PC feeder to be used was developed in an earlier project. The PC feeder was developed to produce a variable feed rate of 1.5 g/s – 6.2 g/s as required by the PC burner.

3.4.2 COMPRESSOR AND COOLING FLUID PUMP

The compressor is used to supply combustion air to the PC burner. The compressor must be capable of producing an adequate mass flow of air at sufficient pressure to overcome pressure losses downstream. The cooling fluid pump must provide sufficient cooling fluid through the cooling fluid jacket and must overcome pressure losses in order to cool down isolation material.

3.4.3 AIR PRE-HEATERS

It was decided that the air pre-heaters were to be electrical because of the reaction time of pre-heating and accurate temperature control. Four electrical air pre-heaters are necessary to provide heat to the air flow streams of CA, PA and SA to reach temperatures of 150^{o}C, 150^{o}C and 280^{o}C respectively. The SA will move through two heaters, namely the SA and TA heater.

3.4.4 MEASURING APPARATUS

According to equations (9) – (11), shown in Section 3.1, the NCVp of coal is calculated by measuring the mass flow and temperature of combustion air, PC, flue gas and cooling fluid.

4 DETAIL DESIGN

The following section explains the detail design of the PC burner and combustion chamber.

Firstly, the material selection for the PC burner was determined by taking into account the temperature and mediums flowing through the burner. Then, calculations based on chemical equations were made to determine the A: F and mass flow of combustion air to ensure proper combustion of PC. The mass flow of combustion air was required in order to size the tubes of the PC burner according to appropriate velocities. After the mass flow of combustion air and sizing of the PC burner had been completed, cold flow modelling was done by using CFD to determine the swirler limits, which produced the desirable flow field patterns from the PC burner into the combustion chamber. The flow modelling was also used to determine the inner dimensions of the combustion chamber to allow for proper residence time (obtained from drop tube furnace data) of the PC particles before exiting the combustion chamber.

Once the inner dimensions of the combustion chamber were known, materials such as the insulation of which the combustion chamber consists were selected. Heat transfer calculations were then completed to determine the thickness of the insulation material.

The PC burner and combustion chamber assembly is shown in Figure 4.1.

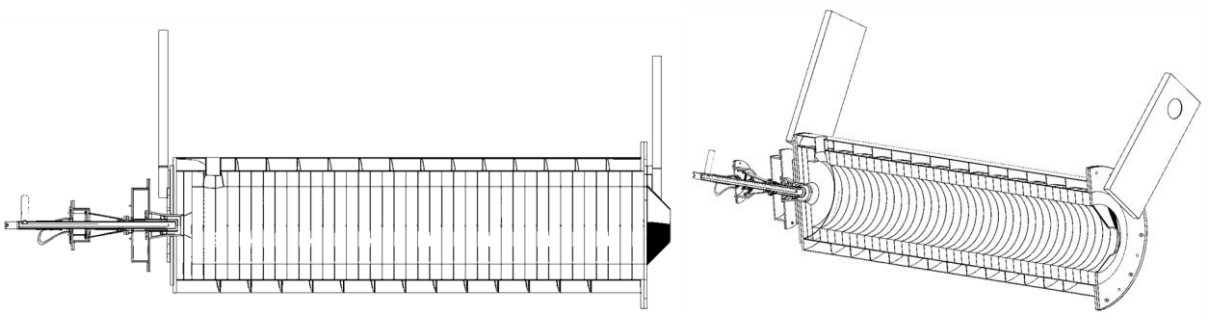

FIGURE 4.1: SECTION VIEWS OF PC BURNER AND COMBUSTION CHAMBER ASSEMBLY MODEL

The detail design of the PC burner and combustion chamber will be discussed in Section 4.1.

4.1 PULVERISED COAL BURNER DESIGN

Figure 4.2 shows the final result of the PC burner as a section view assembly model. The burner is discussed in further detail in Section 4.1.4, “Final design of the PC burner”.

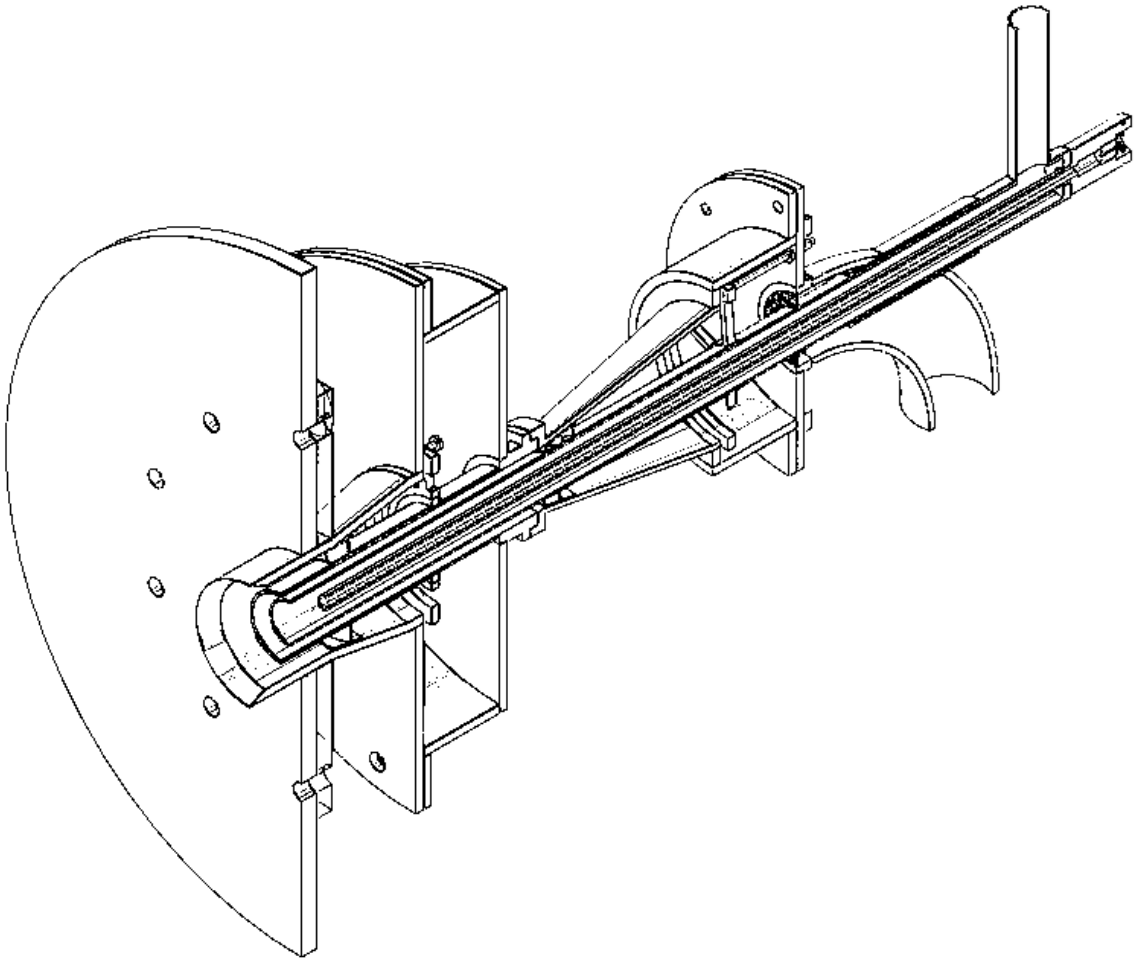

FIGURE 4.2: SECTION VIEW SHOWING GEOMETRY OF THE VISUAL LAYOUT OF THE PC BURNER

The following sections explain the methodology used to obtain this result.

4.1.1 MATERIAL SELECTION FOR THE PULVERISED COAL BURNER COMPONENTS

The materials used to manufacture the PC burner play an important role. Certain properties to which the PC burner was exposed, were considered. These properties include high temperatures due to combustion, erosion due to the abrasiveness of PC, complex geometries of swirlers and cost.

The burner tubes need to withstand very high temperatures. The combustion temperature of high-quality coal is catered to for a value of up to 1600^{o}C. However, the temperature at the burner mouth due to radiation will be reduced significantly by the combustion air flow through the PC burner. It was therefore decided that stainless steel Type 304 would be used for the manufacturing of the tubes, since it has an operating temperature of 1100^{o}C. Stainless steel Type 304 was expected to withstand the abrasiveness of PC and resist corrosion; moreover, manufacturing is relatively cheap and easy.

It was decided to use 3-D printing to manufacture the SA swirler out of high-temperature resin, since the costs are very low compared to other manufacturing possibilities. This was possible since the SA swirler is only exposed to pre-heated combustion air. However, since high temperature resin can only withstand a maximum temperature of 298^{o}C, it was decided that the maximum temperature of the SA would be 280^{o}C.

The PA swirler was machined out of Type 304 stainless steel since it experiences abrasiveness from the PC and is exposed to a temperature of 150^{o}C.

4.1.2 AIR-TO-FUEL RATIO CALCULATIONS

This section focusses on determining the mass flow of combustion air for PC and LPG. By balancing the chemical equations of combustible elements contained in coal and LPG, an A: F for coal and LPG was determined. The mass flow of combustion air was determined for three coal qualities, as explained in Section 3.2.1. The appropriate A: F was then used to determine the amount of combustion air needed for LPG and PC respectively, which was then divided into the required quantities of the CA, PA and SA tubes.

The three coal qualities selected in Section 3.2.1 were used to obtain the air flow limits of the burner (according to their A: Fs) for the selected thermal loading of 40 – 80 kW.

For a pre-selected thermal loading (40 – 80kW) the design is such that the mass flow of air is kept constant and the mass flow of PC is varied to suit the pre-determined A: F. If a lower CV coal is used, the mass flow of coal needs to be higher compared to a higher CV coal. The ultimate analyses of the actual coal qualities obtained (low, intermediate and high CV) were used to determine the above-mentioned A: Fs.

As mentioned in Section 2.3.1, stoichiometric, sub-stoichiometric and hyper-stoichiometric A: Fs exist for a fuel. By supplying a stoichiometric A: F, the theoretical amount of air is provided for coal combustion, as determined by the chemical equations. The stoichiometric A: F assumes that after ideal combustion takes place, all of the combustible elements are fully oxidised and no residual O_2 remains in the combustion products (flue gas). Although this A: F suggests ideal combustion, complete combustion will not occur.

A sub-stoichiometric air quantity proposes that less than stoichiometric air is supplied for combustion. Incomplete combustion will occur and will produce unburned elements such as: C, CO and unburned volatiles. However, no residual O_2 remains after combustion.

A hyper-stoichiometric air quantity proposes that more than stoichiometric air is supplied for combustion. In practice this will result in more complete combustion, which will render less unburned elements. This will subsequently result in residual O_2 in the flue gas.

Since the NCVp coal analyser requires complete combustion, sub-stoichiometric A: Fs were avoided, as this scenario will most probably lead to loss of ignition and combustion. Therefore only hyper-stoichiometric combustion calculations were used. According to Storm (1998), the exact amount of excess air (percentage O_2 in flue gas) to be supplied cannot be explicitly calculated and must be determined experimentally. That optimum quantity also differs for various coal qualities. For complete combustion of most coal qualities, a general guideline for the amount of excess air in this design was calculated to render a 3.5% O_2 in flue gas (Kitto & Stultz, 2005).

A coal analysis can be represented in different modes. Firstly, there is the elemental or proximate analysis of a coal quality as explained in Section 2.1. Then, both these analyses can be expressed in terms of dry basis (no moisture content at all), air-dried basis (inherent moisture content only) and an as received basis (inherent as well as surface moisture incorporated).

It should be noted that the same applies to CV regarding the influence of moisture content. For the initial determination of A: Fs in the design phase, the GCVv was used as heating value, since the NCVp was not yet known at that stage.

Ideal stoichiometric air-to-fuel ratio

Firstly, ideal air-to-fuel ratio calculations were used to determine a stoichiometric A: F for coal on an as received basis. The procedure described below is applied to the three coal qualities; however, the actual intermediate coal quality previously selected was used as an example. Table 4.1 contains these properties:

TABLE 4.1: ULTIMATE ANALYSIS FOR INTERMEDIATE COAL

COAL QUALITY					
GRAVIMETRIC %	**SYMBOL**	**UNITS**	**AS RECEIVED**	**AIR DRIED**	**DRY BASIS**
ULTIMATE ANALYSIS					
Nitrogen	N	%	1.151	1.180	1.227
Oxygen (by difference)	O	%	7.166	7.350	7.640
Carbon TOTAL	C_{TOTAL}	%	53.021	54.380	56.525
Ash	A	%	28.465	29.195	30.347
Sulphur	S	%	0.878	0.900	0.936
Hydrogen	H	%	3.120	3.200	3.326
Surface Moisture	M_S	%	2.500	0.000	0.000
Inherent Moisture	M_i	%	3.700	3.795	0.000
Total moisture	M_T	%	6.200	3.795	0.000
Total		%	100.000	100.000	100.000
Gross calorific value	GCV_v	[MJ/kg]	20.524	21.050	21.880

The balanced chemical equations of the combustible elements for ideal combustion are as follows:

$$C + O_2 = CO_2 \quad (13)$$

$$S + O_2 = SO_2 \quad (14)$$

$$2H_2 + O_2 = 2H_2O \quad (15)$$

An atomic mass is assigned to each of the elements in the chemical equations. By dividing each element of the equation by the atomic mass of the combustible element, the volumetric or mole amount is acquired. This results in the theoretical mole amount of O_2 needed for one of the combustible elements to combust. The ultimate analysis presents the percentage gravimetric mass of each element contained in the intermediate coal. By using these values and multiplying them with the mole amounts of the elements, the gravimetric mass of O_2 needed for combustion of each combustible element is determined on a stoichiometric basis. This procedure is shown below in Table 4.2.

TABLE 4.2: STOICHIOMETRIC COMBUSTION EQUATIONS FOR INTERMEDIATE COAL

(mole)	C	+	O_2	=	CO_2
Atomic mass (g/mole)	12.011		31.999		44.010
(g)	1.000		2.664		3.664
Mass percentage from ultimate analysis (g)	53.021		141.253		194.274
(mole)	S	+	O_2	=	SO_2
Atomic mass (g/mole)	32.060		31.999		64.059
(g)	1.000		0.998		1.998
Mass percentage from ultimate analysis (g)	0.878		0.876		1.753
(mole)	$2H_2$	+	O_2	=	$2H_2O$
Atomic mass (g/mole)	4.032		31.999		36.030
(g)	1.000		7.937		8.937
Mass percentage from ultimate analysis (g)	3.120		24.763		27.883

By adding the amounts of gravimetric O_2 of each equation, the total stoichiometric amount of O_2 needed for combustion of the intermediate coal is determined. However, the elemental analysis indicates that the coal also contains some O_2 and this must therefore be subtracted from the total O_2 needed for combustion, thus:

$$141.253 + 0.876 + 24.763 – 7.166 = 159.726 \text{ g } O_2 / 100 \text{ g coal}$$

Since the PC will be combusted by using air, the amount of air is calculated by dividing the total O_2 by the gravimetric amount of O_2 contained in air (23.194%). The total amounts to 688.647 g air/100 g coal and thus, an ideal stoichiometric A: F for the intermediate coal is 6.886:1.

The following equation is used to determine the mass flow of coal needed to produce an 80 kW flame:

$$\dot{Q}_{thermal} = GCV_{coal} * \dot{m}_{coal} \quad (16)$$

The mass flow of intermediate coal is therefore 3.898 g/s. The total air required for stoichiometric combustion of intermediate coal is thus 26.840 g/s.

Practical hyper-stoichiometric air-to-fuel ratio

During the actual combustion process, incomplete combustion occurs to a certain degree. Incomplete combustion takes place when some of the combustible elements do not have sufficient time or O_2 locally to combust. In addition, a minimal amount of the O_2 is occasionally absorbed by non-combustible elements such as N_2 to form NOx. The non-combustible elements do not produce, but absorb heat.

The same procedure to determine the ideal stoichiometric A: F is used to determine the practical hyper stoichiometric A: F, except for a smaller percentage of C that does not combust, measured as unburned C in ash. Thereafter, the remaining C combusts in two stages. The first reaction of C with O_2 is to form CO and then the major portion, but not all the CO reacts further with O_2 to form CO_2. The non-participating CO is measured as a small percentage in the flue gas.

For the calculations made, the following realistic values of PC burners are assumed:

- The largest portion of NOx formation is N_2O/ NO and has a quantity of up to 1000 ppm contained in the flue gas.
- The value of unburnt C in ash ranges between 0.5 - 2%.
- The quantity of CO in flue gas ranges from 100 - 1000 ppm.

Similar to the methodology used for the ideal stoichiometric A: F calculation above, the amount of excess air to produce 3.5 % O_2 in the flue gas, as well amounted to 30.0 g/s air flow. In addition, this calculation was tailored to accommodate the corrections for unburned C, CO etc. This is equivalent to 13.312 % excess air, an A: F of 7.796:1 and 3.898 g/s intermediate coal flow for 80 kW.

The same procedure was followed to determine the A: Fs of the high and low CV coal qualities. Appendix A shows the coal analyses of the intermediate, high and low grade coal qualities. Appendix B shows the chemical equations used to determine the hyper-stoichiometric A: Fs of the different coal qualities. Appendix C shows the flue gas calculations of both wet and dry flue gas for the different coal qualities. In conclusion, the applicable values for these three coal qualities are shown in Table 4.3.

TABLE 4.3: AIRFLOW, COAL FLOW AND AIR-TO-FUEL RATIOS FOR THE COAL QUALITIES

	Minimum	Intermediate	Maximum
A: F	5.644	7.796	8.949
$\dot{m}_{COAL}$ [g/s]	5.315	3.90	3.352
$\dot{m}_{AIR}$ [g/s]	30.0	30.0	30.0

Sub division of combustion air between the PC burner tubes

Since the total combustion air was determined in the previous section, the total amount of air will be divided into the CA, PA and SA tubes.

To prevent possible combustion upstream of the PC/PA tube to the bunker, the maximum A: F allowed inside the PC/PA tube should be safely below the ideal stoichiometric A: F calculated. Previously in Section 4.1.2., the ideal stoichiometric A: F for intermediate coal was calculated to be 6.886:1 and therefore, the A: F inside the PC/ PA is 1.7:1. By applying this procedure to the selected three coal qualities, it is calculated that the PA amount inside the PC/ PA tube is 6.5 g/s.

After the LPG has been turned off, and a self-sustaining PC flame has been established, the CA will be used to cool tubes and to form part of the PA and SA to provide combustion air for the PC. The amount of CA was chosen to be 3.355 g/s which will be discussed in further detail in the section below.

Since a total of 30.0 g/s combustion air is required, the SA will provide the additional 20.1 g/s.

Air-to-fuel ratio of the LPG gas igniter

In order for the LPG flame to pre-heat the combustion chamber before PC combustion can occur, the thermal amount of the gas flame needs to be determined. The generally considered spontaneous ignition temperature of coal is regarded as 400^{o}C. However, this temperature can vary for different coals and therefore it was decided that the combustion chamber temperature had to reach a minimum of 500^{o}C to ensure spontaneous combustion. When the chamber has reached 500^{o}C, the PC and combustion air will enter the combustion chamber. This will cool down the combustion chamber since it enters at a lower temperature. It was therefore decided to calculate the thermal amount of LPG to ensure that the mixture of the PC and combustion air will not be lower than 500^{o}C.

Using the mass flow and temperature of CA, PA and SA entering the combustion chamber, the heat rate required by the LPG flame was calculated to be 10.9 kW. The NCVp of LPG is known as 46.6 MJ/kg (Chemical engineering, Queens University, 2014), and therefore, a mass flow of 0.237 g/s of LPG is required to produce the required amount of heat.

The next step is to determine the A: F of LPG. Since propane is the prominent composite of the LPG, the known chemical composition can be presented as C_3H_8. The balanced chemical equation is thus:

$$C_3H_8 + 5O_2 = 3CO_2 + 4H_2O \qquad (17)$$

Similar to the process followed to determine the amount of O_2 needed for coal combustion, the O_2 required for LPG combustion is 3.63 gram per gram of LPG, which equates to 15.643 g/s for the amount of air and an A: F of 15.643:1. For a mass flow of 0.237 g/s LPG, the corresponding amount of CA required is 3.335 g/s.

4.1.3 PULVERISED COAL BURNER TUBE SIZING

Since the mass flow and temperature inside the PC burner tubes are known, the tube diameters were determined by using suitable velocities. For confidentiality purposes, the velocities and tube diameters cannot be shown in this thesis.

4.1.4 COLD FLOW MODELLING OF COMBUSTION FLOW FIELD

Since the tube diameters, temperatures and mass flows of LPG, CA, PA, PC and SA for the PC burner were established in Section 4.1.1 and 4.1.2., the desired aerodynamic flow field that was appropriate for PC combustion according to the literature review, was established. As stated previously, cold flow

modelling was employed by making use of CFD in ANSYS FLUENT to determine an internal recirculation zone, using swirl at appropriate velocities.

Swirl limit determination

To design an appropriate aerodynamic flow field for combustion, swirl was the main parameter focussed on. The most crucial part for flame stability is creating a constant ignition zone at the burner mouth in the form of an internal recirculation zone of the air. Therefore, the most important pattern of the flow field, was at the burner mouth.

According to El-Mahallaway and Habik (2002), cold flow modelling adequately represents the flow field in terms of profile, swirl and recirculation when compared to an actual combustion process. According to the literature, a relatively short and intense flame requires high levels of swirl and recirculation. When the flow exits the burner mouth, the centrifugal force of swirl causes the flow to diverge. If the low-pressure zone in the centre of the flow field, created by the swirl, is stronger than the corresponding centrifugal force, the flow is sucked in by the low-pressure zone to converge and recirculate. The diverging-converging flow field after the burner mouth is therefore an important indication of a low-pressure zone being present. If the amount of swirl is too severe, it can cause the centrifugal force of the air flow to be stronger than the low-pressure zone, causing the air flow to only diverge. This will not create a recirculation zone and will dilute the concentration of air and fuel mixture owing to the large volume the mixture occupies. In summary, the desired flow field for a short and intense flame will be created by a diverging-converging, high-swirl, internal recirculating flow pattern. Figures 4.3 and 4.4 show streamlines forming flow patterns of a low amount of swirl and an excess amount of swirl respectively:

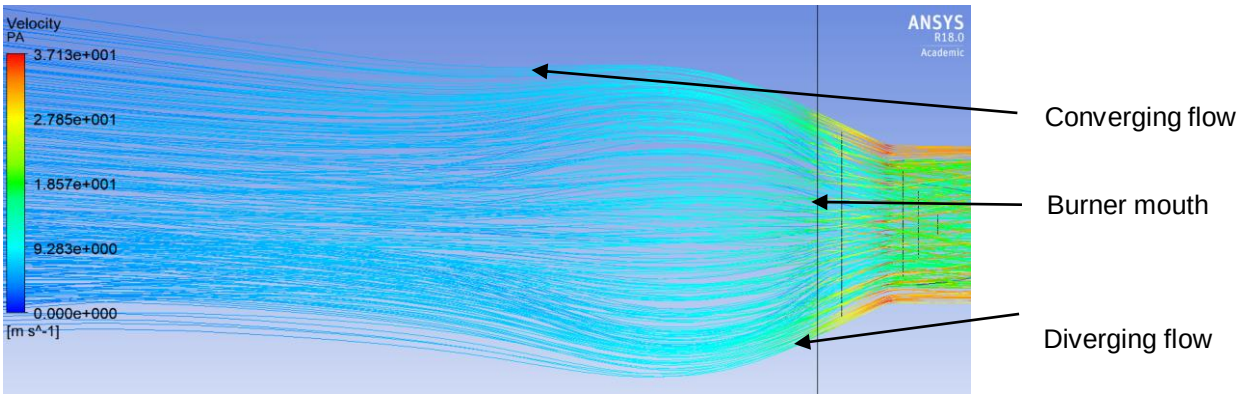

FIGURE 4.3: STREAMLINES REPRESENTING THE FLOW FIELD OF AIR EXITING THE PC BURNER WITH LOW SWIRL

When a low amount of swirl is applied, as can be seen in Figure 4.3, the flow diverges and then converges. This type of flow field ensures that the concentration of PC and air will be high. However, no recirculation is created owing to the low amount of swirl.

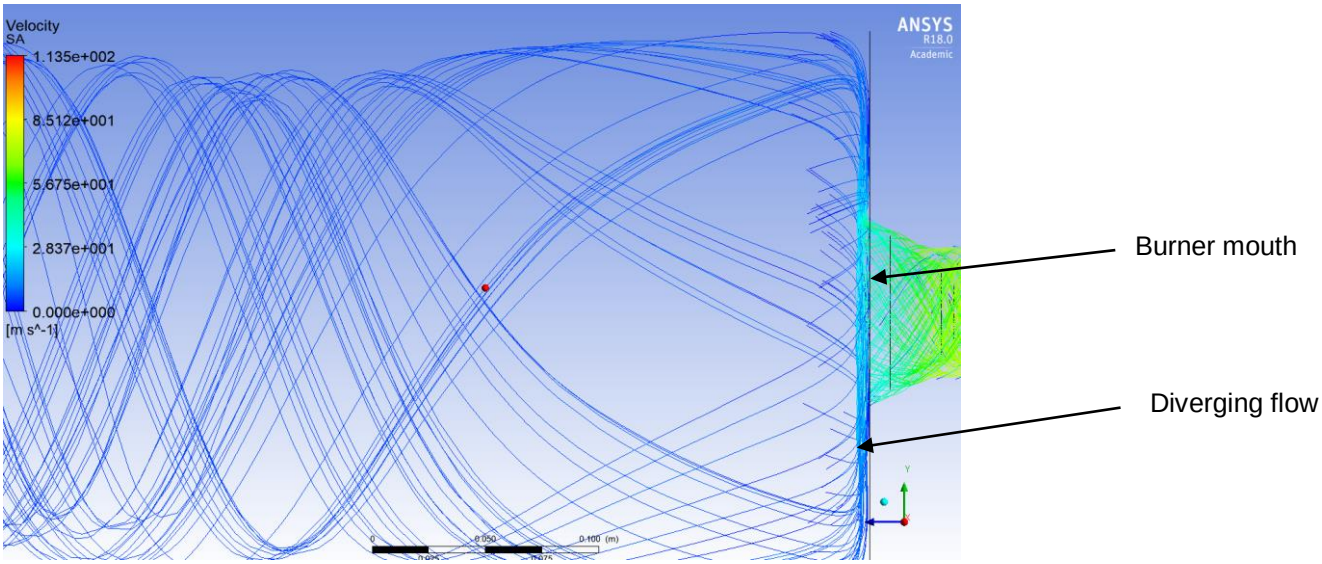

FIGURE 4.4: STREAMLINES REPRESENTING THE FLOW FIELD OF AIR EXITING THE PC BURNER WITH EXCESSIVE SWIRL

When an excessive amount of swirl is provided, the flow will only diverge and not converge owing to an excessive amount of centrifugal force, as seen in Figure 4.4. This will allow the concentration of PC and air to be low because of the larger volume it occupies, and will lead to poor combustion despite the fact that a high amount of swirl is present.

The desired amount of swirl required for an effective flow profile must be high enough to create an internal recirculation zone, but not too high to cause diverging flow.

The amount of swirl and recirculation for optimum coal combustion cannot be explicitly pre-determined, and therefore the aim in this section will be to determine the maximum limits of swirl while still being able to create a converging-diverging, high-swirl and internal recirculation pattern (Wróblewska *et al.*, 1977). For different coal qualities, the desired flow patterns do not require the same amount of swirl.

CFD modelling methodology

The aerodynamic flow field produced in the combustion chamber, is governed by the geometry of the PC burner. To design the PC burner, a series of different geometries were experimented with in order to create the flow field described in the previous section. For each geometry, a CFD model was completed and evaluated. This iteration process was followed until the geometry for maximum swirl was determined.

Since the creation of different geometries was time consuming, certain CFD parameters needed to be considered to reduce the computation time of CFD modelling in the iteration phase. The CFD parameters that influenced the computation time were mesh fineness, mesh type, cell type and turbulence models.

- **Turbulence models**

The parameter that influences the computation time and accuracy of the results most is the CFD turbulence model used. According to the literature review, although many turbulence models exist, the most appropriate model used for turbulence modelling is the so-called RANS model. RANS models make use of basically two methods, namely the k-ε and RSM model. According to literature, the k-ε method is less time-consuming but also less accurate compared to the RSM method. It was therefore decided that the k-ε method would be used in the iteration phase of modelling because of its lower computation time. However, the final geometry was modelled by comparing both the k-ε and RSM methods to evaluate the flow field more accurately.

- **Mesh fineness and structure**

Another parameter that influences time and accuracy greatly is the mesh. In theory, a finer mesh will always yield more accurate results opposed to a courser mesh; however, using it is more time-consuming owing to lengthier computational time. A structured or unstructured mesh also influences the results of the CFD cell type used. Since the PC burner consists of complicated geometries, it is necessary to make use of an unstructured mesh.

According to the literature review, hexahedral and polyhedral cell types are more appropriate to use for turbulence modelling. It is suggested that the results delivered by using polyhedral cells are similar to those of hexahedral cells (Ranade & Gupta, 2015). However, the number of cells for a polyhedral mesh is much lower when compared to a hexahedral mesh, which will decrease solving time.

Since it was unclear how many cells to use for this CFD application, it was decided that two comparative trial runs of CFD modelling would be done to determine what type and number of cells to use prior to the iteration phase. The two trial runs were: polyhedral vs hexahedral mesh, and fine vs course mesh. The two trial runs compared the similarity of the flow fields, number of cells used and computation time.

Hexahedral cell vs polyhedral cell mesh

Since the polyhedral mesh contains fewer cells compared to a hexahedral mesh, it can be very useful to reduce computation time. However, to establish the accuracy of a polyhedral mesh, two trial burner models were compared to each other. One of the models makes use of a hexahedral mesh and the other of a polyhedral mesh. The flow domain of the trial burner and combustion chamber is shown below:

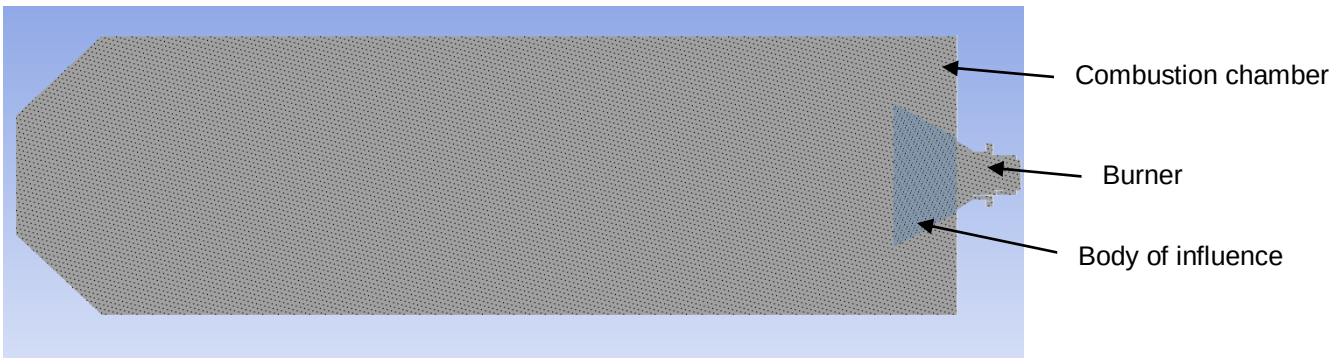

FIGURE 4.5: FLOW DOMAIN OF TRIAL BURNER AND COMBUSTION CHAMBER

Figure 4.5 shows the flow domain that was used for both meshes. A body of influence is used to make the mesh finer (which produces more accurate results) at the burner mouth, which is the critical part for ignition.

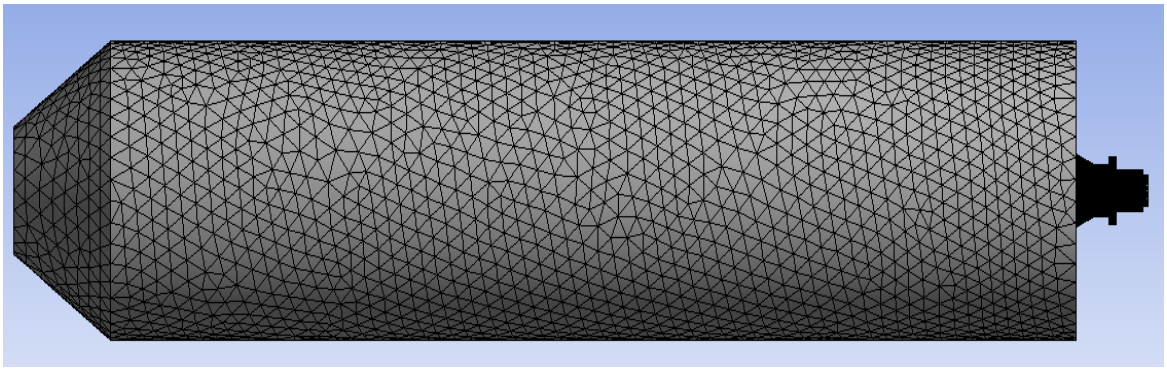

FIGURE 4.6: HEXAHEDRAL MESH OF FLOW DOMAIN

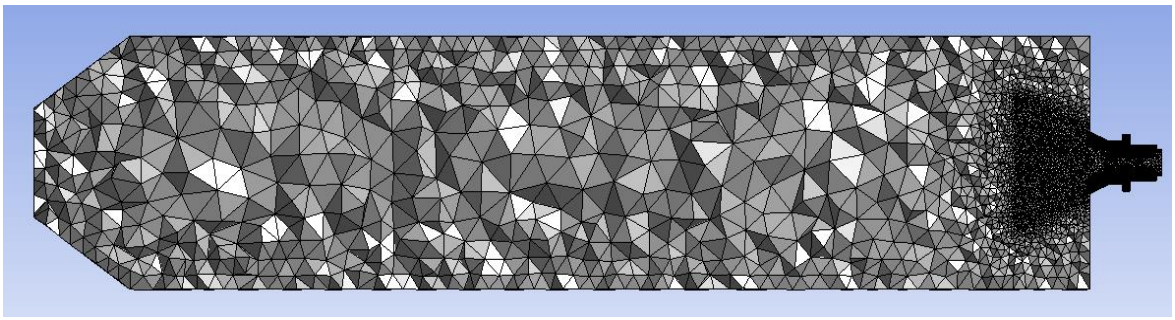

FIGURE 4.7: SECTION VIEW OF HEXAHEDRAL MESH OF FLOW DOMAIN

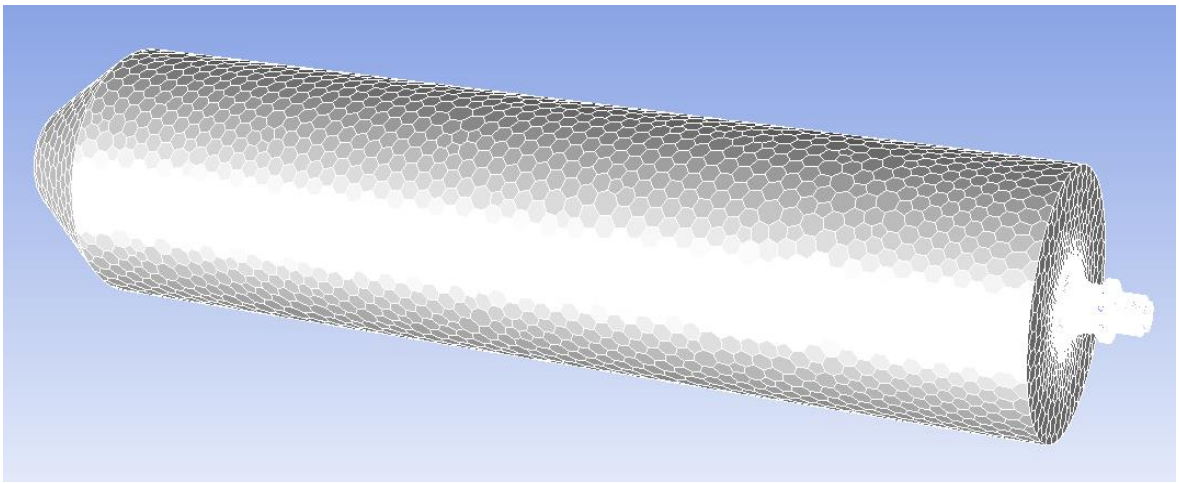

FIGURE 4.8: POLYHEDRAL MESH OF FLOW DOMAIN

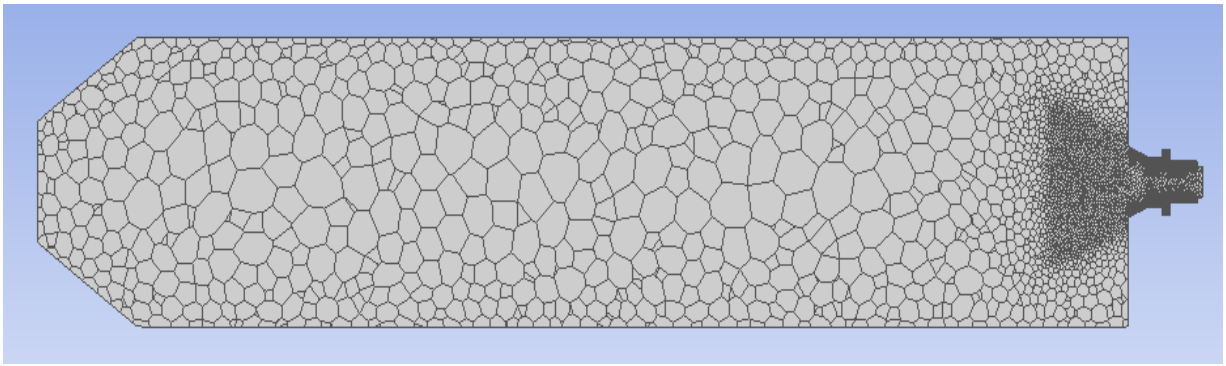

FIGURE 4.9: SECTION VIEW OF POLYHEDRAL MESH OF FLOW DOMAIN

Figures 4.6 and 4.7 show the hexahedral mesh, while Figures 4.8 and 4.9 show the polyhedral mesh of the same flow domain. It can be seen in Figures 4.7 and 4.9 that both of the meshes are finer at the burner mouth owing to the body of influence. The number of cells of the hexahedral mesh is 2 800 135, and for the polyhedral mesh 636 526, which is significantly lower. The solving time for the hexahedral mesh model took 3.5 times longer than for the polyhedral mesh model.

The flow fields produced by each mesh are compared below:

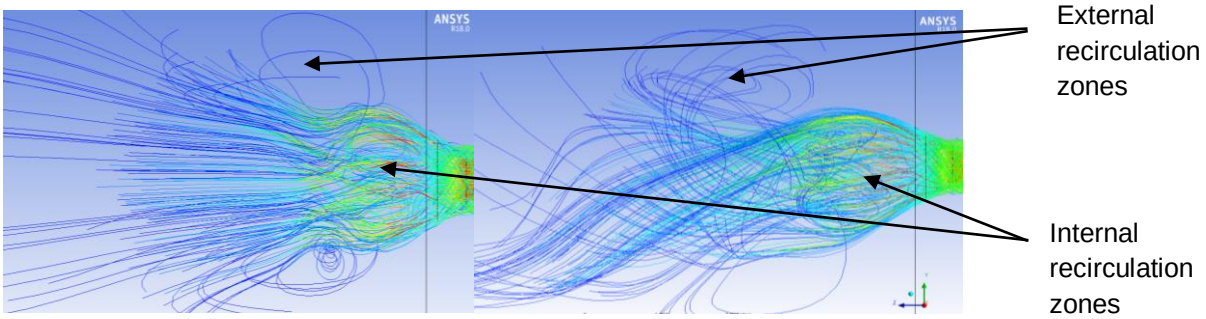

FIGURE 4.10: VELOCITY STREAMLINES PRODUCED BY HEXAHEDRAL (LEFT) AND POLYHEDRAL (RIGHT) MESHES

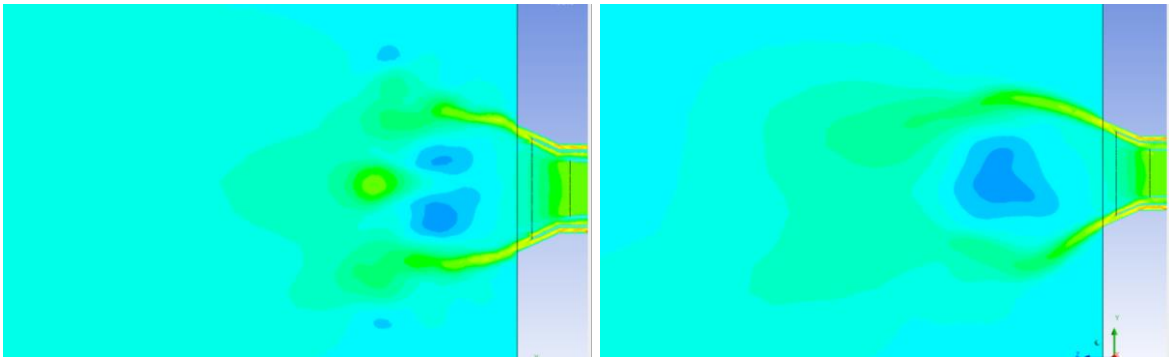

FIGURE 4.11: VELOCITY CONTOURS PRODUCED BY HEXAHEDRAL (LEFT) AND POLYHEDRAL (RIGHT) MESHES

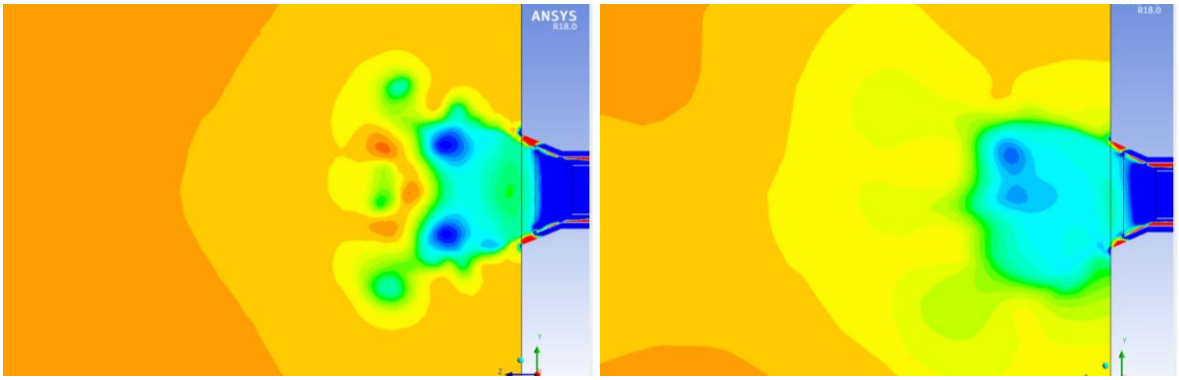

FIGURE 4.12: PRESSURE CONTOURS PRODUCED BY HEXAHEDRAL (LEFT) AND POLYHEDRAL (RIGHT) MESHES

When considering Figures 4.10 – 4.12, it can be seen that the hexahedral mesh is more accurate than the polyhedral mesh only in a symmetrical sense. However, there are also many similarities between the results of the two meshes. Both represent external recirculation zones as well as an internal recirculation zone, have the same amount of swirl, and more or less the same converging-diverging flow at the burner mouth. The velocity and pressure distributions are similar, since they are compared on the same scale. Since the maximum amount of swirl for the formation of an internal recirculation zone will be the crux of the swirl limit design, the polyhedral mesh provides a sufficient amount of information in this regard. Therefore, the polyhedral mesh was used in the iteration phase of the design because the computational time is much less. However, since the hexahedral mesh seems more accurate, the final design will be evaluated by using a hexahedral mesh as well.

- **Fine mesh vs coarser mesh**

It was established in the previous section that a polyhedral mesh will be used in the iteration phase, because of reduced computational time. The next step is to determine the coarsest polyhedral mesh to yield sufficient results and to reduce solving time.

Once again, two trial models were compared to each other. Both of the models make use of a polyhedral mesh, where the first consists of 636 526 cells and the second of 307 951 cells. The comparison is shown below:

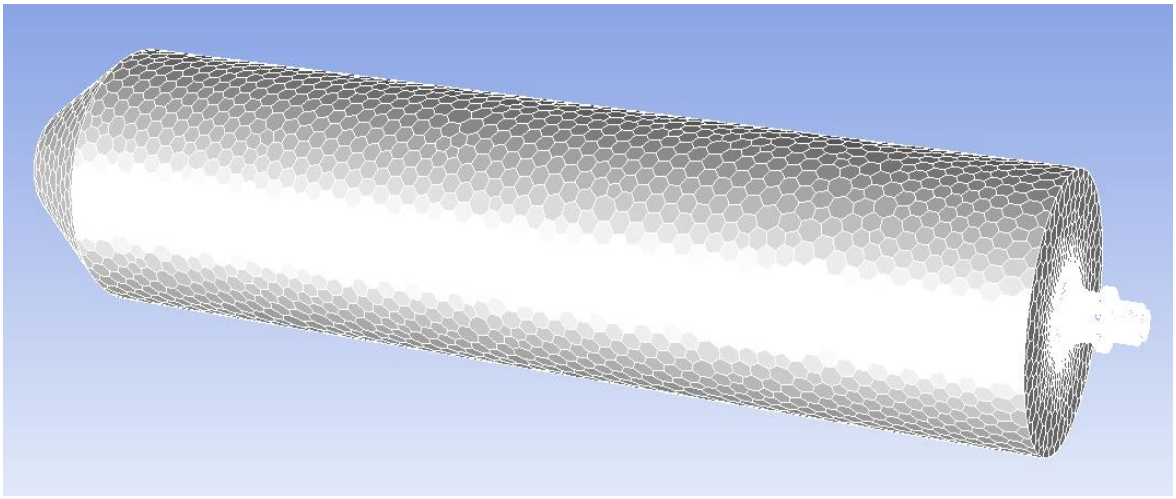

FIGURE 4.13: FINE POLYHEDRAL MESH OF FLOW DOMAIN

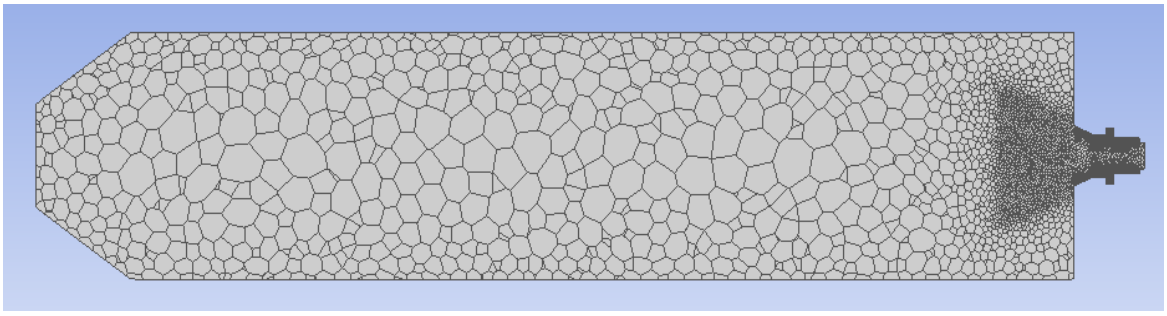

FIGURE 4.14: SECTION VIEW OF FINE POLYHEDRAL MESH OF FLOW DOMAIN

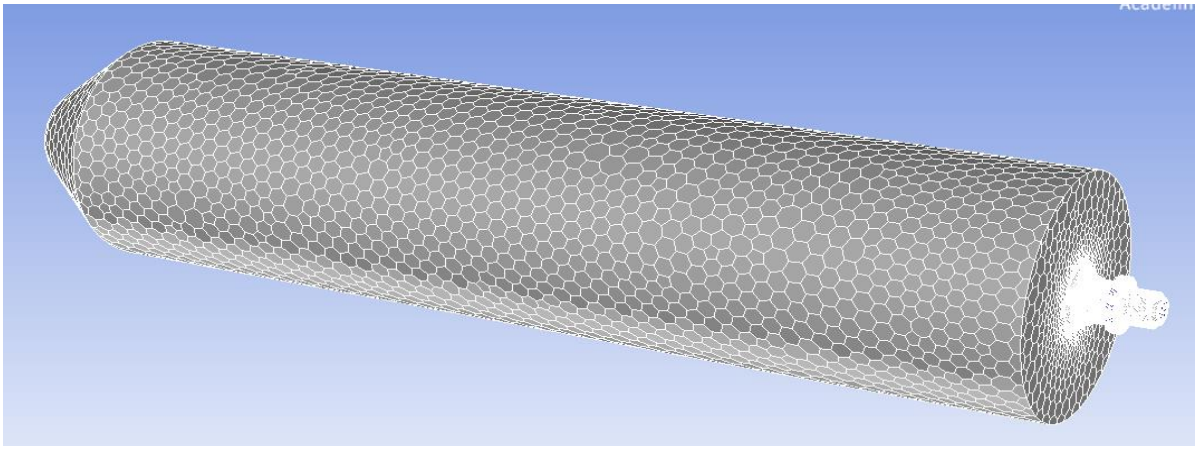

FIGURE 4.15: COARSE POLYHEDRAL MESH OF FLOW DOMAIN

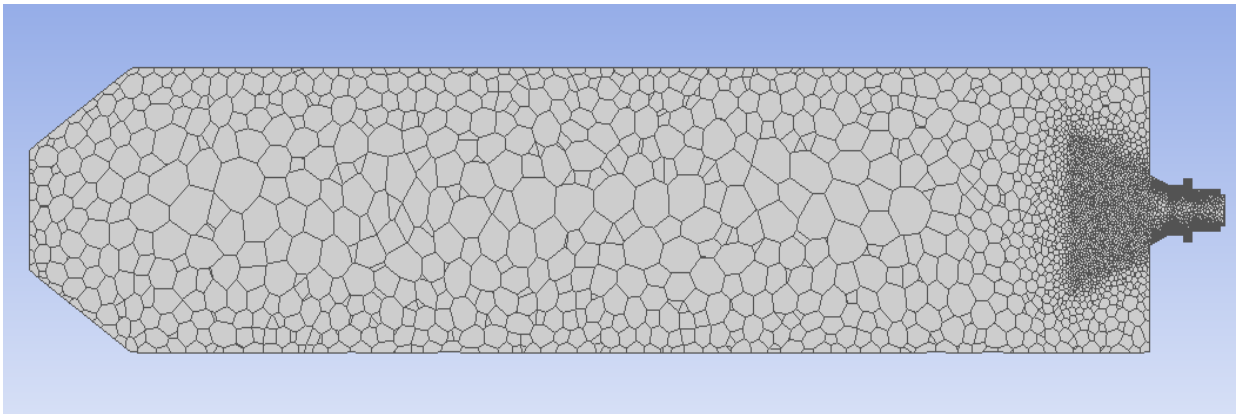

FIGURE 4.16: SECTION VIEW OF COARSE POLYHEDRAL MESH OF FLOW DOMAIN

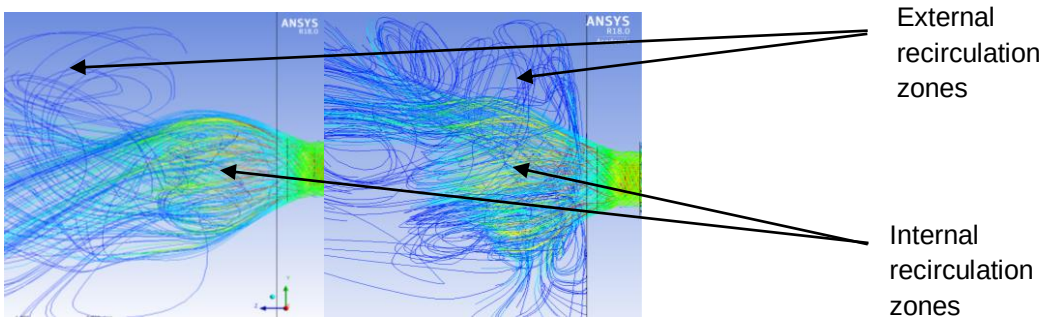

FIGURE 4.17: VELOCITY STREAMLINES PRODUCED BY FINE POLYHEDRAL (LEFT) AND COARSE POLYHEDRAL (RIGHT) MESHES

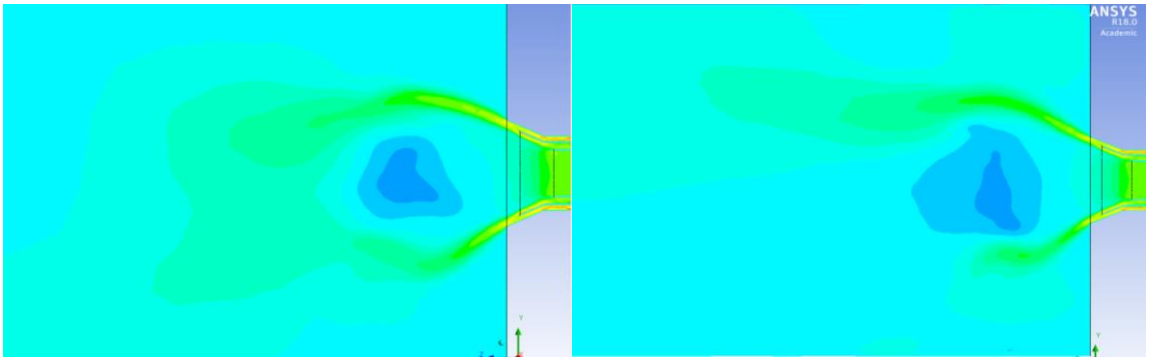

FIGURE 4.18: VELOCITY CONTOURS PRODUCED BY FINE POLYHEDRAL (LEFT) AND COARSE POLYHEDRAL (RIGHT) MESHES

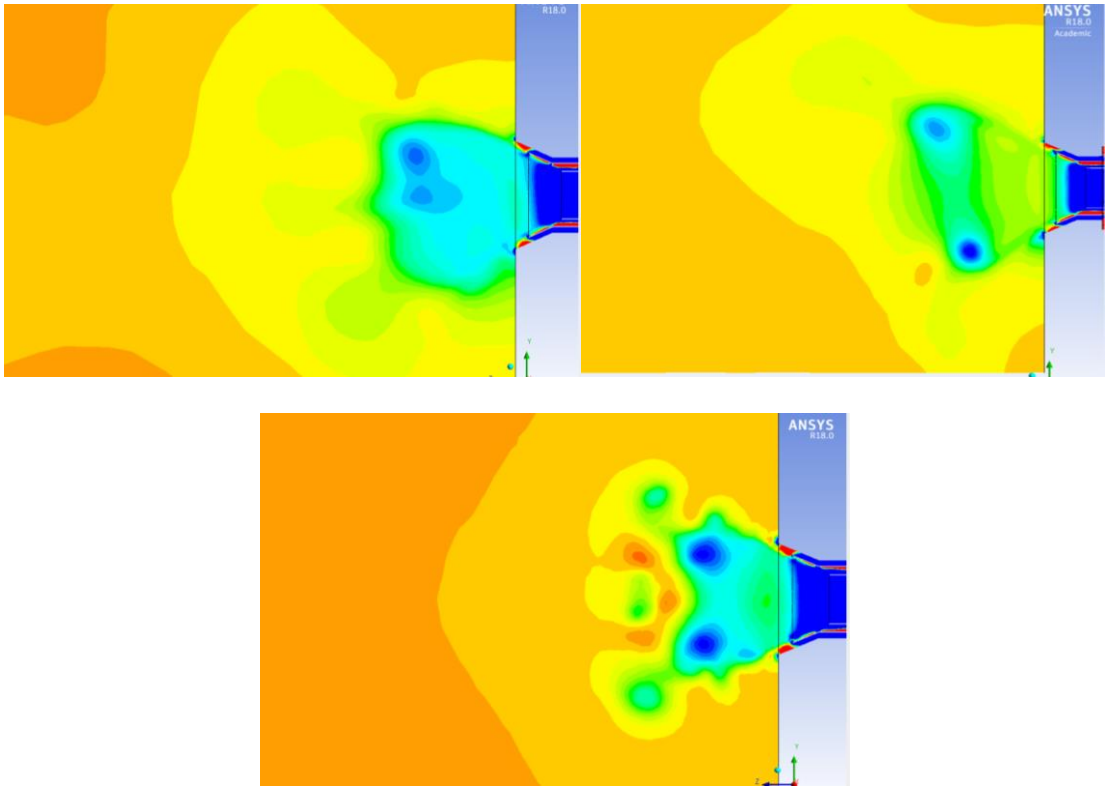

FIGURE 4.19: PRESSURE CONTOURS PRODUCED BY FINE POLYHEDRAL (LEFT), COARSE POLYHEDRAL (RIGHT) AND HEXAHEDRAL (BOTTOM) MESHES

When comparing the results of the coarse and fine polyhedral mesh, it can be seen that the streamlines differ to some extent. Even though there are differences, similarities also exist, such as the external recirculation zone and amount of internal recirculation and swirl. When comparing the velocity contours, much similarity can be seen. The pressure contours differ to some degree, yet the coarser polyhedral mesh compares well to the hexahedral mesh in the previous section. The solving time of the fine mesh was double that of the coarser mesh.

Hence, a polyhedral mesh consisting of approximately 307 951 cells can be used in the iteration phase of PC burner swirler design to reduce the solving time.

Final design of the PC burner:

After many iterations of CFD modelling, more detail of the burner became known. In Figure 4.2 only a qualitative visual of the layout was shown. The quantitative detail now known after the CFD iterations is shown in Figure 4.20:

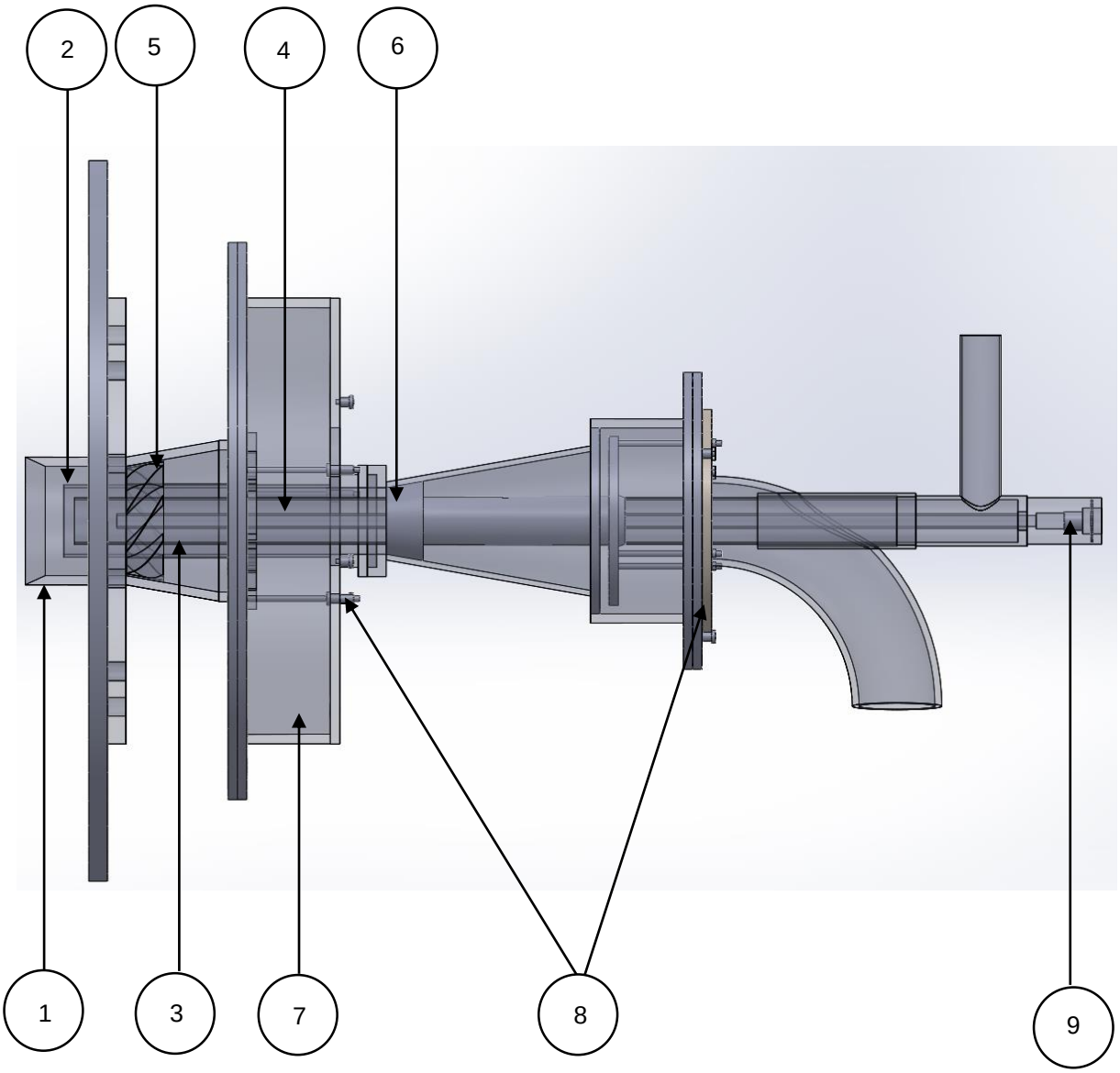

1) SA tube, 2) PA tube, 3) CA tube, 4) LPG tube, 5) SA swirler, 6) PA swirler, 7) SA wind box, 8) Swirl adjuster, 9) LPG insert

FIGURE 4.20: GEOMETRY OF FINAL DESIGNED PC BURNER

The SA and PA swirlers are conical axial swirlers to allow for variable swirl. In Figure 4.20, the swirlers are situated at maximum swirl, since there is no space between the swirler and the tube. Less swirl can thus be created by moving the swirlers in a direction away from the burner mouth by using the swirl adjustor.

It is very important that the air is distributed evenly inside the SA and PC/PA tube before entering the swirlers. If the air is not distributed evenly (non-concentrically) this will create a roping effect. Therefore,

the SA wind box was designed in a way that enables it to distribute the SA evenly in the SA tube before it enters the SA swirler. This velocity distribution obtained from the CFD results reflects the desired distribution of air and is illustrated in Figure 4.21:

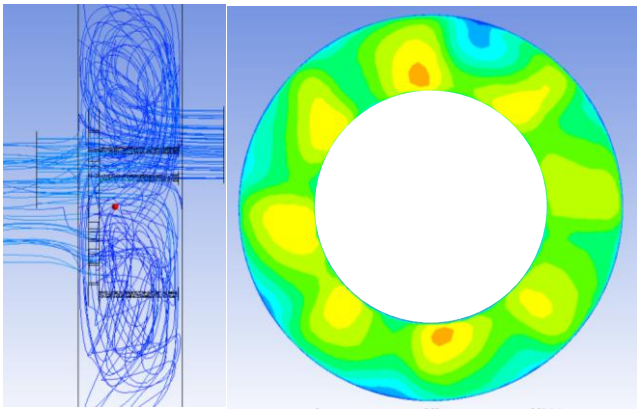

FIGURE 4.21: SA VELOCITY STREAMLINES PRODUCED INSIDE THE SA WIND BOX (LEFT), FRONT VIEW OF THE SA VELOCITY CONTOURS BEFORE ENTERING THE SA SWIRLER (RIGHT)

The PC/PA tube cannot make use of a wind box for even distribution purposes since the wind box creates very low velocities compared to the PC settling velocity. As can be seen in Figure 4.20, the PC/PA enters the burner with a 90^{o} bend. At the PC/PA swirler, most of the air and PC are situated at the bottom half of the pipe, as shown in Figure 4.22:

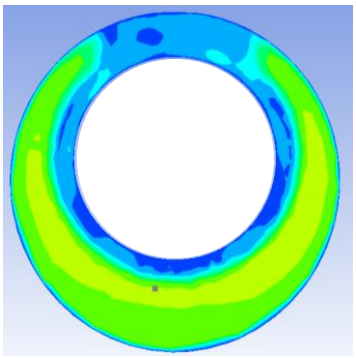

FIGURE 4.22: FRONT VIEW OF PA VELOCITY CONTOURS WHEN EXITING THE BEND

To solve this problem, in order to have better distribution of PA and PC, a coarse mesh sieve was placed at the end of the bend. This is illustrated in Figure 4.23:

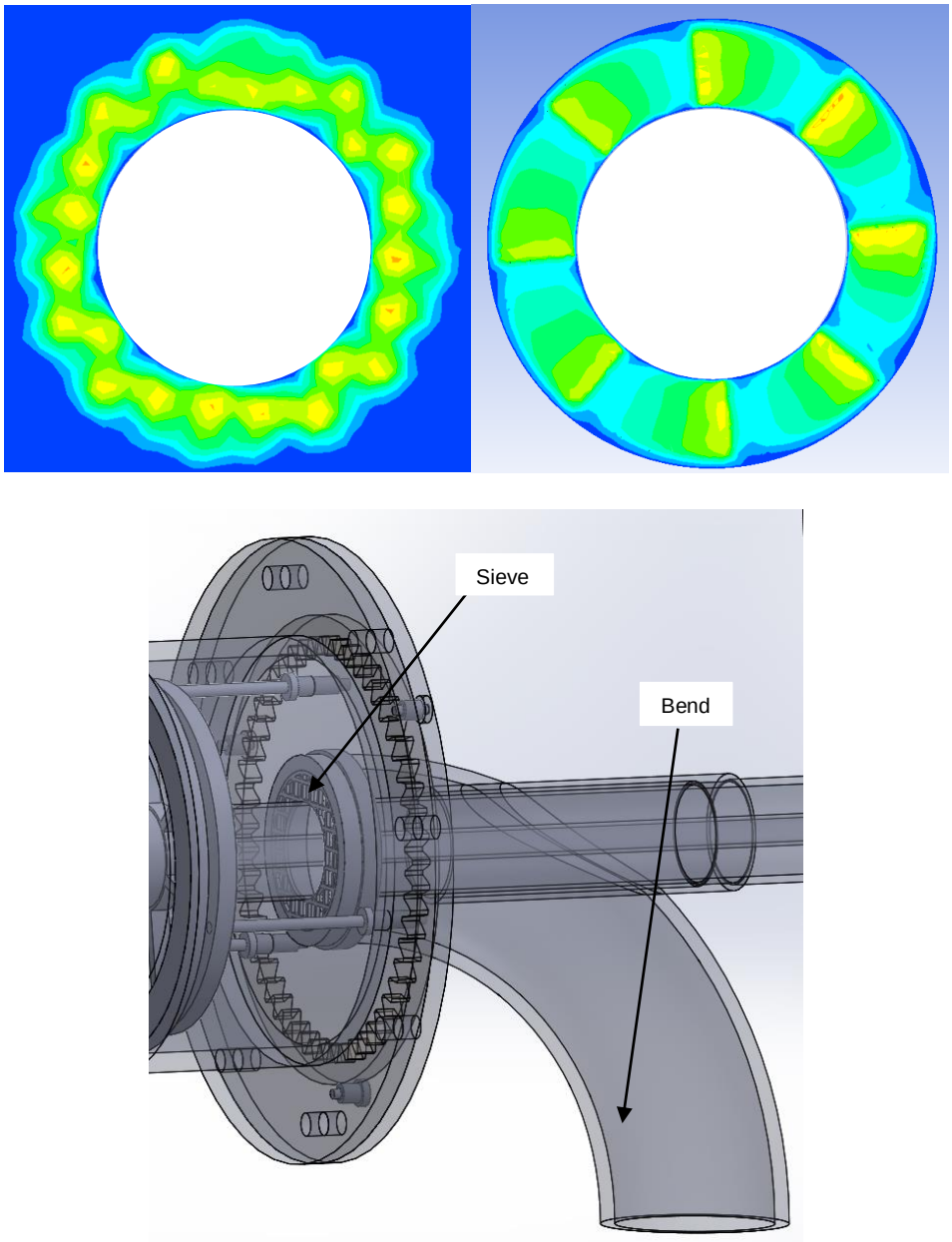

FIGURE 4.23: PA VELOCITY CONTOURS DOWNSTREAM OF THE SIEVE (LEFT), PA VELOCITY CONTOURS UPSTREAM OF THE SWIRLER (RIGHT), GEOMETRY OF SIEVE PLACEMENT (BOTTOM)

LPG orifice sizing

Since the mass flow of LPG is very low (0.237 g/s), it is difficult to regulate the flow with conventional measuring equipment. The amount of LPG flow can be regulated by using a pressure regulator, pressure gauge and gas orifice with a specific diameter. A certain gauge pressure will be used to force 0.237 g/s LPG through the orifice diameter hole.

The pressure and orifice diameter were conveniently chosen to be in a suitable range of pressure diameter. CFD was used to determine the gauge pressure for an orifice diameter to provide 0.237 g/s LPG. It was determined that a pressure of 8040 Pascal was required for a 1.5 mm orifice diameter. Figure 4.24 shows the pressure contours before and after the gas insert:

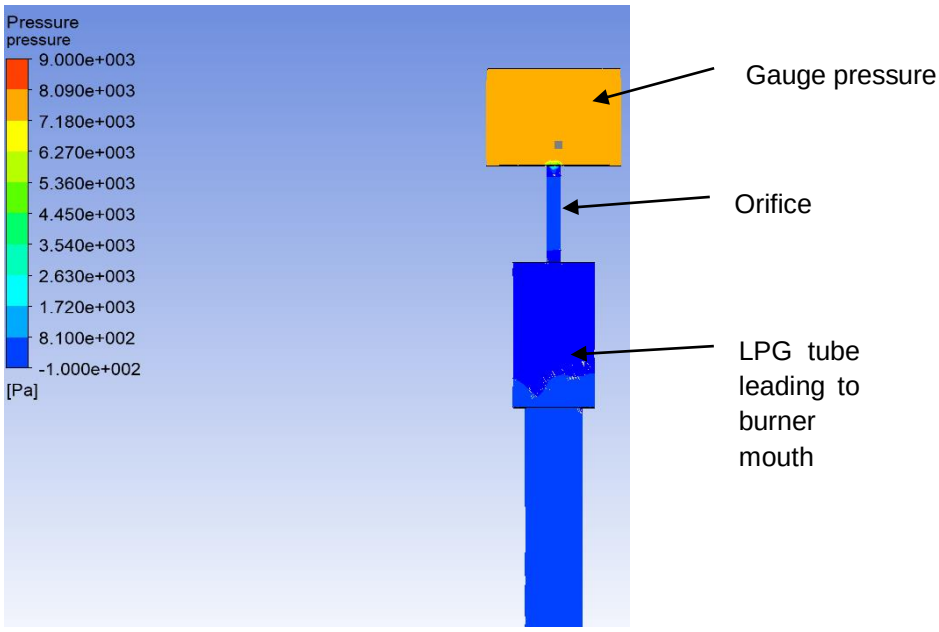

FIGURE 4.24: PRESSURE CONTOURS OF LPG TUBE

By using the pressure determined by CFD, and the mass flow, the coefficient of discharge (Cd) factor was calculated. The value of the Cd factor can indicate if the CFD was done correctly.

$$\dot{m} = \rho A C \tag{18}$$

$$P_{DYNAMIC} = P_{STAGNATION} - P_{STATIC} \tag{19}$$

$$P_{DYNAMIC} = P_{GAUGE} \tag{20}$$

$$\frac{1}{2}\rho C^2 = P_{GAUGE} \tag{21}$$

$$C = \sqrt{\frac{2\Delta P * 1000}{\rho}} * Cd \tag{22}$$

where,

- P is the pressure [kPa]
- $\dot{m}$ is the mass flow [kg/s]
- ρ is the density [kg/m^3]

- *A* is the area [m^2]
- *C* is the velocity [m/s]
- *Cd* is the coefficient of discharge [-]

It was calculated that the Cd factor is 0.76, which is a realistic value.

Verification of the resulting flow field

As stated previously, the final geometry was evaluated by using three different models to determine if the maximum swirl limits at 80 kW still produced an adequate flow pattern. Model 1 was the final model obtained during the iteration phase. This was done by using the k-ε turbulence model and a polyhedral mesh. Model 2 used a hexahedral mesh and RSM turbulence model. Lastly, model 3 used a polyhedral mesh and RSM turbulence model. Models 1 and 3 were solved by using the same polyhedral mesh.

The comparison between the three models will now be discussed:

FIGURE 4.25: FLOW DOMAIN OF FINAL DESIGN

Each of the three models used the same flow domain seen in Figure 4.25.

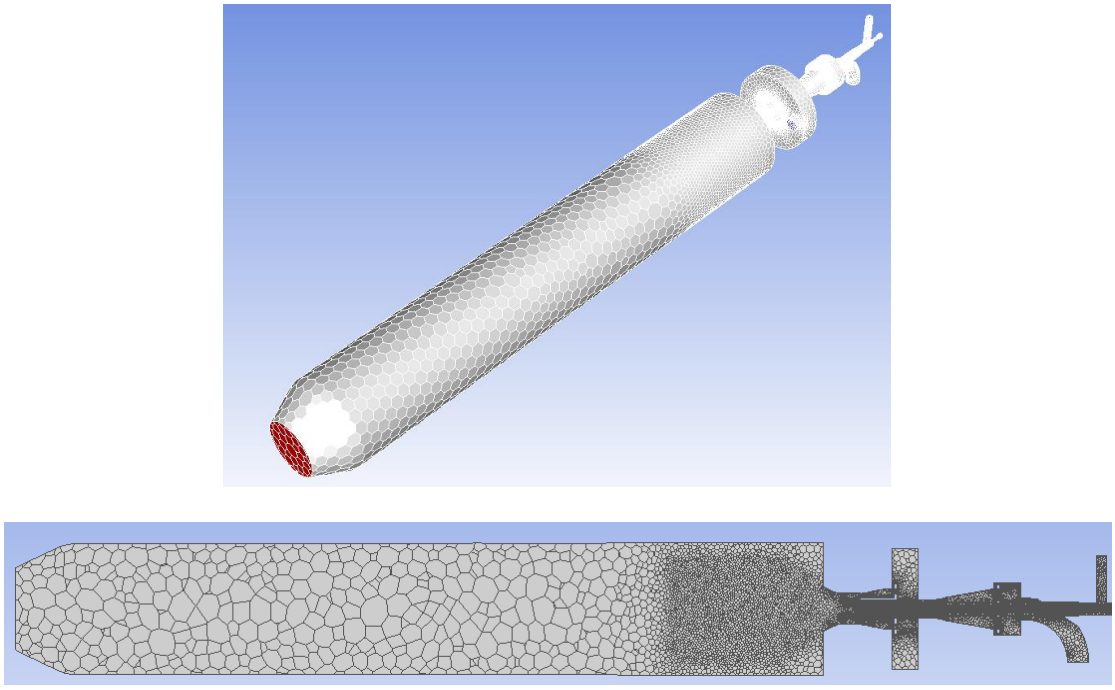

FIGURE 4.26: POLYHEDRAL MESH (TOP) AND SECTION VIEW OF POLYHEDRAL MESH (BOTTOM) OF FINAL DESIGN

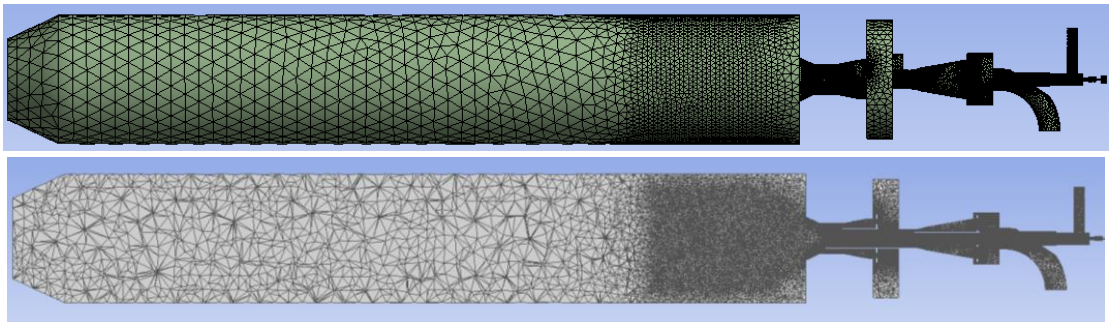

FIGURE 4.27: HEXAHEDRAL MESH (TOP) AND SECTION VIEW OF HEXAHEDRAL MESH (BOTTOM) OF FINAL DESIGN

Figures 4.26 and Figure 4.27 illustrate the polyhedral and hexahedral mesh used for solving. The polyhedral mesh contained 620 002 cells, while the hexahedral mesh contained 2 670 595 cells.

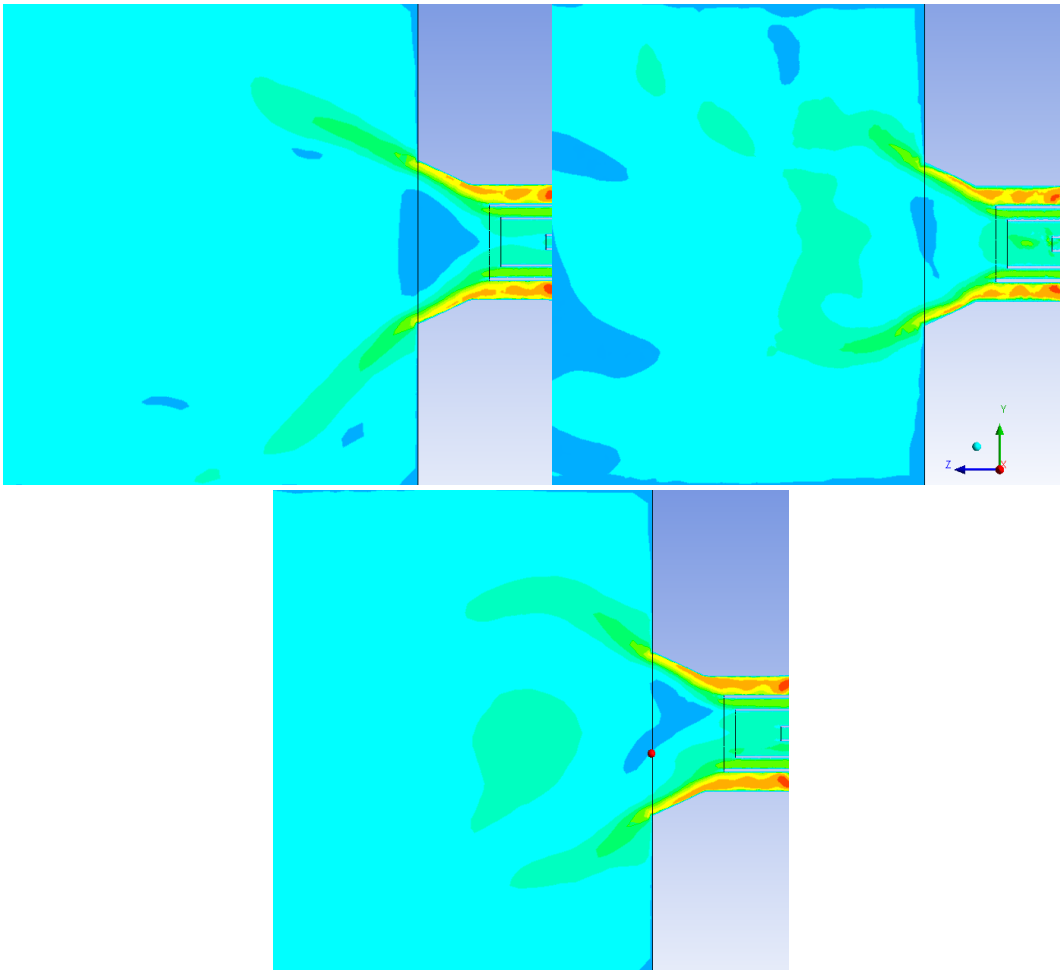

FIGURE 4.28: VELOCITY CONTOURS PRODUCED BY MODEL 1 (LEFT), MODEL 2 (RIGHT), MODEL 3 (BOTTOM)

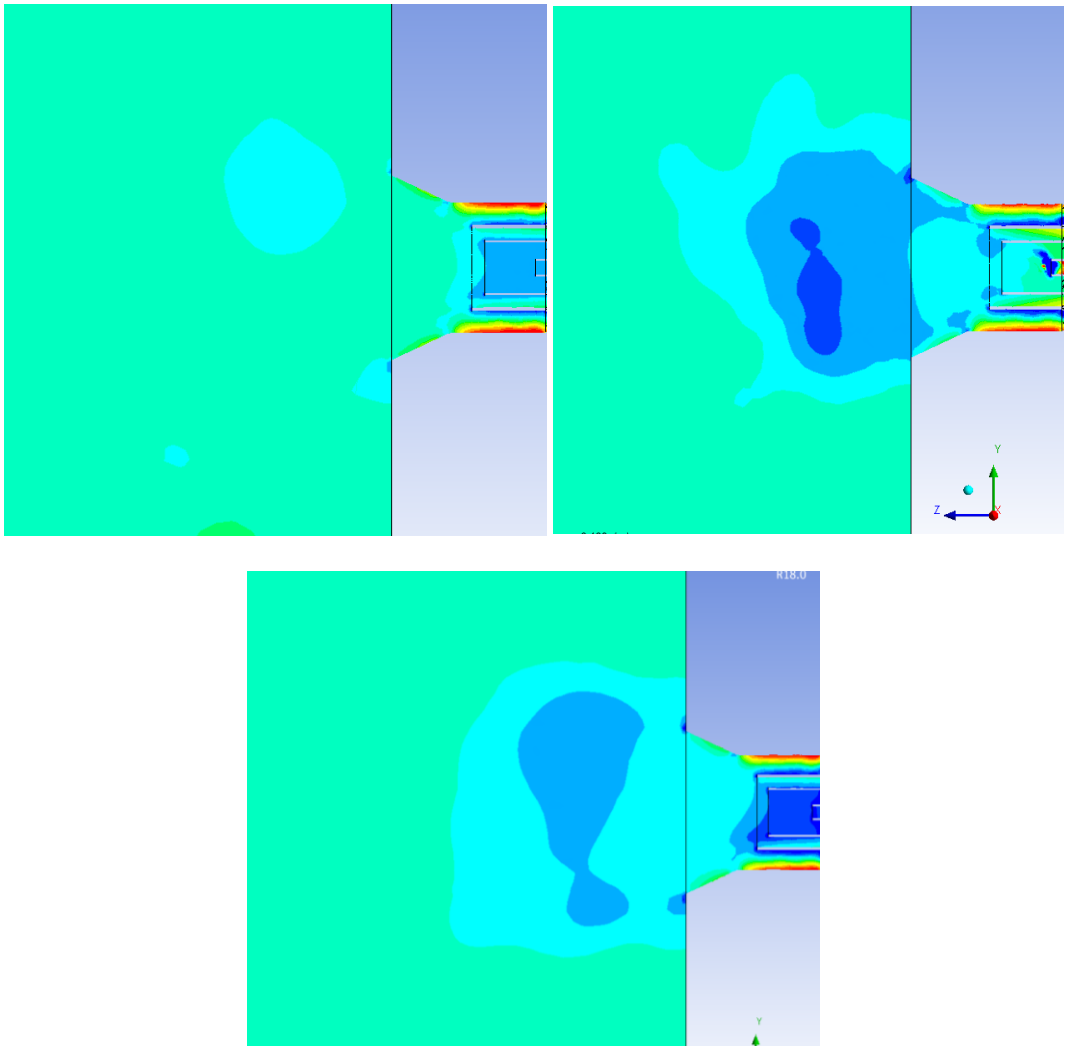

FIGURE 4.29: PRESSURE CONTOURS PRODUCED BY MODEL 1 (LEFT), MODEL 2 (RIGHT), MODEL 3 (BOTTOM)

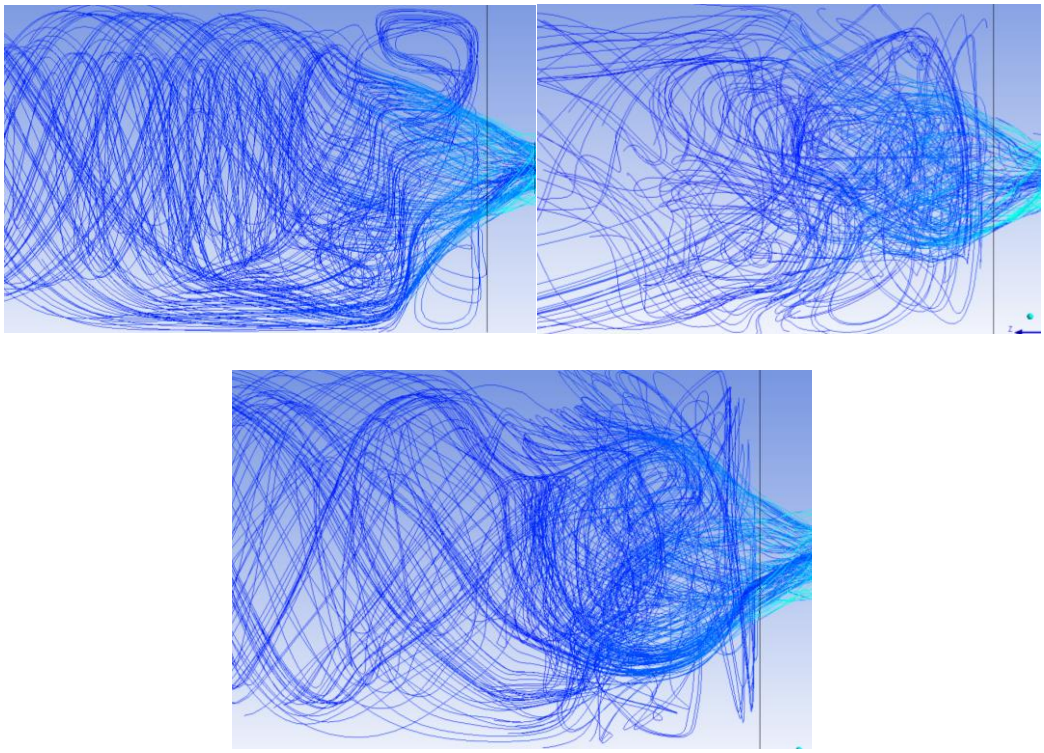

FIGURE 4.30: VELOCITY STREAMLINES PRODUCED BY MODEL 1 (LEFT), MODEL 2 (RIGHT), MODEL 3 (BOTTOM)

When evaluating the velocity contours of Figure 4.28, pressure contours of Figure 4.29, and velocity streamlines of Figure 4.30 of the three models, it can be seen that model 2 and model 3 are more similar compared to model 1. Model 1 shows that the swirl limit is on the verge of excessive swirl and little converging flow follows. However, an internal recirculation zone exists. Unlike model 1, models 2 and 3 show a diverging-converging flow pattern. All the models show a large amount of swirl. Because the k-ε turbulence model is generally regarded as less accurate than the RSM model, the results of models 2 and 3 are considered more representative.

It can be seen that the polyhedral and hexahedral meshes correlate very well when observing the velocity and pressure contours. The streamlines differ to a lesser extent, but show that there is a similar amount of recirculation and swirl.

Because models 2 and 3 are very similar, model 3 will be evaluated and discussed in further detail in the following section.

Detailed discussion of model 3 using a polyhedral mesh and RSM model

When this mesh was created, it was necessary to evaluate the mesh quality. Two types of parameters were used to assess the mesh quality namely: orthogonal quality and aspect ratio. According to ANSYS FLUENT (2019), the orthogonal quality is a measure between the direct connections of the neighbouring element's centre, to the median line of that element's face. It is regarded that it is better to have a value closer to 1, and worse to have a value closer to 0. It is suggested that the minimum orthogonal quality should not be less than 0.01 for an acceptable mesh quality. The aspect ratio indicates a measure of the stretching of a cell and it is suggested that the maximum aspect ratio should not exceed 35.

The following information was used to run model 3:

The minimum orthogonal quality obtained for the polyhedral mesh was 1.58211e-01, which was well above the recommended minimum. The maximum aspect ratio was 2.15071e+01 which was well below the recommended maximum value. The mesh used can be seen in Figure 4.26; and contained 620 002 cells.

The boundary conditions were the following:

TABLE 4.4: BOUNDARY CONDITIONS FOR MODEL 3

	LPG	CA	PA	SA	Outlet
Inlet Mass Flow [g/s]	0.237	3.355	6.5	20.1	-
Inlet Temperature [^{o}C]	20	150	150	280	-
Outlet Pressure [kPa]	-	-	-	-	86

The following figures show each of the LPG, CA, PA, PC and SA streamlines separately, although with the effect of the other streams present. The PC particles were simulated by using the discrete phase method (DPM) in FLUENT, since the PC might have a different flow field compared to that of the PA. The particle fineness distribution was based on a Rosin-Rammler logarithmic scale common for PC used on power stations in South Africa and can be seen in Appendix D. These particle sizes vary between 300 and 75 µm. The mass flow of PC was set at 3.9 g/s, which was the same as for the intermediate coal.

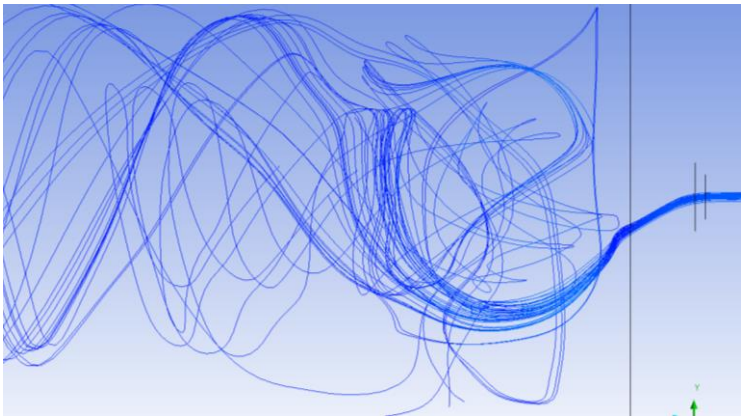

FIGURE 4.31: VELOCITY STREAMLINES OF LPG

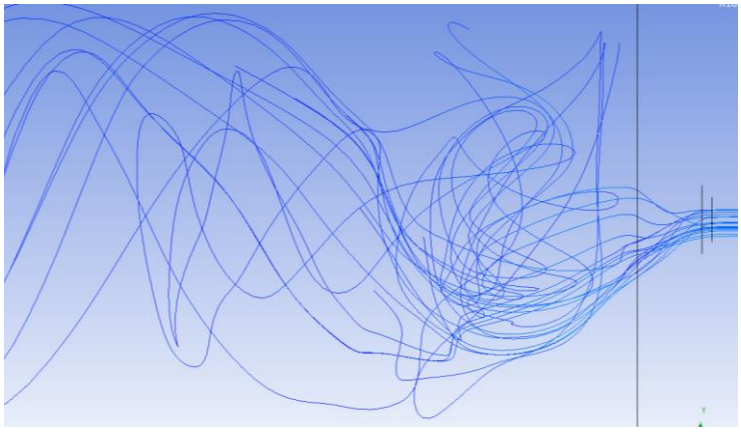

FIGURE 4.32: VELOCITY STREAMLINES OF CA

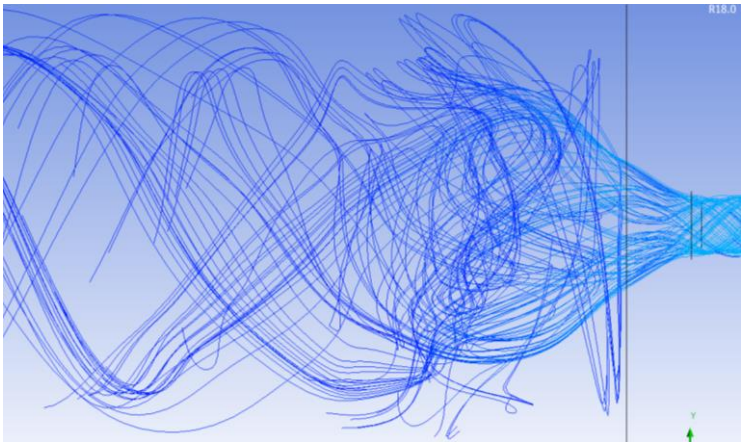

FIGURE 4.33: VELOCITY STREAMLINES OF PA

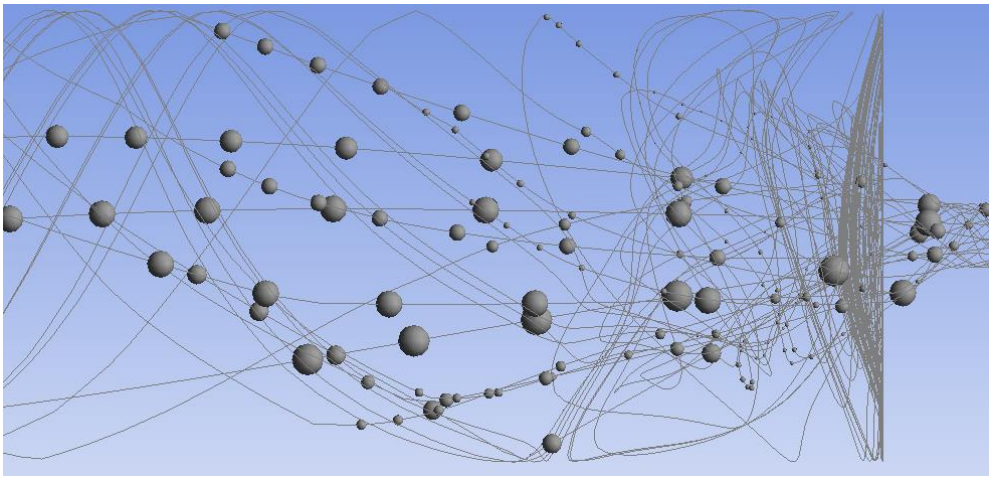

FIGURE 4.34: STREAMLINES OF PC

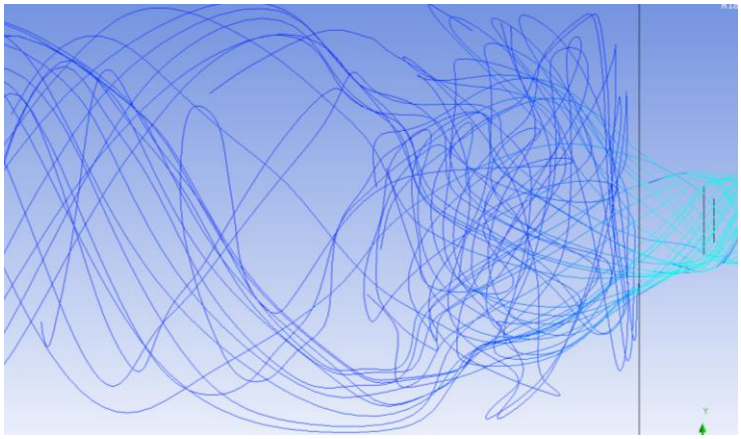

FIGURE 4.35: VELOCITY STREAMLINES OF SA

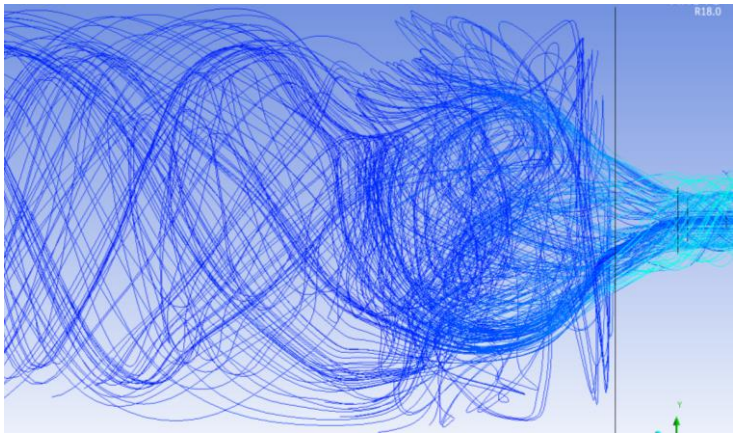

FIGURE 4.36: VELOCITY STREAMLINES OF LPG, CA, PA AND SA

When considering the flow of LPG, CA, PA, PC and SA, it can be seen that all the streams are recirculating into the internal recirculation zone close to the burner mouth. This leads to rapid mixing of PC and air, just after the burner mouth. The rapid mixing and recirculation will create an intense and short flame and a constant ignition zone, which will promote flame stability. The entrainment effect can be seen in the flow field, since all the different streams (LPG, CA, PC and PA) follow the path of the dominant SA stream, because it has the largest momentum.

The streamlines representing the PC paths in Figure 4.34 show the fineness of the PC entering the flow field by using an over-exaggerated size scale of spheres. The smaller particles seem to recirculate in the internal recirculation zone, while a few of the coarser particles appear to penetrate the recirculation zone. It can be seen that all of the PC particles have continuous contact with air at the burner mouth which enables ignition and combustion.

Bear in mind, that this CFD model represents the flow field at maximum swirl, where a diverging-converging flow still exists. The amount of swirl can still be adjusted to create a desired flow field that corresponds to a desired flame. It was decided not to model all of the possible flow fields that the burner can produce in respect to the different amounts of swirl, since doing this will require numerous iterations and too much computational time. During testing, the amount of swirl can be adjusted to obtain the most suitable flame profile for a specific coal.

The volume of the combustion chamber is also very important with regards to burnout time of PC. According to the literature review, the coarsest PC particles take approximately 2 seconds for complete burnout. However, this amount varies for different types of coal. Information on burnout time for typically used PC on South African power stations was acquired. The drop tube furnace (DTF) at RT&D Rosherville, was used to determine the burnout time of a single PC particle. The results can be seen in Appendix E. According to the data, the particle with the longest burnout time took 2.9 seconds to burn out. This time will be used to size the combustion chamber to ensure that the fastest travelling particle still has a residence time of at least 2.9 seconds. In Figure 4.37, the streamlines of the PC are shown just before the first particle exits the combustion chamber (left-hand side of Figure 4.37). According to the CFD model, the fastest PC particle, takes approximately 3.2 seconds to exit the combustion chamber, which is sufficient residence time to allow for complete burnout. The size of the flow domain inside the combustion chamber was determined to have a length of 1.5 m and a diameter of 250 mm.

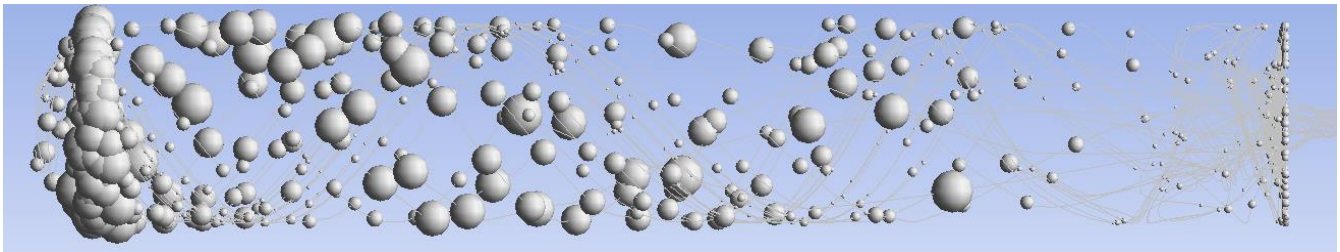

FIGURE 4.37: STREAMLINES OF PC OVER THE LENGTH OF THE COMBUSTION CHAMBER

Evaluation of the flow field at 40 kW thermal loading

Since the burner operates between 40 and 80 kW, the flow field had to be evaluated at 40 kW thermal loading as well. The set-up for the 40 kW model was the same as the 80 kW model 3, except for changed inlet mass flow boundary conditions. The inlet boundary conditions are shown in Table 4.5.

TABLE 4.5: BOUNDARY CONDITIONS FOR 40 kW MODEL

	LPG	CA	PA	SA	Outlet
Inlet Mass Flow [g/s]	0.1185	1.6775	3.25	10.05	-
Inlet Temperature [°C]	20	150	150	280	-
Outlet Pressure [kPa]	-	-	-	-	86

The following figures show a comparison between the 40 kW and 80 kW models:

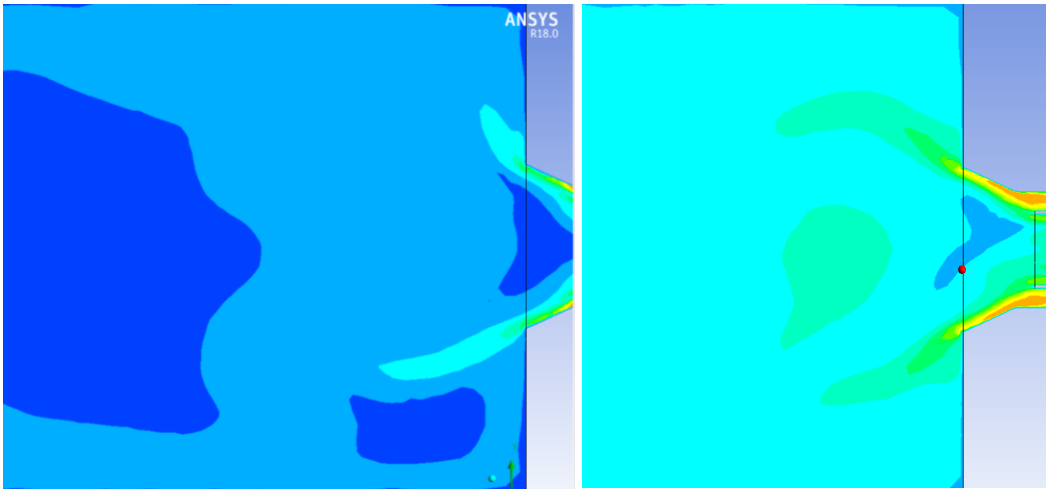

FIGURE 4.38: VELOCITY CONTOURS PRODUCED: 40 kW (LEFT) AND 80 kW (RIGHT)

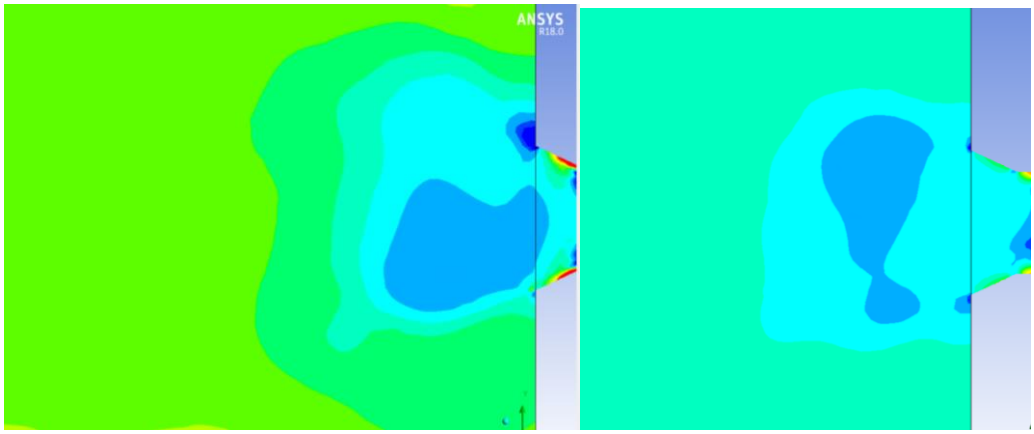

FIGURE 4.39: PRESSURE CONTOURS PRODUCED OF: 40 kW (LEFT) AND 80 kW (RIGHT)

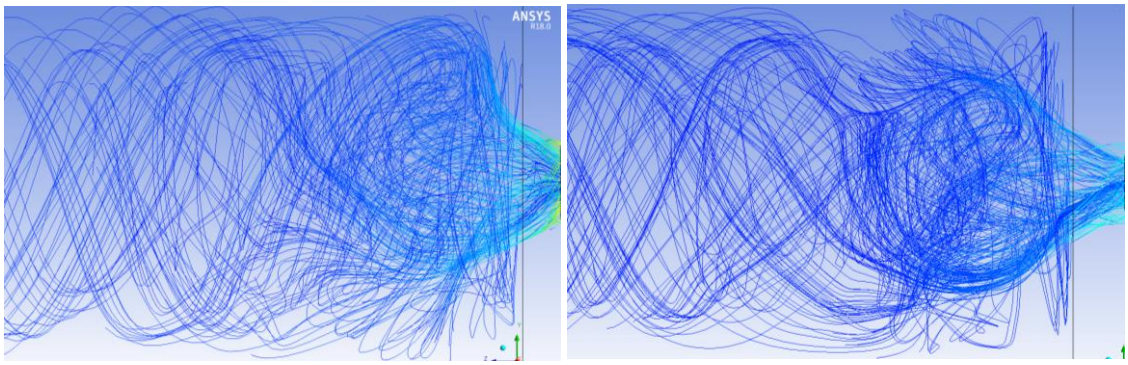

FIGURE 4.40: VELOCITY STREAMLINES RPODUCED OF: 40 kW (LEFT) AND 80 kW (RIGHT)

It can be seen that the 40 kW model has a similar aerodynamic flow field as the 80 kW model.

FIGURE 4.41: IMAGES OF: PC BURNER (LEFT AND MIDDLE), SWIRLER CONSTRUCTED FROM HIGH TEMPERATURE RESIN (RIGHT)

4.2 COMBUSTION CHAMBER DESIGN

The combustion chamber plays an important role in the NCVp coal analyser. It needs to be cooled to prevent temperature excursions of the materials, create a high temperature environment in which combustion can take place, and withstand high combustion temperatures of up to 1600°C.

It was therefore required to design a combustion environment consisting of a refractory or insulating material that is able to withstand high temperatures, with a cooling jacket surrounding the refractory material. The following figure shows transparent views to display the refractory insulation discs, the helix guiding the cooling air, inspection ports, quarl and burner interface:

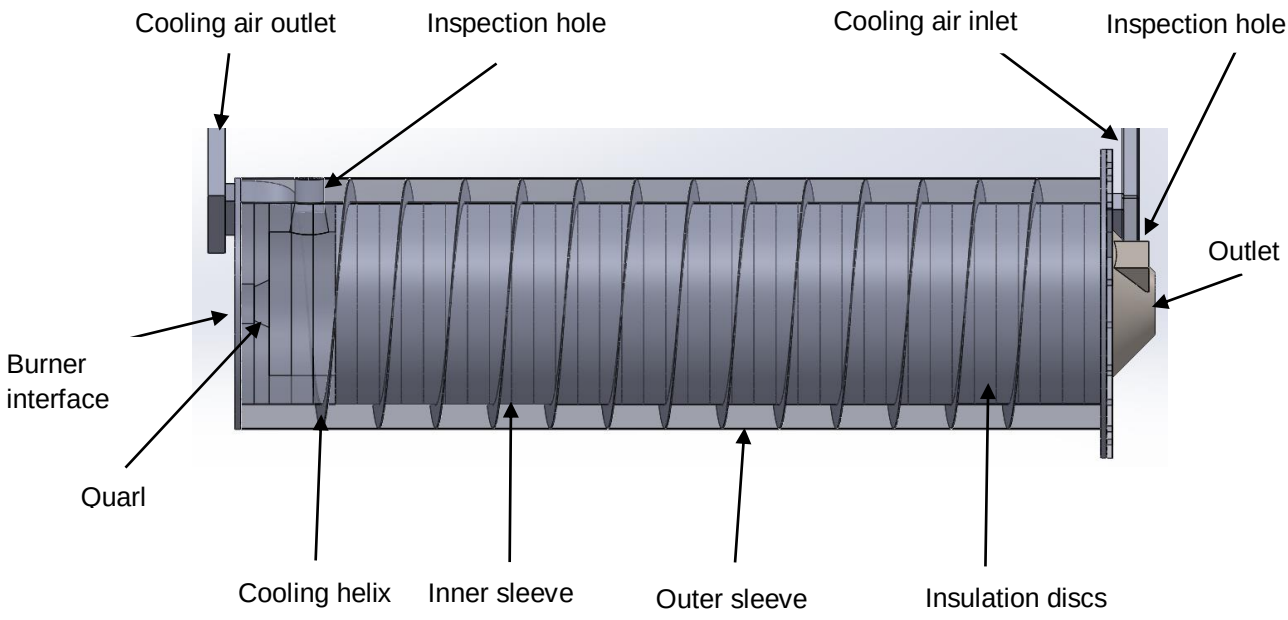

FIGURE 4.42: GEOMETRIC MODEL OF COMBUSTION CHAMBER

The functionality of the combustion chamber will now be explained. The insulation material was chosen to form an environment in which combustion can take place. This material can withstand high temperatures and promotes combustion of PC since it has a low thermal conductivity.

The insulation material was manufactured in the form of discs that were situated inside the inner sleeve. The concentric inner sleeve and the outer sleeve form an air-cooling jacket. Air was selected as cooling medium rather than water, this is explained in Section 4.2.1. Between the inner and outer sleeves is the cooling helix, which causes air to circulate, preventing temperature hot spots from forming. The air enters the cooling jacket at the flue gas outlet end and exits at the burner end, for counter-flow heat exchange. The combustion chamber has a converging outlet that will force the flue gas to concentrate and will make the temperature measurement more representative.

Two inspection holes enable the flame to be observed during testing, one from the side at the burner mouth and the other from the front at the outlet. The burner is connected to the combustion chamber at the burner interface. Insulation material was chosen as the material of the quarl, since the flame will ignite in that area.

4.2.1 COMBUSTION CHAMBER MATERIAL SELECTION

According to the Kitto and Stultz (2005) the flame temperature inside a PC-fired furnace can reach up to 1600°C. Generally, it is common to use insulating or refractory material that can be in direct contact with the flame. The insulating material must also be able to reduce the amount of heat that is absorbed by the cooling air in the cooling jacket. This requires the insulating material to have low thermal conductivity in order to reflect heat back to the flame. This promotes ignition for combustion.

The insulating material chosen is ZIRCAR Type AL-30. ZIRCAR Type AL-30, which is a medium-density, high-strength, uniformly rigid refractory structural board material composed of high-alpha polycrystalline alumina fibres and high-purity inorganic binders. This ceramic can withstand a temperature of up to 1700°C, has a thermal conductivity ranging from 0.09 – 0.27 at temperatures of 250 – 1650°C respectively, and has good machinability. The properties of Al-30 can be seen in Appendix F.

To allow for improved flow inside the combustion chamber, the insulating material needs to be circular in shape. Since the AL-30 was in the form of rectangular discs with a thickness of 40 mm, it needed to be reshaped into circular discs.

The cooling jacket will act as a cylindrical housing or sleeve for the AL-30 discs. Although traditionally, water is used in the cooling fluid-jacket on traditional gas flow calorimeters, there is the risk of water leakage onto the AL-30 discs, since the cooling jacket surrounds the insulation. The AL-30 material is extremely hygroscopic and will absorb water rapidly. This water can be turned into steam, which can cause an explosion. It was therefore decided to use air as the cooling medium inside the cooling jacket for safety reasons.

The other material used in the cooling chamber (concentric sleeves and helix) is also introduced to relatively high temperatures. During start-up and cooling-down of the device, moisture forms from combustion products as well as the relative humidity of air. To prevent subsequent corrosion stainless steel Type 304 was used.

4.2.2 COMBUSTION CHAMBER HEAT TRANSFER CALCULATIONS

After the type of materials and size of the combustion chamber flow domain had been established, the next step was to determine the radial thickness of the AL-30 material for an acceptable amount of heat loss. This was determined by using heat transfer calculations.

Most of the heat from the flame is in the form of radiation. The heat loss of the flame is transferred to the cooling jacket in the form of conduction heat through the insulating material. The heat absorbed by the cooling jacket will be in the form of convection.

Heat balance equations were compiled for the flow of heat from the flame as heat source to the atmosphere via the insulation material, stainless steel sleeves and cooling air through the cooling jacket. Iterations were performed by varying the radial thickness of the AL-30 and the amount of heat absorbed by the cooling air, until the radiant heat loss balanced with the heat absorbed by the air. The following equations were used to obtain a solution:

$$Radiation: \quad \dot{Q} = A\varepsilon\sigma * (T_{FLAME}^4 - T_{AL-30,INNER}^4) \tag{23}$$

$$Conduction: \quad \dot{Q} = Ak * (T_{INNER} - T_{OUTER}) \tag{24}$$

$$Heat\ rate: \quad \dot{Q} = \dot{m}_{AIR} cp_{AIR} * (T_{OUTLET} - T_{INLET}) \tag{25}$$

where,

- $\dot{Q}$ is the heat rate [kW]
- A is the area [m^2]
- ε is the emissivity [-]
- σ is the Stefan Boltzmann constant [-]
- T is the temperature [^oC]
- k is the thermal conductivity coefficient [-]
- $\dot{m}_{AIR}$ is the mass flow of air [kg/s]
- cp_{AIR} is the specific heat capacity at constant pressure [kJ/kg-K]

The following figure illustrates a front view schematic of the combustion chamber that will be used in the heat transfer calculations:

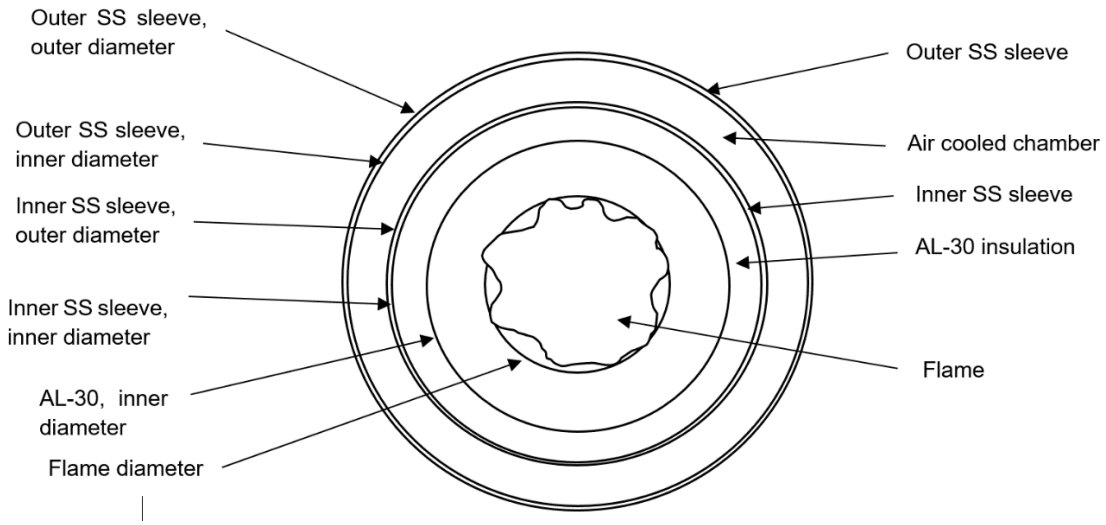

FIGURE 4.43: FRONT VIEW SCHEMATIC OF COMBUSTION CHAMBER

The input parameters used to solve the heat transfer equations can be seen in Table 4.6:

TABLE 4.6: INPUT PARAMETERS FOR COMBUSTION CHAMBER HEAT TRANSFER CALCULATIONS

$D_{AL\text{-}30\ INNER}$ [mm]	250.000	$t_{AL\text{-}30}$ [mm]	50.000	$T_{SS,OUTER}$ [°C]	95.000	D_{FLAME} [mm]	150.000
T_{FLAME} [°C]	1250.000	L_{FLAME} [m]	0.650	k_{SS} [W/m-K]	23.000	ε_{FLAME} [-]	0.800
$k_{AL\text{-}30}$ [W/m-K]	0.200	$L_{CHAMBER}$ [m]	1.500	$T_{AIR,OUT}$ [°C]	150.00	σ	0.00000005670
$c_{P\ AIR}$ [kJ/kg-K]	1.000	t_{SS} [mm]	1.500	$T_{AIR,IN}$ [°C]	40.000		

Table 4.6 shows the input parameters used to calculate the heat of cooling air, heat from radiated flame loss, mass flow of cooling air, and the temperatures of the stainless steel inner wall and the AL-30 inner wall. The diameter of the flame was assumed to be 150 mm which is obtained from the CFD modelling. The emissivity of the flame and wall is assumed to be 0.8, since this is a common value used for the brightness of PC flames (Viskanta & Menguc, 1987). The stainless steel sleeves were manufactured from 1.5 mm thick sheet metal. The temperature of the flame was assumed to be that of typical flame temperatures on power stations in South Africa.

TABLE 4.7: RESULTS OF COMBUSTION CHAMBER HEAT TRANSFER CALCULATIONS

Q_{AIR} [kW]	$T_{SS,INNER}$ [°C]	$T_{AL\text{-}30,INNER}$ [°C]	$m_{COOLING\ AIR}$ [kg/s]	$Q_{FLAME\ LOSS}$ [kW]
6.410	95.247	1216.252	0.0571	6.410

After the iterations, the results obtained are shown in Table 4.7. The radial thickness of the AL-30 for 50 mm allows 6.41 kW of heat to be absorbed by the cooling air. The cooling air must have a mass flow of 0.0571 kg/s, entering at 40°C and exiting at 150°C. These values are practically acceptable.

FIGURE 4.44: PHYSICAL MODEL OF COMBUSTION CHAMBER

5 COMMISSIONING AND TESTING

After the PC burner and combustion chamber had been designed and manufactured, the auxiliaries of the NCVp coal analyser were selected and all the components were assembled. This section explains the commissioning and testing of the NCVp coal analyser. In this section, the combustion produced by the burner is shown. Figure 5.1 shows the main components of the NCVp coal analyser assembly:

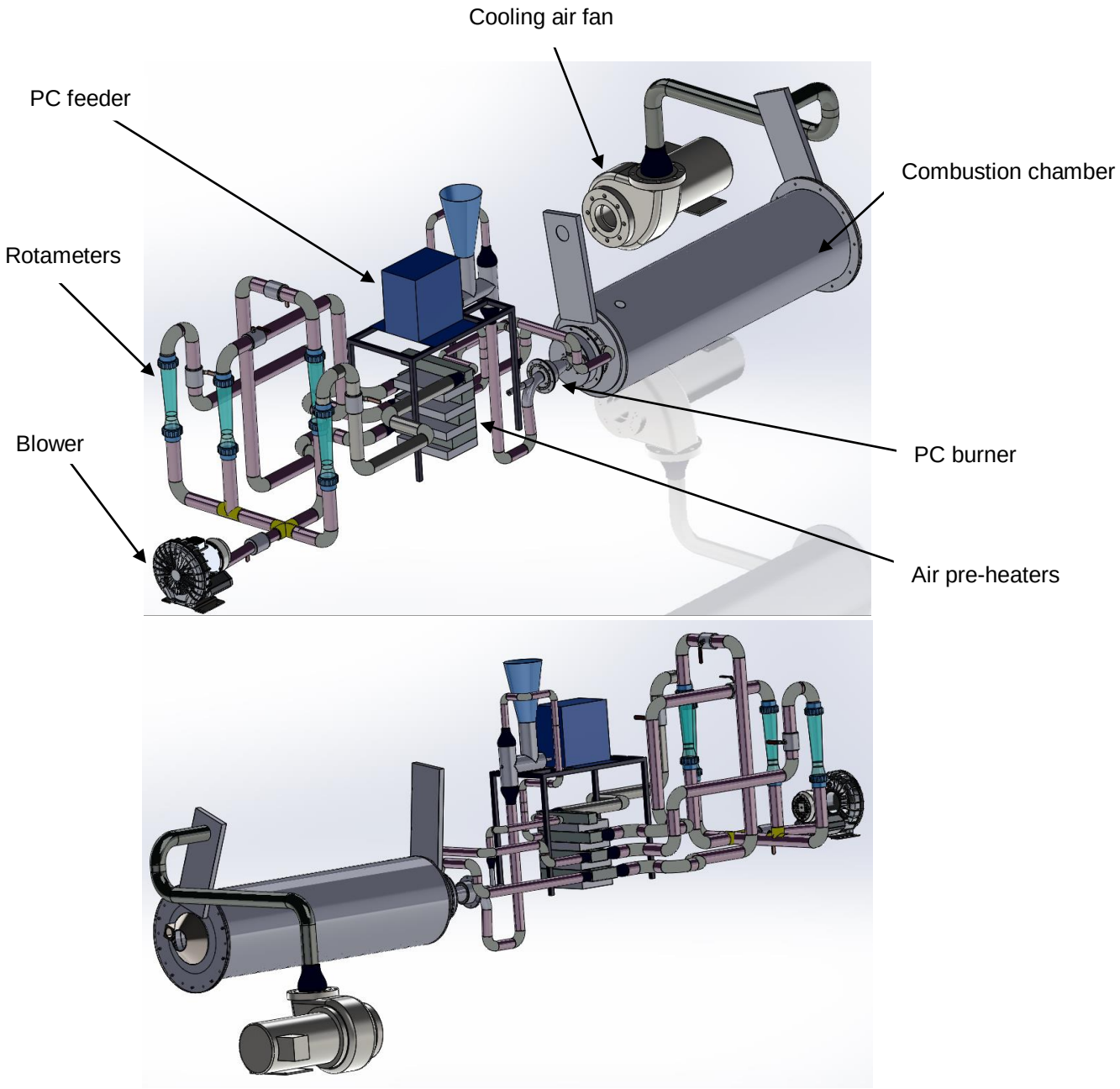

FIGURE 5.1: TWO VIEWS OF THE ASSEMBLY DRAWING OF NCV$_P$ COAL ANALYSER

5.1 COMMISSIONING OF THE NCV_P COAL ANALYSER

The following auxiliaries were needed to make the NCVp coal analyser functional:

5.1.1 PULVERISED COAL FEEDER

As explained in Section 3.4.1, a PC feeder was used to feed PC to the burner. The PC feeder consists of a storage bunker, screw conveyor, variable speed drive (VSD) AC induction motor and a load cell. The storage bunker contains the PC, which feeds into the burner. The induction motor drives the screw conveyor that is situated at the outlet of the storage bunker and conveys the PC from the bunker into the PA tube at a specific mass flow.

The VSD is used to control the speed at which the induction motor's shaft rotates and therefore, controls the speed at which the screw conveyor rotates. The speed of the screw conveyor dictates the rate at which PC is discharged from the PC bunker. The load cell serves as an indicator of PC mass flow that is delivered by the PC feeder. The load cell is connected to the PC feeder and measures the loss of weight. The loss of weight is then divided by a time interval and the mass flow is calculated and displayed. The commissioning of this feeder comprised of calibration, by correlating the volumetric feed to mass flow.

The PC feeder is shown in Figures 5.2 and 5.3.

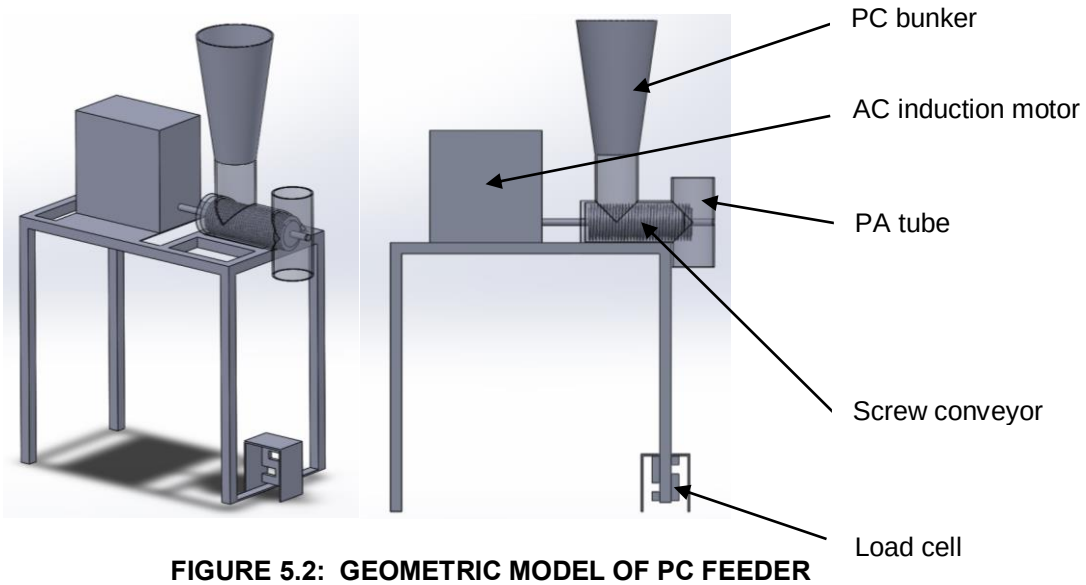

FIGURE 5.2: GEOMETRIC MODEL OF PC FEEDER

FIGURE 5.3: IMAGE OF PC FEEDER

5.1.2 ELECTRICAL AIR HEATERS

The electrical air heaters consist of a box constructed of mild steel, with an air flow inlet and outlet. Inside the box are cylindrical shaped electrical elements as well as guide vanes situated between the elements. As the air enters the electrical air heater at the inlet, it is forced to flow over the electrical elements by the guide vanes, thus absorbing the emitted heat from the elements, and exiting at the outlet. Situated at the outlet of each air heater is a thermocouple. The thermocouple is connected to a proportional–integral–derivative (PID) controller, which in turn is connected to the circuit breaker. The thermocouple measures the temperature of the air exiting the air heater and sends a signal of temperature to the PID controller. Once the PID controller receives this signal, it regulates the heat at a constant temperature set-point by switching the electrical air heaters on-and-off. The desired temperature can be set on the PID controller.

The flow models of the air heaters with temperature streamlines are shown in Figures 5.4 and 5.5.

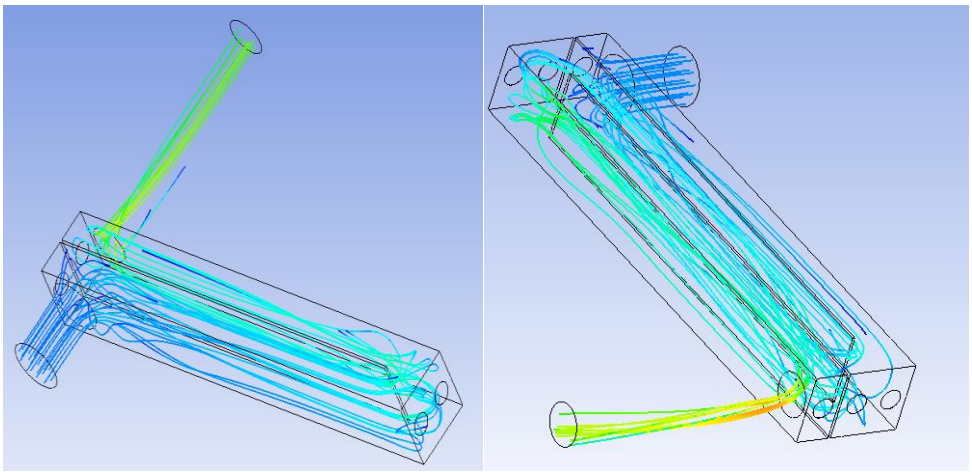

FIGURE 5.4: MODELS OF CA HEATER (LEFT) AND PA HEATER (RIGHT) WITH TEMPERATURE STREAMLINES

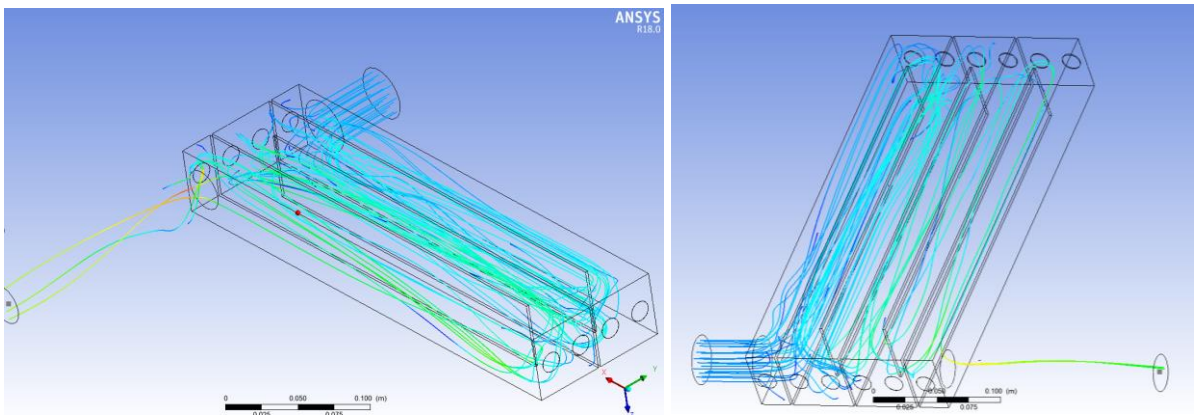

FIGURE 5.5: MODELS OF SA HEATER (LEFT) AND TA HEATER (RIGHT) WITH TEMPERATURE STREAMLINES

The internal view of the actual CA heater is shown in Figure 5.6, as well as the air heater set-up in Figure 5.7. The PID controllers for each air heater are shown in Figure 5.8.

FIGURE 5.6: IMAGE SHOWING INTERNAL VIEW OF ACTUAL CA HEATER

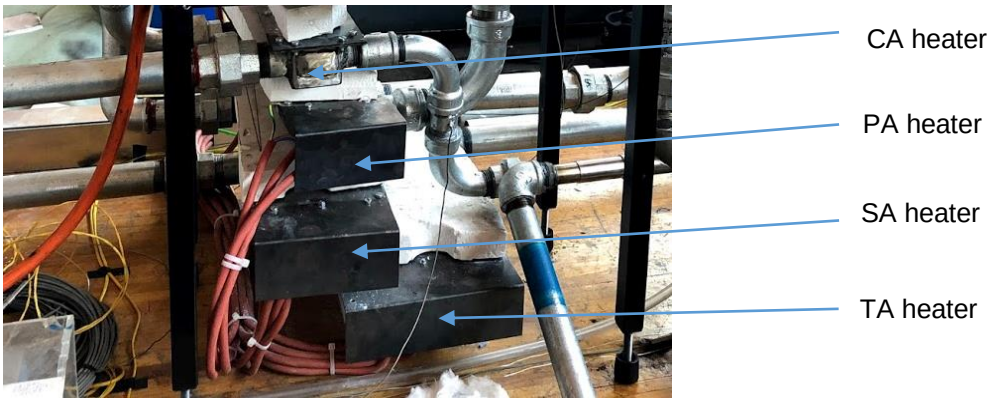

FIGURE 5.7: IMAGE SHOWING ACTUAL AIR HEATERS

FIGURE 5.8: PID CONTROLLERS

5.1.3 COMBUSTION AIR BLOWER

The air compressor needs to be able to deliver a sufficient amount of combustion air to the burner and overcome the back pressure created by the rotameters, air heaters and the burner.

It was established previously that the maximum amount of combustion air was 30.0 g/s. The blower discharges air to the burner by using a single tube. The tube then splits into four parallel tubes, each connected to the rotameters used to measure the volume flows of CA, PA, SA and TA air heaters respectively. As mentioned before, the SA and TA air streams supply heated air to the SA tube of the burner. After the air heaters, each air stream is connected to the respective burner tube. Since the air flows of CA, PA, SA and TA are in parallel, the airflow stream that produces the highest back pressure was the limiting factor. The pressure required by the air compressor was determined by using CFD on each air heater and burner tube, as well as the pressure loss due to the rotameters.

The CFD results of the air heater pressures were determined and are shown in the following table:

TABLE 5.1: PRESSURE LOSSES OF AIR HEATERS

	CA heater	PA heater	SA heater	TA heater
Pressure loss [kPa]	0.142	0.418	1.322	1.989

The CFD results of the burner tube pressure losses were determined and are shown in the following table:

TABLE 5.2: PRESSURE LOSSES OF BURNER TUBES

	CA tube	PA tube	SA tube	TA tube
Pressure loss [kPa]	0.112	0.700	0.734	0.740

The pressure loss of the rotameters stated by the supplier is 0.3 kPa.

Thus the total head loss of each stream is given in Table 5.3:

TABLE 5.3: TOTAL PRESSURE LOSSES

	CA	PA	SA	TA
Pressure loss [kPa]	0.454	1.418	2.357	3.029

The CFD results of the air heaters and burner tubes pressure distributions can be seen in Appendix G.

The stream with the highest pressure loss is the TA stream. Therefore, it was determined that an air blower is required to deliver 30.0 g/s at a pressure greater than 3.029 kPa.

The air blower that was chosen is a side channel air blower and exhauster. It can be seen in Appendix H, that the blower can deliver 40 l/s (40 g/s @ 40 ^{o}C) at 20 kPa which is suitable for this application.

FIGURE 5.9: IMAGE OF SIDE CHANNEL AIR BLOWER AND EXHAUSTER

5.1.4 CENTRIFUGAL AIR FAN

Since it was determined that the cooling fluid inside the cooling jacket would be air, a fan with suitable capacity was required. The fan needed to deliver a sufficient amount of air and overcome any pressure losses inside the cooling jacket. It was determined in Section 4.2.2 that the amount of cooling air required was 0.0571 kg/s.

Using a CFD model, which can be seen in Appendix I, it was determined that the pressure loss inside the cooling jacket was 1.898 kPa. A centrifugal fan was chosen to deliver the correct amount of cooling air at sufficient pressure. This can be seen in Appendix J.

FIGURE 5.10: IMAGE OF CENTRIFUGAL COOLING FAN

5.1.5 ROTAMETERS

Rotameters were chosen as suitable measuring devices for the combustion air, since according to the supplier the accuracy is within 2.5% at a relatively favourable cost. The calibration certificate is included in Appendix K.

However, rotameters measure volumetrically, but a gravimetric value is required for calculations. The rotameters were calibrated in terms of a normal temperature and pressure (NTP) reference. To determine the gravimetric amount, the actual temperature and pressure of the air at the rotameter were measured and the gravimetric amount was then calculated.

5.1.6 THERMOCOUPLES

Thermocouples were chosen to measure the temperatures of the NCVp coal analyser. In total, eight thermocouples were used and these were placed at the following locations:

- The outlet of the blower to determine the mass flow of combustion air;
- After each air heater, to regulate the temperature of the air streams giving an input to a PID controller;
- The burner mouth inside the combustion chamber, to monitor the flame temperature;
- Inside the AL-30 wall, near the burner mouth, to monitor the wall temperature;
- At the outlet of the combustion chamber to measure the temperature at which the flue gas exits;
- The in-and-outlet of the cooling jacket of the combustion chamber.

The following table shows the material composition, accuracy and temperature ranges of different thermocouples:

TABLE 5.4: ACCURACY AND TEMPERATURE RANGES OF DIFFERENT THERMOCOUPLES (MODIFIED AFTER WUHAN GLOBAL METAL ENGINEERING CO., LTD. 2019)

Conductor material	Wire Calibration	Accuracy			
		Class		Class	
		Accuracy	Temperature range(℃)	Accuracy	Temperature range()
Ni Cr-Ni Si	K	1.5 or 0.4%t	-40-1000	2.5 or 0.75%t	-40-1000
Ni Cr Si-Ni Si	E		-40-1100		-40-1200
NiCr-Konstantan	N		-40-800		-40-800
Fe-Konstantan	J		-40-750		-40-750
Cu-Konstantan	T	1 or 0.4%t	-40-350	1.5 or 0.75%t	-40-350
Pt Rh 10-Pt	S	1or 1+t-1100× 0.003	0-1600	1.5 or 0.25%t	0-1600
PtRh 13-Pt	R		0-1600		
Pt Rh30-PtRh 6	B				600-1700

K-type thermocouples were used at the blower outlet, the outlets of the air heaters and the in- and-outlet of the cooling jacket, since the temperature ranges from 20°C - 300°C. The thermocouples used at the burner mouth, AL-30 wall, and combustion chamber outlet were B-type thermocouples because of temperature ranges of 600°C – 1600°C. The thermocouples were calibrated by using a calibration oven. The calibration certificate for the oven is attached in Appendix L.

FIGURE 5.11: B-TYPE THERMOCOUPLE

5.1.7 ANEMOMETER

An anemometer was used to measure the velocity of the cooling air inside the cooling jacket, by utilising the pressure and temperature, the mass flow was then calculated.

FIGURE 5.12: IMAGE OF ANEMOMETER

5.1.8 MANOMETERS

To determine the mass flows of combustion air and cooling air from volume flow and temperature, water manometers were used to determine the gauge pressures. The manometers were placed at the blower outlet, rotameter outlets and centrifugal fan outlet.

FIGURE 5.13: IMAGE OF MANOMETERS

The figure below shows the assembled NCVp coal analyser including the PC burner, combustion chamber and auxiliaries:

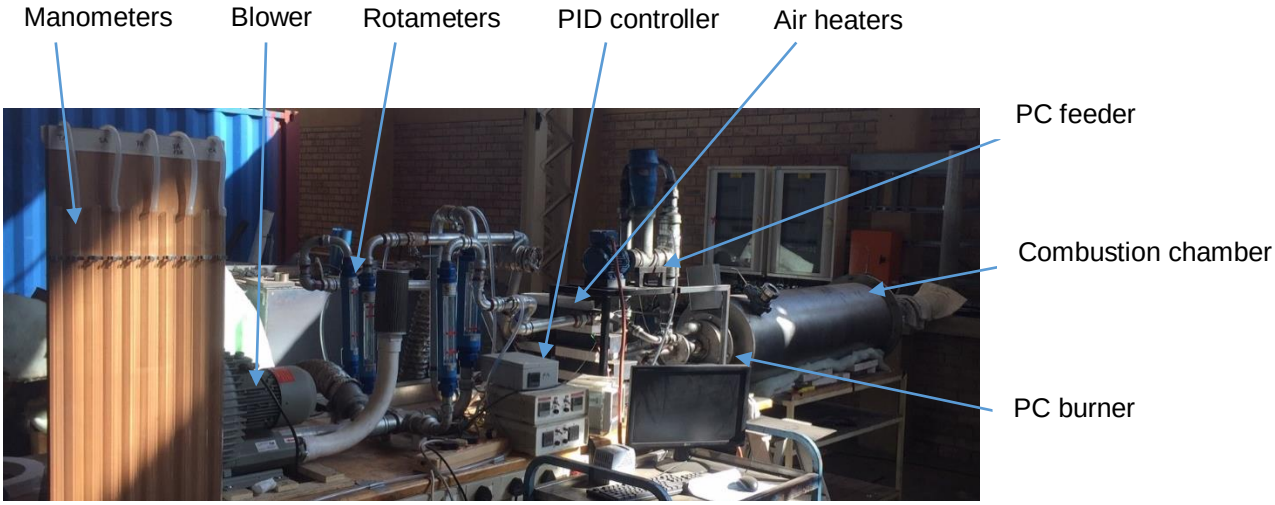

FIGURE 5.14: IMAGE OF ASSEMBLED NCV_P COAL ANALYSER

5.1.9 PRELIMINARY TESTS

After the NCVp coal analyser had been assembled, certain tests were carried out to confirm proper functioning. These tests related to air leak checks and air heater temperature control. Soap was used on the piping connections to see if any air leaks were present.

After the air leaks had been checked, the air heaters were tested to establish if the temperature could be controlled at a certain set-point. As stated before, the CA and PA heaters must heat air to a temperature of 150°C and the SA and TA heaters must heat air to a temperature of 280°C. The tests were performed and as seen in Figure 5.15, the PID controllers were able to keep the temperatures within 2°C of their respective set-points.

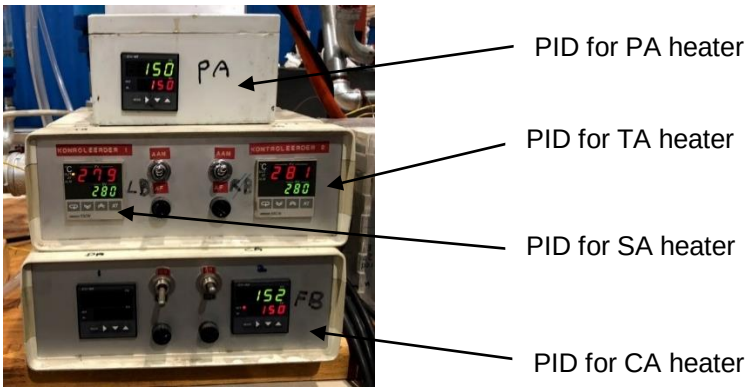

FIGURE 5.15: IMAGE OF PID CONTROLLERS DISPLAYING TEMPERATURES OF AIR HEATERS

5.1.10 LPG COMBUSTION TESTING

The first test run done on combustion involved applying an LPG flame only. This was to establish if the combustion chamber could withstand relatively high temperatures and if the thermocouples registered, as well as to evaluate and compare the aerodynamic flow field of the burner to the CFD. Therefore, the swirl angles were set at maximum. The test was carried out by introducing a minimum amount of LPG at first and then igniting it. After the LPG had been lit, an amount of CA was provided to avoid blow-off. The correct amounts of CA, PA and SA were then provided to the PC burner, as designed for the 80 kW heat rate. However, the LPG was then set at 0.3 g/s, which equates to 13.5 kW heat rate (25% higher than the designed heat rate), to create a longer flame in order to observe and evaluate the aerodynamic flow field. Figure 5.16 shows the LPG flame as seen from the side and front inspection holes:

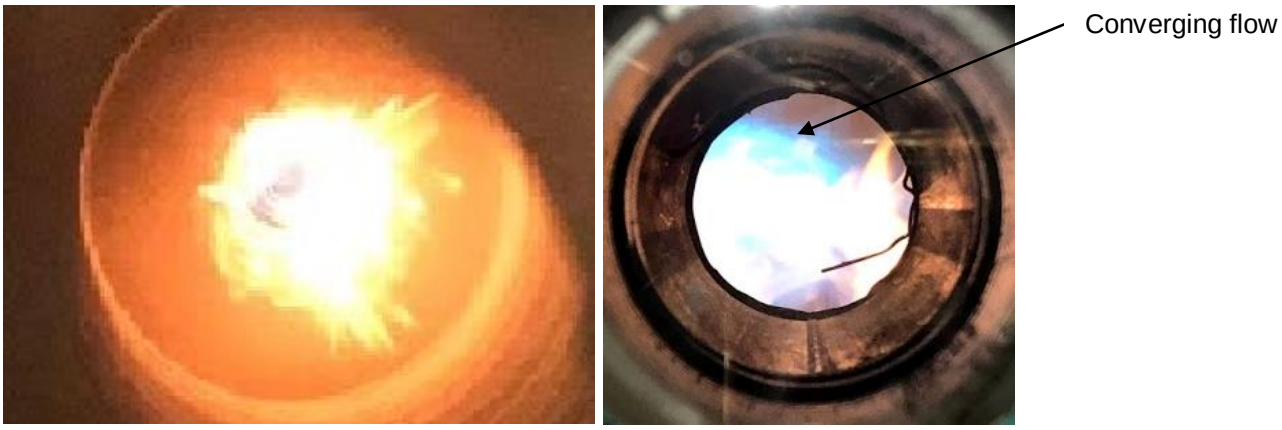

FIGURE 5.16: IMAGES OF THE LPG FLAME TAKEN THROUGH THE FRONT (LEFT) AND SIDE (RIGHT) SIGHT GLASSES OF THE COMBUSTION CHAMBER

The front view only reveals the yellow part of the flame. The side view shows the flame transitioning from a blue to a yellow flame. The blueish part of the flame cannot be seen in the front view owing to the over shadowing of the yellow front part of the flame. The side view (blue part of the flame) shows a converging flow profile. The front view shows evidence of turbulence in the flow.

5.1.11 CALIBRATION OF THE NCV_P COAL ANALYSER

The purpose of this exercise was to validate the accuracy of the NCVp coal analyser and simultaneously establish the magnitude of possible unaccounted heat losses. To accomplish this, the NCVp coal analyser was calibrated by utilising LPG only, which has an independently tested NCVp of 46.6 MJ/kg (Chemical engineering, Queens University, 2014). This known NCVp of LPG was also determined by gas flow calorimeters. Therefore, this established value was used to compare to the NCVp of LPG as obtained by this NCVp coal analyser.

The test was carried out by burning LPG until steady state conditions of the NCVp coal analyser had been reached. The mass flows, temperatures and pressures measured at that stage were used to calculate the NCVp of LPG. The results are shown in Table 5.5 below:

TABLE 5.5: RESULTS OF LPG NCV_P DETERMINATION WITH NCV_P COAL ANALAYSER

TESTED NCV_P LPG MASS - ENERGY BALANCE						
	MASS - ENERGY IN					
Property	**CA**	**PA**	**SA**	**TA**	**LPG**	**Total**
$\dot{m}$ [g/s]	3,661	1,967	1,788	2,281	0,247	9,944
c_P [kJ/kg-K]	1,043841	1,044031	1,043841	1,044052	***1,658000***	
Temperature [°C]	150,000	150,000	150,000	150,000	18,000	
$\dot{Q}$ [kW]	1,617	0,869	0,790	1,008	0,119	4,403
	MASS - ENERGY OUT					
Property	**Flue Gas**	**Cooling Air**	**Losses**			**Total**
$\dot{m}$ [g/s]	9,943942	76,28696935				
c_P [kJ/kg-K]	1,216656099	1,052016				
Temperature [°C]	664	59,000				
$\dot{Q}$ [kW]	11,33797568	**4,735**	**0,000**			16,073
	MASS - ENERGY BALANCE					
$\dot{Q}$ [kW]	11,670					
NCV_P [MJ/kg]	**47,248**					

The results show that the 47.248 MJ/kg NCVp of LPG, obtained by using the NCVp coal analyser, differs only by 1.4% compared to the known reference NCVp of LPG. Therefore, this marginal difference indicates that the NCVp coal analyser is adequately accurate, as well as that possible unaccounted heat losses are negligible.

5.1.12 PULVERISED COAL SETTLING FLOW TEST

After LPG combustion had been tested, a test run was performed to evaluate the flow of PC through the burner. The airflows of the CA, PA and SA were unchanged from the conditions in Section 5.1.10, and the feed rate of PC was set at 1.5 g/s. After the test had been completed, it was noticed that some PC had settled in the tapered part of the PC/PA tube, before the PA swirler as shown in Figure 5.17 (left). To explain this phenomenon, the velocity streamlines of the PA, where the PC settling took place, needed to be analysed carefully by using a CFD analysis. This CFD analysis is shown in Figure 5.17 (right):

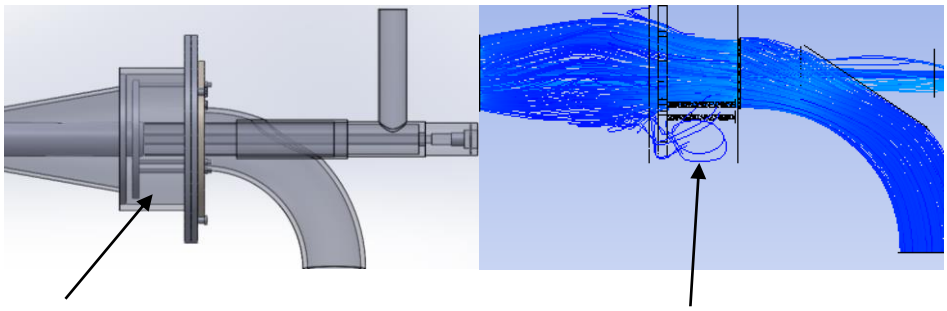

FIGURE 5.17: LOCATION IN THE BURNER WHERE PC SETTLING OCCURED (LEFT) AND STREAMLINES SHOWING PREDICTED PC SETTLING (RIGHT)

Figure 5.17 indicates the area where some PC settled, as well as the streamlines of the PA. The streamlines indicate that that there is a recirculation zone indicating a low velocity-area in the same location where PC settling took place. To solve this problem, it was decided that a tube had to be connected to the swirler at the end of the elbow, to prevent a low- velocity- recirculating area from forming. This would, however, prevent adjustable swirl. It was also deemed necessary to increase the PA from 6.5 g/s to 7.5 g/s, to increase the velocity in the PA/ PC tube and prevent PC settling. The A: F

in the PC/ PA tube was still safe regarding possible upstream combustion. The modification to the PA tube is shown in Figure 5.18:

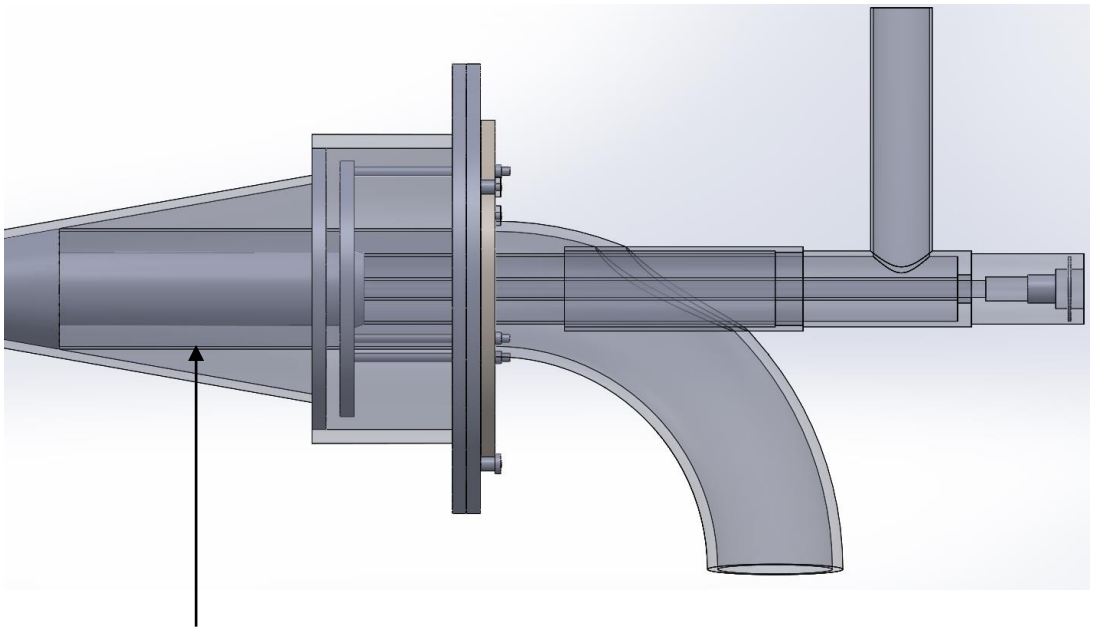

FIGURE 5.18: FRONT VIEW OF LPG FLAME AT A PORTIAN AMOUNT OF MASS FLOW WITHOUT CA AFTER IGNITION

5.2 ACTUAL COAL COMBUSTION TESTING

The main objective described in this section was to demonstrate proof of concept, that is, to establish continuous, self-sustaining combustion of PC without any LPG flame support, for a single burner at this relatively small thermal heat rate. The results of this section were used to evaluate the PC flame using CFD, and to determine the NCVp of the tested coal, as will be explained in Chapter 6.

Unfortunately, the exact analysis of the coal that was tested, was not yet available at that time. Therefore, the planning and settings for this test were done for a coal quality in the intermediate range as explained in Section 4.1.2. However, the test was carried out successfully, and after the tested coal's analysis was obtained, the subsequent calculated A: Fs etc., are shown and explained in Chapter 6.

Because the tested coal's analysis was unknown, the A: F for an intermediate coal was increased to ensure that combustion occurred for a lower or a higher quality coal, since the most prominent reason for flame-outs is due to an insufficient amount of combustion air.

5.2.1 COAL PREPARATION

The PC was dried before testing, at 100^{o}C for 1 hour, to obtain a dry basis. A dry basis was used for better coal combustion and ignition purposes and provided a more consistent base for NCVp calculation, since coal does not contain constant surface moisture. The inherent and surface moisture can be included in the calculations to obtain the NCVp for coal on an air-dried and as received basis.

5.2.2 START-UP PROCEDURE

- Firstly, the cooling air was supplied to cool the combustion chamber via the cooling jacket.
- Thereafter, a partial amount of the designed mass flow of LPG was supplied to be ignited, as seen in Figure 5.19. This pilot flame burned with the ambient air in the combustion chamber without any CA.

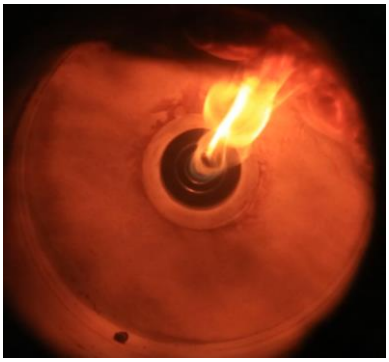

FIGURE 5.19: IMAGE SHOWING FRONT VIEW OF FLAME AT A PARTIAL AMOUNT OF LPG MASS FLOW

- After the LPG had been ignited, a relatively small amount of CA was supplied. When the LPG flame stabilised, the correct mass flows of LPG and CA were provided. The purpose of the LPG flame was to pre-heat the combustion chamber before supplying the PC.
- Small amounts of PA and SA were also provided to cool the tubes of the PC burner to prevent damage and avoid cooling down the chamber, which would prolong the pre-heating of the LPG flame.
- At this stage the air heaters were set at the respective set-points of 150 and 280^{o}C.
- These settings stayed the same until the combustion chamber wall's thermocouple had reached 600^{o}C.

The following figure shows the LPG flame that was produced to pre-heat the combustion chamber:

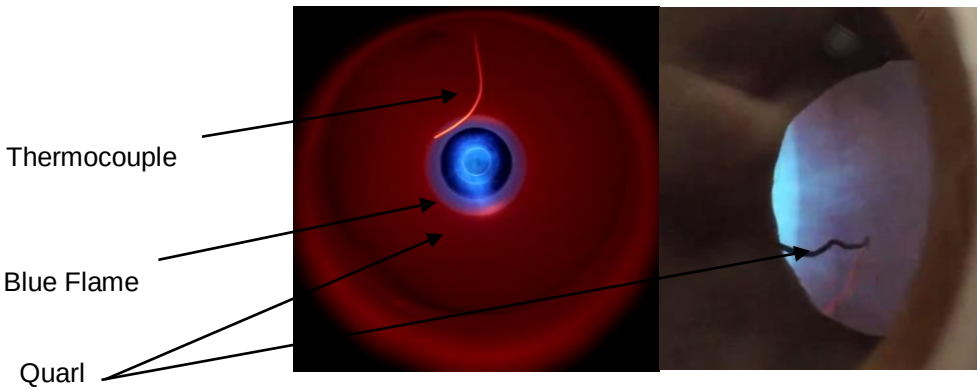

FIGURE 5.20: FRONT VIEW (LEFT) AND SIDE VIEW (RIGHT) SHOWING IMAGES OF LPG FLAME AT DESIGNED MASS FLOWS OF LPG AND CA

From Figure 5.20, it can be seen that the blue flame is very short which indicates rapid combustion. The red glow of the AL-30 indicates that the flame heats up the combustion chamber, but more importantly,

the quarl. As the fuel – air mixture exits the burner, it firstly makes contact with the hot quarl which promotes ignition. The thermocouple is situated near the flame to measure the flame temperature.

5.2.3 PULVERISED COAL FIRING PROCEDURE

- To prevent thermal shock to the combustion chamber, it was decided that the PC was to be admitted in stages to increase the thermal load gradually until the maximum thermal load for the test was reached.
- Since the minimum PC mass flow the feeder can deliver is 1.5 g/s, this was the starting point of the test.
- The PA and SA were then set for the assumed intermediate coal A: F since the analysis of the test coal tested was not yet available.
- The PA and SA were supplied prior to the PC, since the air heaters first had to stabilise and reach the set temperatures.

Some PC was entrained when the PA was applied (prior to the PC feeder being started) because of some remaining PC from the previous test in the PC/PA tube. Figure 5.21 shows the ignition of this entrained PC:

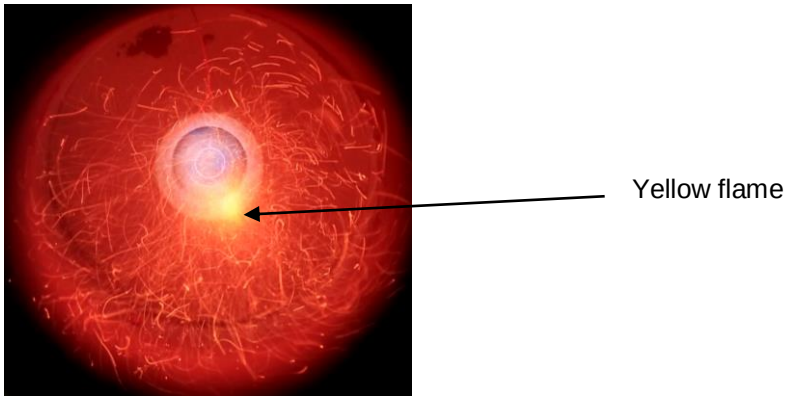

FIGURE 5.21: IMAGE SHOWING THE FRONT VIEW OF THE LPG FLAME WITH IGNITION OF A PORTION OF ENTRAINED PC

It can be seen from Figure 5.21 that a yellow PC flame starts to form near the burner mouth and coal particles continue to burn in the form of glowing sparks. The streamlines of the coal particles show a lot of recirculation and turbulence.

- After the air temperatures had stabilised, the feeder was set to supply the minimum of 1.5 g/s. Figure 5.22 shows the combustion in the transition of the PC feed increasing to the set point:

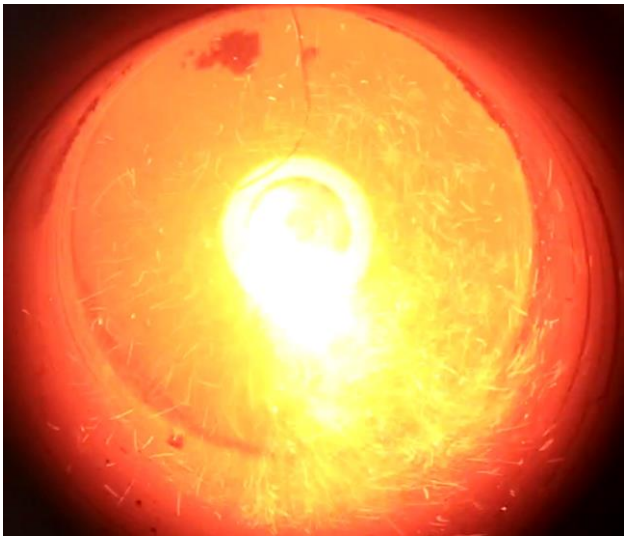

FIGURE 5.22: IMAGE SHOWING THE FRONT VIEW OF THE INCREASING PC COMBUSTION

- As the mass flow of PC started to approach the set point of 1.5 g/s, the brilliance increased such that no detail of the flame could be seen from the front inspection hole. However, when a dark filter was used on the camera, some of the glare was removed and more detail of the flame could be seen.

Figures 5.23 and 5.24 show the front view and side view of the flame as the degree of the dark filter was increased progressively:

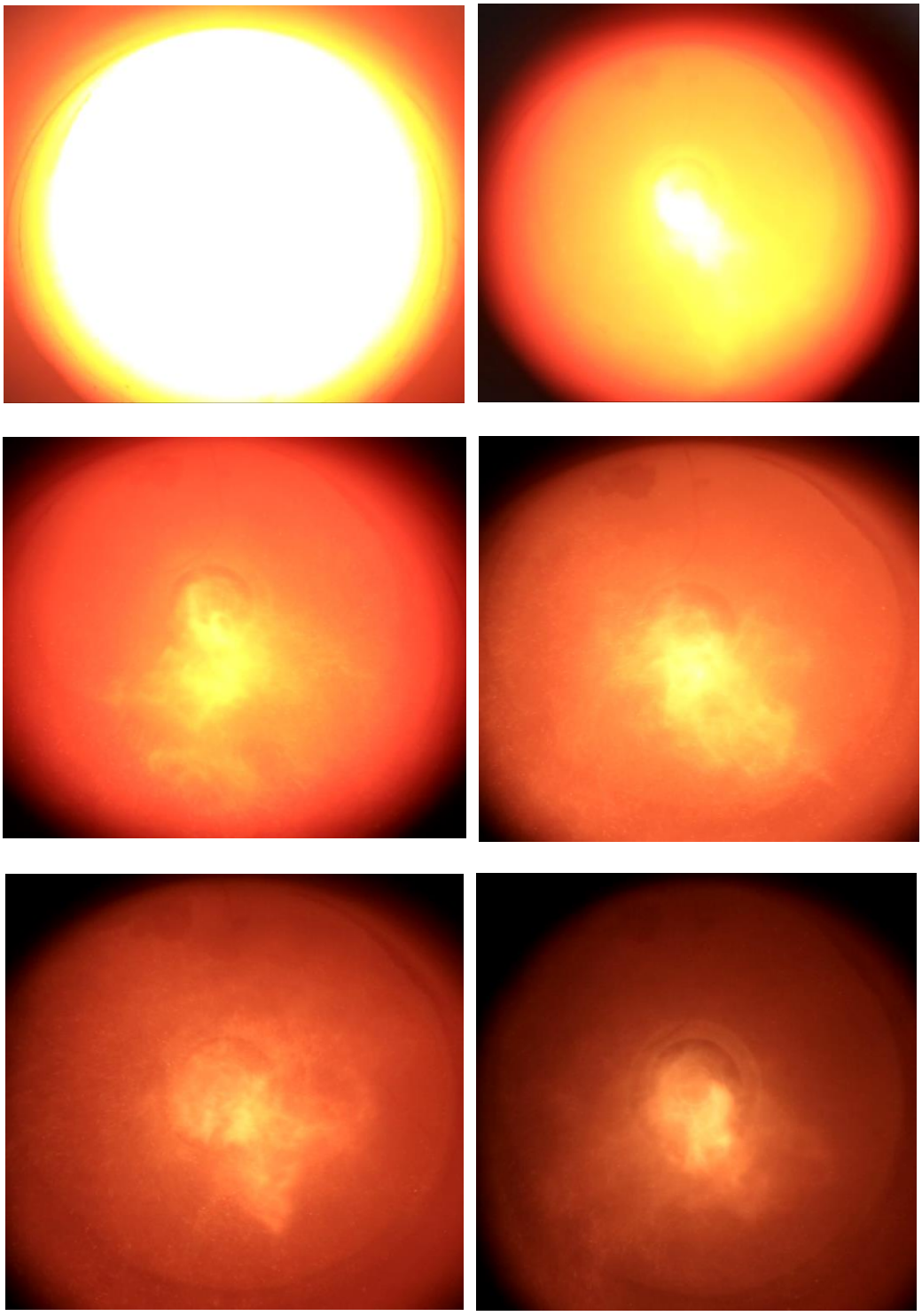

FIGURE 5.23: IMAGES SHOWING THE FRONT VIEW OF LPG-PC FLAME WHILE INCREASING THE DEGREE OF DARK FILTERING

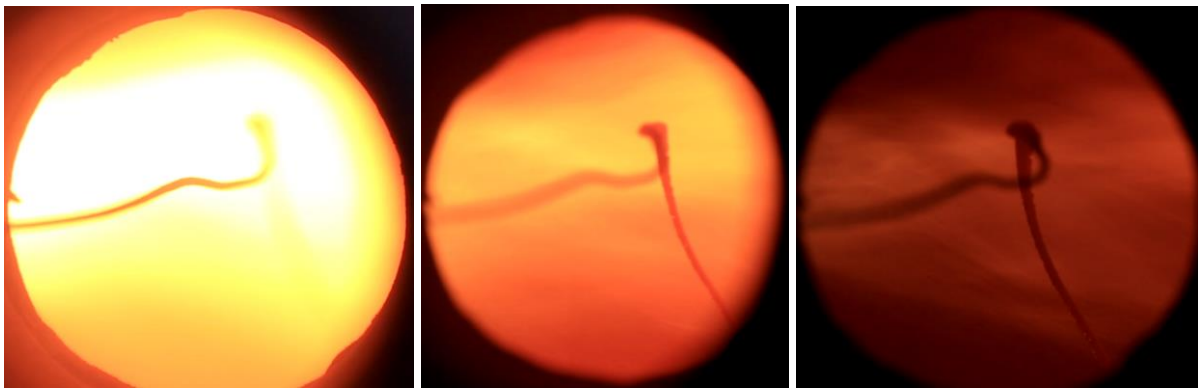

FIGURE 5.24: IMAGES SHOWING THE SIDE VIEW OF THE LPG-PC FLAME WHILE INCREASING THE DEGREE OF DARK FILTERING

- The settings of the LPG and PC flame were unchanged to allow for the flame and combustion chamber temperatures to stabilise.
- The next step was to reduce the LPG supply gradually to zero, in order to establish if the PC flame could continuously be self-sustaining without any LPG flame support.
- After turning off the LPG completely, a continuously self-sustaining PC flame occurred.

Figure 5.25 shows the self-sustaining PC flame without any LPG support. A dark filter was once again applied to reduce the brilliance of the PC flame, which was equivalent to the first image shown in Figure 5.23.

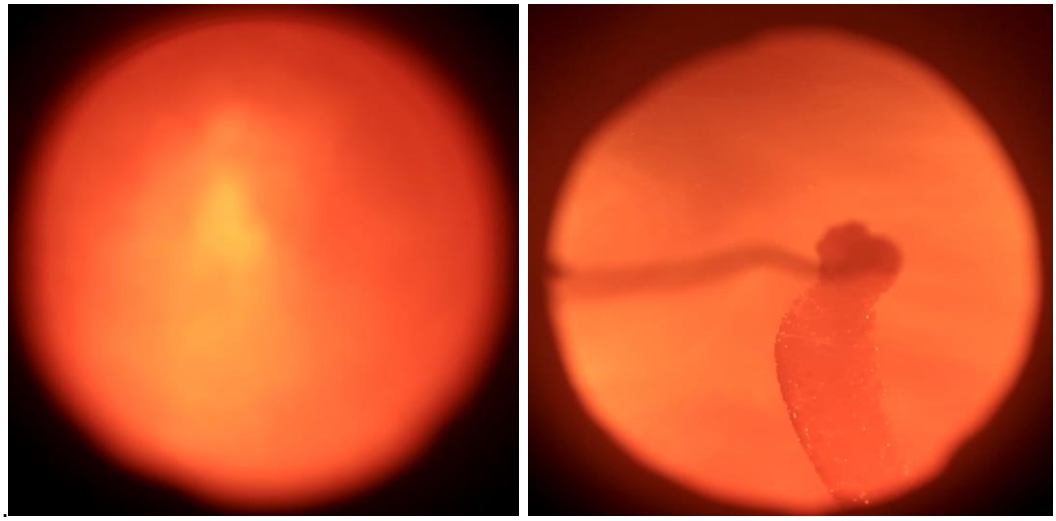

FIGURE 5.25: IMAGES OF FRONT VIEW (LEFT), AND SIDE VIEW (RIGHT) OF SELF-SUSTAINING PC FLAME WHILE USING DARK FILTERING

The quality of Figure 5.25 is worse than that of previous figures because of fly ash particles starting to precipitate on the inspection hole glasses. Slight fly ash clinkering started to form on the thermocouple measuring the flame temperature, which can be seen in Figure 5.25 on the right.

While the self-sustaining PC flame burned, a slight pulsating effect was noticed in the flame. This can be seen in Figures 5.26 and 5.27, showing a front and side view comparison. The images on the left show a more prominent flame image than the images on the right, respectively.

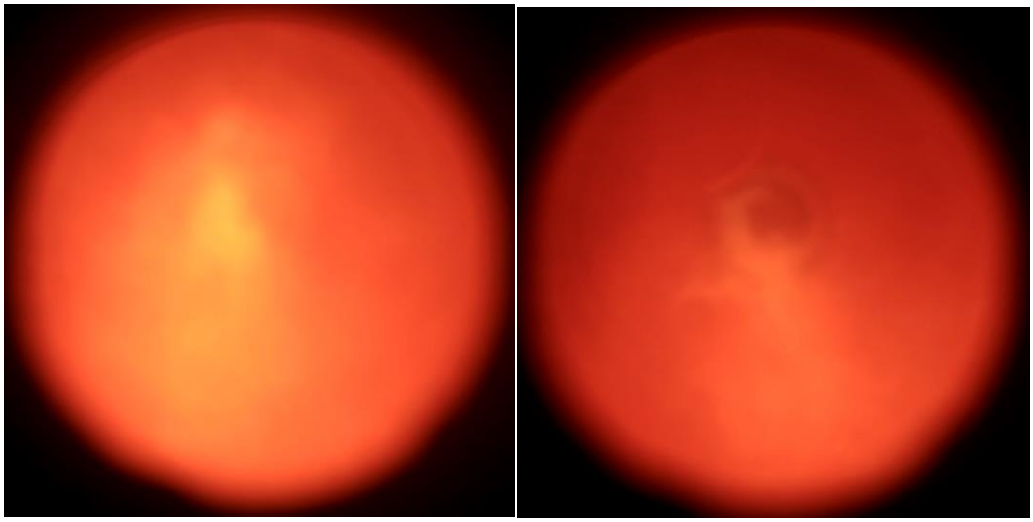

FIGURE 5.26: IMAGES SHOWING THE FRONT VIEW COMPARISON OF THE MORE PROMINENT (LEFT) AND LESS PROMINENT (RIGHT) PULSATING FLAME

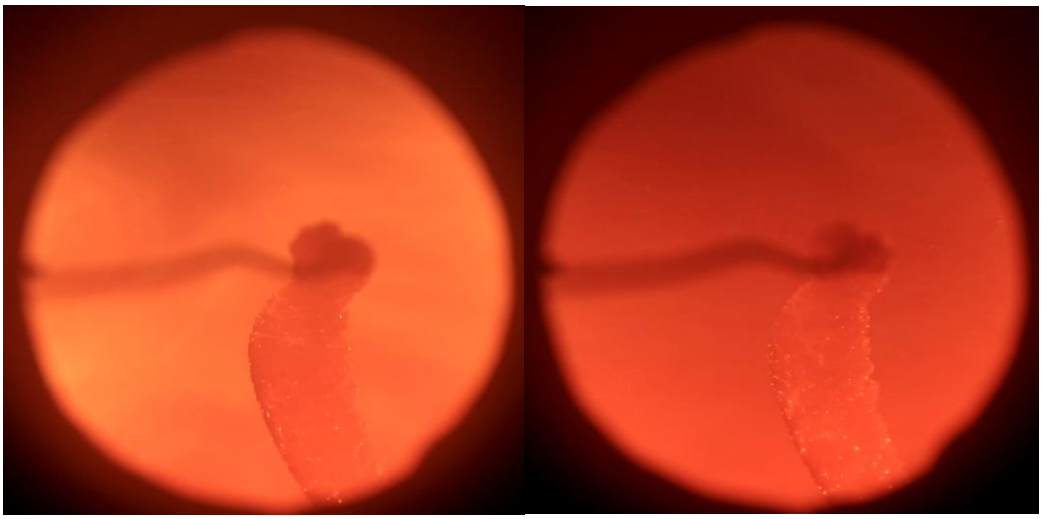

FIGURE 5.27: IMAGES SHOWING THE SIDE VIEW COMPARISON OF THE MORE PROMINENT (LEFT) AND LESS PROMINENT (RIGHT) PULSATING FLAME

This pulsating effect of the flame was due to the feeder producing pulsating flow when feeding PC at 1.5 g/s.

5.3 CONCLUSION OF COAL COMBUSTION TEST

The actions and the achievements described in this section are the following:

- The primary device (PC burner and combustion chamber) and the supporting auxiliaries were commissioned and tested successfully.
- Combustion testing with LPG only was performed for validation of the CFD flow field in Chapter 4. Moreover, this LPG test was used to test all temperature measurements, as well as material durability.
- By firing LPG with a known NCVp, the NCVp coal analyser was calibrated within an acceptable margin. Unaccounted heat losses were found to be negligible.
- PC flow testing was performed and the observed deficiency of PC settling was corrected with a design modification.
- The main objective of this test was to demonstrate the proof of concept, that is, to attain a self-sustaining, continuous PC flame without any LPG flame support for a single burner of this relatively small thermal rating. The proof of concept was indeed demonstrated.

Since a self-sustaining PC flame was established, and the analysis of the tested coal was not yet available, it was decided not to increase the thermal load at this stage. However, the conditions were such that an NCVp calculation of the tested coal was possible, since all the necessary temperatures, pressures, volume flows and mass flows were documented at steady state conditions after 27 minutes of continuous coal combustion.

6 CALCULATIONS AND INTERPRETATION OF RESULTS

In this chapter, the following is discussed:

- Validating the PC burner design by comparing the LPG flame profile with the CFD obtained;
- Air flow calculations of actual test, with known tested coal analysis;
- Self-sustaining, PC flame profile evaluation of actual test, by using CFD;
- PC burner performance and combustion efficiency;
- NCVp calculation of tested coal.

6.1 VALIDATION OF PC BURNER DESIGN

To validate the CFD used for the PC burner design at a load of 80 kW, the LPG flame test, done in Section 5.1.10, was used. As mentioned, all the air settings were as per design. In addition, the LPG amount was increased to create a larger flame to enable better analysis of the flame profile. In comparing the CFD with the LPG flame, only the outer profile could be compared, since it is difficult to do exact observation of the LPG flame's internal profile, such as recirculation and swirl, on an image.

In Figure 6.1, the left image shows the front view of the LPG flame, which is yellow and white, as seen from the inspection hole. The right image shows the cold flow streamlines obtained from CFD, used to design the PC burner, where the large circle indicates where the flame is observed from the front inspection hole. Both images in Figure 6.1 were front views that were slightly angled. When comparing the profile of the cold flow streamlines (obtained from CFD), and the actual flame profile, it can be seen that they are quite similar. This is an indication that cold flow streamlines represent the flame quite accurately.

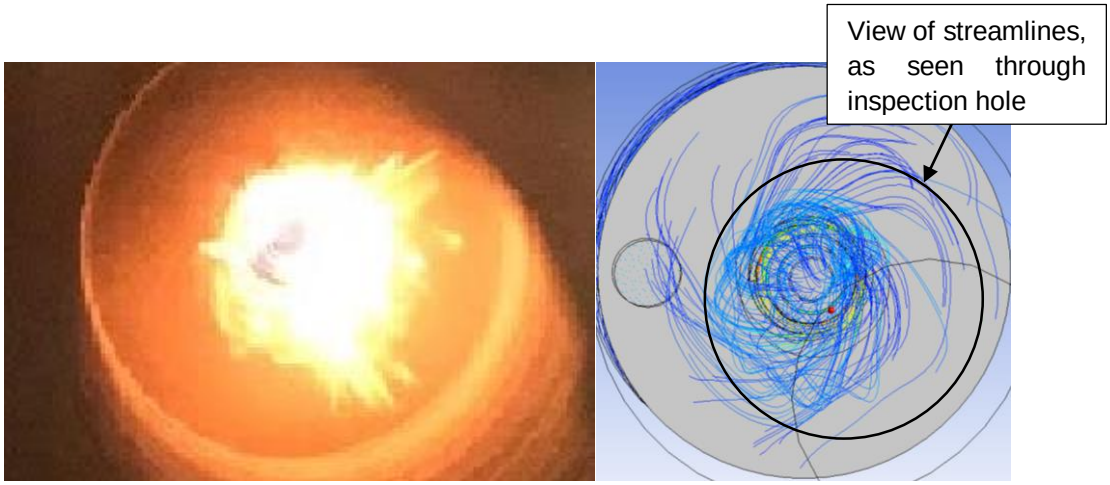

FIGURE 6.1: FRONT VIEW OF LPG FLAME IMAGE (LEFT) COMPARED TO CFD STREAMLINES (RIGHT)

Figure 6.2 shows the side views of the same LPG flame and CFD streamlines as in Figure 6.1. Again, the circle in the CFD streamlines image (right) indicate the inspection hole view. It seems as if the flame consists of a blue part and a yellow part. Close to the burner mouth, the flame is blueish. The flame then gradually turns yellow which can only be seen clearly in the front view of Figure 6.1. The blue part of the flame shows a converging flow pattern, while the yellow part shows a diverging flow pattern.

All the converging, diverging and recirculation streamlines can be realistically correlated to the image of the actual flame on the left. It can therefore be concluded that the actual flame represents the cold flow CFD streamlines model closely.

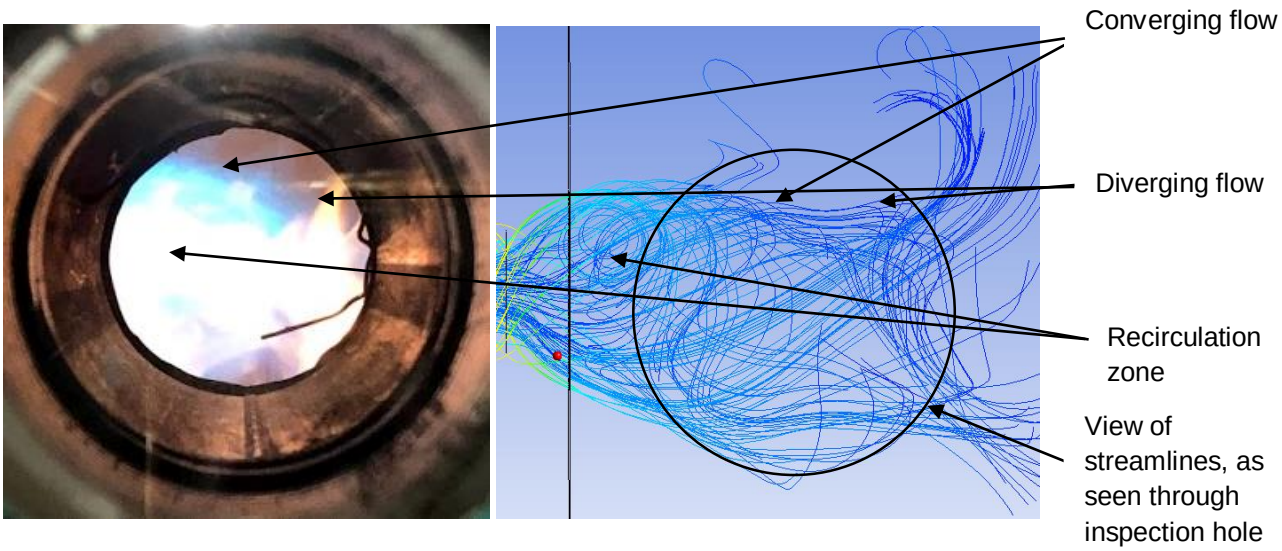

FIGURE 6.2: SIDE VIEW OF LPG FLAME IMAGE (LEFT) COMPARED TO CFD STREAMLINES (RIGHT)

6.2 AIR FLOW CALCULATIONS OF ACTUAL TEST

As mentioned in Section 5.2, the coal that was used during the test had not yet been analysed, and the A: F and excess air were calculated on the basis of an assumed intermediate coal analysis. However, after the test had been completed, the coal was analysed, and the analysis was used to determine the actual A: F and excess air of the test. The coal analysis can be seen in Table 6.1, which is on an air-dried basis:

TABLE 6.1: ANALYSIS OF ACTUAL TESTED COAL

Component	Unit	Value
Analytical Moisture	%	3.3
Ash	%	41.3
Volatile Matter	%	20.5
Fixed Carbon (by difference)	%	34.9
Carbon	%	40.35
Hydrogen	%	1.84
Nitrogen	%	1.16
Total Sulphur	%	0.84
Carbonate	%	2.02
Oxygen (by difference)	%	9.19
Gross Calorific Value	MJ/kg	15.18

Since the NCVp test was carried out on a dry basis of coal, the air-dried analyses provided in Table 6.1 needed to be converted to a dry basis. The results are given in Table 6.2. It can be noted that the results of the air-dried and as received basis are the same, since no information was received on the surface moisture and it was taken as zero.

TABLE 6.2: PROXIMATE AND ELEMENTAL ANALYSIS OF TESTED COAL ON AN AS RECEIVED, AIR-DRIED AND DRY BASIS

COAL QUALITY					
GRAVIMETRIC %	**SYMBOL**	**UNITS**	**AS RECEIVED**	**AIR DRIED**	**DRY BASIS**
PROXIMATE ANALYSIS					
Carbon $_{FIXED}$ (by difference)	C_{FIX}	%	34.900	34.900	36.091
Volatile matter	VM	%	20.500	20.500	21.200
Ash	Ash	%	41.300	41.300	42.709
Surface moisture	M_s	%	0.000	0.000	0.000
Inherent moisture	M_i	%	3.300	3.300	0.000
Total moisture	M_t	%	3.300	3.300	0.000
Gross calorific value (Bomb)	GCV_V	[MJ/kg]	15.180	15.180	15.698
Total		%	100.000	100.000	100.000
ELEMENTAL ANALYSIS					
Nitrogen	N	%	1.160	1.160	1.200
Oxygen (by difference)	O	%	9.190	9.190	9.504
Carbon $_{TOTAL}$	C_{TOTAL}	%	40.350	40.350	41.727
Ash	A	%	41.300	41.300	42.709
Sulphur	S	%	0.840	0.840	0.869
Hydrogen	H	%	1.840	1.840	1.903
Carbonates	CO_2	%	2.020	2.020	2.089
Other	Cl, F	%	0.000	0.000	0.000
Surface Moisture	M_S	%	0.000	0.000	0.000
Inherent Moisture	M_i	%	3.300	3.300	0.000
Total moisture	M_T	%	3.300	3.300	0.000
Total		%	100.000	100.000	100.000

Next, the mass flows used for CA, PA and SA during the test had to be calculated, since the rotameters measure volumetrically. To calculate the mass flows, the temperatures and volume flows and pressures were required. The rotameters display the volume flow as a percentage of 0 – 100 %, where 100% is equal to the maximum of each respective rotameter used for CA, PA, SA and TA. Note that the TA and SA were both used to supply air to the SA tube. The maximum of the CA, PA and SA rotameters was calibrated as 7.753 l/s, while the maximum of the TA rotameter was 12.406 l/s at standard temperature and pressure (STP) which is at 0ºC and 101.325 kPa. The following table shows what the target percentage of each rotameter was at STP:

TABLE 6.3: MASS FLOW AND VOLUME FLOW AT STP FOR THE ROTAMETERS

STP VOLUME TO MASS						
	CA	**PA**	**SA**	**TA**	**SA + TA**	**Total**
R_{AIR} @ STP [kJ/kg-K]	0,287726	0,287726	0,287726	0,287726	0,287726	0,287726
Standard Temperature [°C]	0,000	0,000	0,000	0,000	0,000	0,000
Standard Pressure [kPa]	101,325	101,325	101,325	101,325	101,325	101,325
100% Meter Volume Flow @ STP [l/s]	7,753	7,753	7,753	12,406	20,159	35,665
100% Meter Massflow @ STP [g/s]	9,996	9,996	9,996	15,994	25,990	45,981
Target Meter Massflow @ STP [g/s]	3,698	7,887	2,635	2,083	4,718	16,303
Target Meter Volume Flow @ STP [l/s]	36,999%	78,903%	26,365%	13,023%		

However, the conditions of testing were not at STP. The actual temperature, atmospheric pressure and gauge pressure of CA, PA, SA and TA during the test were used to convert the volume flow and mass flow at 100% and target set points. The results are shown in Table 6.4:

TABLE 6.4: MASS FLOW AND VOLUME FLOW AT ACTUAL TEMPERATURES AND PRESSURES FOR ROTAMETERS

ACTUAL VOLUME TO MASS						
	CA	PA	SA	TA	SA + TA	Total
R_{AIR} Actual [kJ/kg-K]	0,288869	0,288869	0,288869	0,288869	0,288869	0,288869
Actual Temperature [°C]	45,100	45,100	45,100	45,100	45,100	45,100
Actual Atmospheric Pressure [kPa]	86,400	86,400	86,400	86,400	86,400	86,400
Actual Gauge Pressure [kPa]	4,776	4,338	4,776	4,289		4,545
100% Meter Volume Flow Actual [l/s]	6,813	6,797	6,813	10,873	17,687	31,297
100% Meter Massflow Actual [g/s]	8,784	8,763	8,784	14,019	22,803	40,350
Target Meter Mass Flow Actual with Gas [g/s]	3,698	7,887	2,635	2,083	4,718	12,605
Target Meter Volume Flow Actual with Gas [%]	42,100%	90,000%	30,000%	14,859%		
A:F with Gas	15,604	5,543				8,860
A:F with Gas [% of Stoichiometric]	100,000%	109,046%			*(2.43 % O_2)*	174,283%
Target Meter Mass Flow Actual without Gas [g/s]	3,698	7,887	2,635	2,083	4,718	16,303
Target Meter Volume Flow Actual without Gas [%]	42,100%	90,000%	30,000%	14,859%		
ACTUAL VOLUME TO MASS CORE AIR REDUCED WITHOUT GAS						
Target Meter Mass Flow Actual without Gas [g/s]	1,054	7,887	2,131	2,243	4,374	13,315
Target Meter Volume Flow Actual without Gas [%]	12,000%	90,000%	24,265%	16,000%		

The following step was to determine the actual and intended A: F and excess air during the test, after the mass flows of combustion air had been calculated in Table 6.4. However, the dry combustion air was required since the air used during the test contained some moisture. The amount of dry air and water vapour is shown in Table 6.5:

TABLE 6.5: MASS FLOW OF DRY COMBUSTION AIR AND WATER VAPOUR

M atmospheric air, actual	[g/s]	13.315
M dry air actual	[g/s]	13.211
M water vapour actual	[g/s]	0.104

During the test, the actual mass flow of PC was found to be 1.423 g/s. This mass flow of PC, dry combustion air and water vapour was used to determine the actual and intended A: Fs and excess air on a gravimetric dry basis. The same procedure was followed as in Section 4.1.2 and the summary results are shown in Table 6.6, whereas the detailed calculations can be seen in Appendix M. Note that, the O_2 in the flue gas is the volumetric wet value, corresponding to the other gravimetric dry values.

TABLE 6.6: SUMMARY OF AIRFLOW CALCULATIONS OF TEST

	Actual	Intended
A: F	9.285	5.778
Excess air	82.403%	13.503
O_2 in flue gas	9.467%	3.5%

Table 6.6 shows that the actual PC combustion test was completed by using a high amount of excess air compared to the intended amounts. Using the mass flow of PC, and the GCVv obtained from the test coal analysis, the actual thermal rating of the PC burner during the test was calculated at approximately 21.6 kW.

6.3 PULVERISED COAL FLAME ANALYSIS OF ACTUAL TEST

The actual self-sustaining PC flame test had a lower thermal loading (21.6 kW) than the maximum it was designed for (80 kW), as explained in the previous section. Consequently, the initial cold flow CFD could not be used to evaluate and analyse the actual test flame. Therefore, another cold flow CFD model was developed to evaluate the self-sustaining PC flame more accurately at the reduced load.

To accomplish the above, a CFD model was developed with the boundary conditions corresponding to the settings of the actual 20 kW PC flame test, shown in Table 6.7. The same mesh and turbulence model was used as for Model 3 in Section 4.1.4 (80 kW).

TABLE 6.7: BOUNDARY CONDITIONS FOR COLD FLOW CFD ON SELF-SUSTAINING 20kW PC FLAME TEST

	LPG	CA	PA	SA	Outlet
Inlet Mass Flow [g/s]	0	1.054	7.887	4.374	-
Inlet Temperature [^{o}C]	-	150	150	280	-
Outlet Pressure [kPa]	-	-	-	-	86

A comparison between the actual flame and the cold flow CFD streamlines was done, as in Section 6.1. Figure 6.3 shows the actual PC flame (left image) and cold flow CFD streamlines (right) at the same angled front view. The circle in the right image represents the front view through the inspection hole.

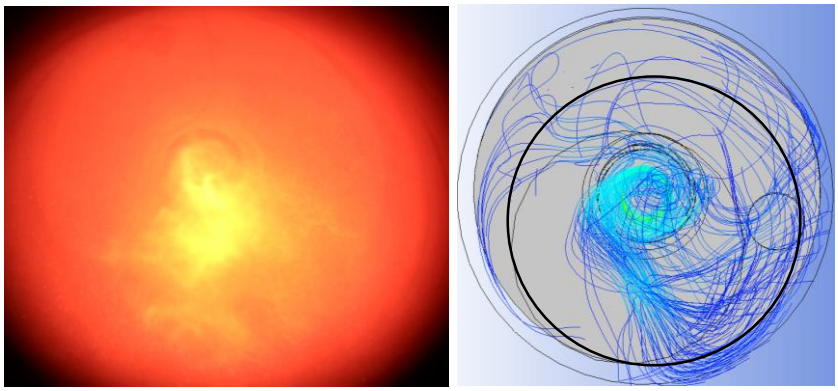

FIGURE 6.3: FRONT VIEW IMAGE COMPARISON OF ACTUAL PC FLAME (LEFT) AND CFD STREAMLINES (RIGHT)

Figure 6.4 shows the side view of the PC flame (left) and the CFD streamlines (right). The circle in the right image represents the sight from the inspection hole of the left image.

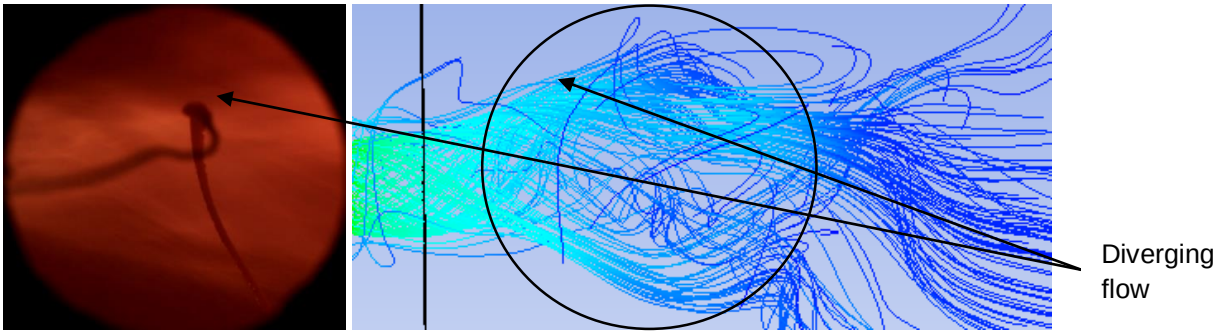

FIGURE 6.4: SIDE VIEW IMAGE COMPARISON OF ACTUAL PC FLAME (LEFT) AND CFD STREAMLINES (RIGHT)

Similar to Section 6.1, this actual flame at 21.6 kW, compares favourably with the cold flow CFD streamlines. It can be seen that the flame diverges similar to the streamlines and that the overall similarities validate the CFD.

The cold flow CFD streamlines of CA, PA, and SA separately (but with the combined influence), and all of the streams together are shown in Figure 6.5 – 6.8. The velocity and pressure contours are also shown in Figures 6.9 and 6.10:

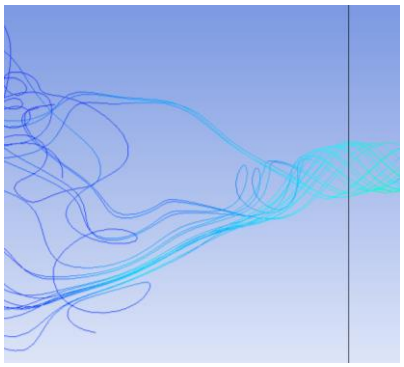

FIGURE 6.5: COLD FLOW STREAMLINES OF CA

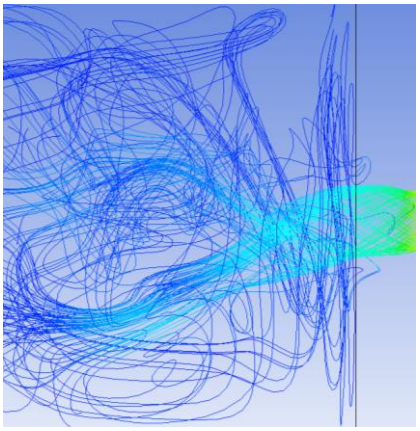

FIGURE 6.6: COLD FLOW STREAMLINES OF PA

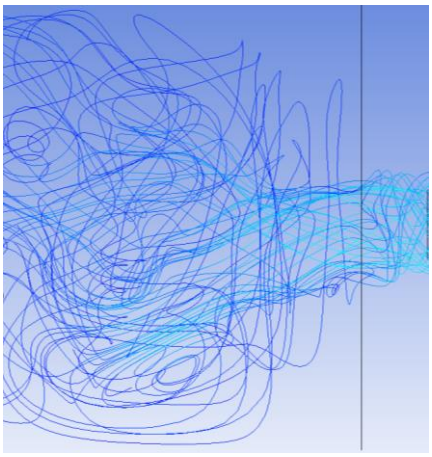

FIGURE 6.7: COLD FLOW STREAMLINES OF SA

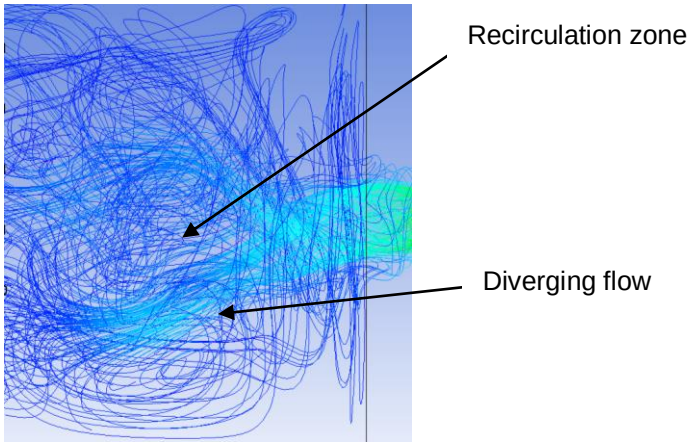

FIGURE 6.8: COLD FLOW STREAMLINES OF THE COMBINED STREAMS

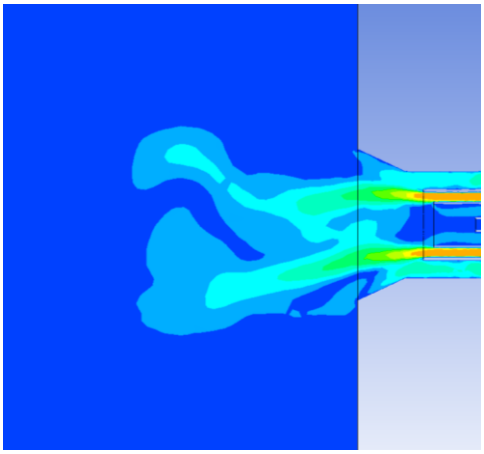

FIGURE 6.9: VELOCITY CONTOURS OF THE COMBINED STREAMS

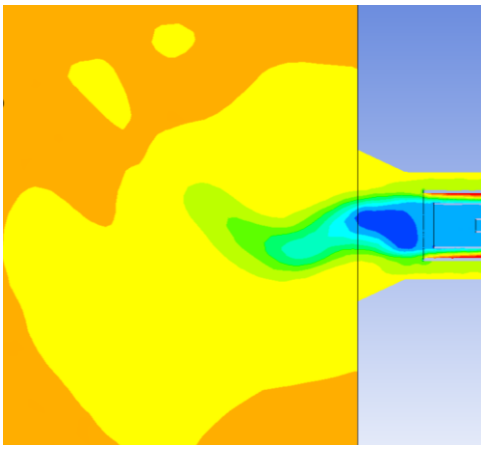

FIGURE 6.10: PRESSURE CONTOURS OF THE COMBINED STREAMS

The CFD of the self-sustaining PC flame test, shows that the flow exits the burner at a diverging angle. A certain distance after the burner mouth, a low-pressure recirculation zone is formed, which provides flame stabilisation and constant ignition. This correlates with what was seen during the test. The flame did not seem to stabilise at the burner mouth, but slightly further downstream.

6.4 COMBUSTION EFFICIENCY OF PC BURNER

During the combustion of coal, all of the fixed C does not fully combust. The percentage of C remaining after combustion is contained in the ash. The ash formed can either be fly ash or bottom ash. Fly ash is normally finer, and lighter in colour, since it contains less unburnt fixed carbon. Fly ash is carried by the flue gas stream to the back end of the boiler. Bottom ash is coarser in structure and darker in colour, since it contains more unburnt C, and normally falls to the bottom in the ash hopper. In large boilers, the ratio of fly ash to bottom ash is approximately 90:10.

In the case of this device, the combustion chamber is horizontal, resulting in a mixture of fly ash and bottom ash in the combustion chamber, representing a ratio closer to 50:50. However, this exact ratio is of no concern here, since an accumulative mixture of fly and bottom ash was tested as reflected in Table 6.8.

As in the standard procedure, an ash sample is dried to get rid of any accumulated moisture, weighed and then placed in an oven at 800ºC for 2 hours, to combust the remaining C in ash. The unburnt C in the ash is then calculated as a percentage of the ash. The unburnt C in the ash is a measure of the combustion efficiency of a burner.

The results of the unburnt fixed C in ash is given in Table 6.8:

TABLE 6.8: UNBURNT FIXED CARBON IN ASH ANALYSIS

	Crucible mass [g]	Dry mass [g]	Ash only [g]	Carbon [g]
Sample 1	11,3446	12,3714	12,3668	0,0046
Sample 2	94,3193	95,0104	95,0071	0,0033
Sample 3	82,4451	84,6496	84,6369	0,0127
UNBURNED CARBON IN ASH				
	Initial mass [g]	**Burnt carbon mass [g]**	**%Unburnt Carbon**	**Ratio**
Sample 1	1,0268	0,0046	0,4480	90,000
Sample 2	0,6911	0,0033	0,4775	10,000
Sample 3	2,2045	0,0127	0,5761	
Average	1,3075	0,0069	0,5005	
% Unburnt Carbon of Coal			0,2138	
% Unburnt Carbon of Carbon			0,5923	

Table 6.8 shows that the unburnt C in ash is 0.500%, which converts to 0.592% unburnt fixed C in a 100% coal sample, and 0.214% unburnt fixed C of total C in a 100% coal sample. This indicates that this burner achieved a combustion efficiency of 99.785%. As mentioned in Section 2.2, a good combustion efficiency is considered to be at least 97%. It therefore indicates that the burner achieved extremely good combustion efficiency.

6.5 NCV_P CALCULATION OF TESTED COAL

The NCVp of the tested coal was determined by using the proof of concept test results at steady state conditions. The mass-energy balance as explained in Section 3.1 was used, which is shown below:

$$\dot{Q}_{in} = \dot{Q}_{out} \tag{9}$$

$$(\dot{m} * cp * T)_{coal} + (\dot{m} * cp * T)_{combustion\ air} + \dot{Q}_{combustion} = (\dot{m} * cp * \Delta T)_{cooling\ fluid} + (\dot{m} * cp * T)_{flue\ gas} \tag{10}$$

$$NCVp = \frac{\dot{Q}_{combustion}}{\dot{m}_{coal}} \tag{11}$$

where:

- $\dot{Q}$ is the heat rate [kW]
- $\dot{m}$ is mass flow [kg/s]
- T is temperature [K]
- cp is the specific heat capacity at constant pressure [kJ/kg-K]
- $NCVp$ is the heat content in the coal [MJ/kg]

The mass flow of coal during the test was 1.423 g/s, while the temperature thereof was 30°C in the PC bunker. The specific heat capacity (cp) value of coal was taken as 1.31 kJ/kg-K since this is a common value used for coal (Porgis, 1982). The combustion air comprised CA, PA and SA at their respective temperatures (which was measured by thermocouples). The corresponding cp values at their respective temperatures and pressures were used. The mass flows of the combustion air used were as calculated in Table 6.4. The heat content of the cooling air was determined by using the mass flow, corresponding cp value, and inlet and outlet temperatures.

The temperature of the flue gas was measured by a thermocouple, and the cp value was calculated by using the weighted average of the cp values of the different components in the flue gas. The flue gas basically comprised N_2, NOx, O_2, CO, CO_2, H_2O and SO_2, shown in the gravimetric wet, flue gas analysis table in Appendix M. In Section 6.4, it was stated that 50% of the ash was in the form of fly ash exiting the combustion chamber. Consequently, because of the conservation of mass, the mass flow of the flue gas was determined by adding the mass flows of the combustion air and PC and subtracting 50% of the ash quantity in the coal. Table 6.9 summarises the results of the NCVp of coal:

TABLE 6.9: SUMMARISED RESULTS OF THE NCV_P OF THE TEST COAL

TESTED NCV_P MASS - ENERGY BALANCE						
	MASS - ENERGY IN					
Property	**CA**	**PA**	**SA**	**TA**	**Pf**	**Total**
ṁ [g/s]	1,054	7,887	2,131	2,243	1,423	14,738
c_P [kJ/kg-K]	1,043841	1,044031	1,043841	1,044052	***1,310000***	
Temperature [°C]	150,000	150,000	280,000	280,000	30,000	
Q̇ [kW]	0,466	3,484	1,231	1,295	0,565	7,041
	MASS - ENERGY OUT					
Property	**Flue Gas**	**Cooling Air**	**Losses**	**Fly ash**		**Total**
ṁ [g/s]	14,118461	48,57850401		0,2937987		
c_P [kJ/kg-K]	1,219156158	1,052016		1,3		
Temperature [°C]	820,115	122,900		820,115		
Q̇ [kW]	18,81794248	**6,281**	**0,000**	0,4175598		25,516
	MASS - ENERGY BALANCE					
Q̇ [kW]	18,475					
NCV_P [MJ/kg]	**13,013**					

Conclusively, an NCVp of 13.013 MJ/kg was determined for the tested coal. Since there is no direct method standard to compare this value with, the closest is to compare it with the calculated GCVv of Dulong, GCVv of the Bomb, NCVp of the BS-Dulong, the NCVp of the BS-Bomb and the NCVp determined by Dulong. Table 6.10 shows the comparative CVs:

TABLE 6.10: COMPARATIVE CALORIFIC VALUES OF COAL

Method	Type	Units	Dry basis	% difference
Gross calorific value (Bomb)	GCV_v	[MJ/kg]	15.698	20.633
Gross calorific value (Dulong)	GCV_v	[MJ/kg]	16.915	29.985
Nett calorific value (BS-Bomb)	NCV_p	[MJ/kg]	15.185	16.691
Nett calorific value (BS-Dulong)	NCV_p	[MJ/kg]	16.401	26.036
Nett calorific value (Dulong)	NCV_p	[MJ/kg]	16.511	26.880
Net calorific value by NCVp coal analyser	NCV_p	[MJ/kg]	**13.013**	-

The NCVp of the tested coal, according to this analyser, is the only value determined entirely by means of a direct method. The other remaining CVs are either entirely calculated, or derived from the GCVv direct method (Bomb calorimeter). The percentage difference between the NCVp coal analyser and the other direct method for GCVv by the Bomb calorimeter is approximately 20%. This emphasises the argument for using the NCVp for boiler utilities. A further problem is presented by the comparison of the NCVp as determined by the BS Bomb derived value, which has the smallest percentage difference (approximately 16%) in the above table. These percentage differences do not show a constant deviance from that determined by this device either, but vary greatly among themselves each other.

Since the calibration of this NCVp coal analyser in Section 5.1.11 showed a deviation of only 1.4% from the established value of LPG, the larger deviances from the other calculated values for coal in Table 6.10 justify the development of an NCVp coal analyser.

7 CONCLUSION AND RECOMMENDATIONS

The following chapter draws a conclusion on what was set out to be achieved in this study and emanating from that, certain recommendations are made.

7.1 CONCLUSION

7.1.1 LITERATURE REVIEW

From the literature review the following main aspects were found:

- NCVp is obtained if moisture cannot condensate inside the measuring apparatus.
- NCVp must be determined directly.
- The flow calorimeter is the direct method used to determine the NCVp of gaseous fuels.
- No flow calorimeters for coal are available on the market.
- A flow calorimeter consists mainly of a combustion chamber, burner, water jacket and measuring apparatus.
- The procedure of using a flow calorimeter is basically the following:
    - The burner is used to combust fuel inside the water-cooled furnace.
    - The fuel gives off heat; some of this heat is absorbed by the water-cooled furnace walls and some of the heat exits the furnace to the atmosphere.
    - The NCVp is determined from a mass-energy balance, which depends on the measurements of:
        - inlet and outlet water temperature;
        - mass flow of water;
        - inlet temperature of fuel;
        - mass flow of fuel;
        - inlet temperature of combustion air;
        - mass flow of combustion air;
        - outlet temperature of flue gas.
- Mass flow of flue gas is calculated by using the conservation law of mass for combustion air and fuel.
- It is important that the fuel is completely combusted.
- The test duration must be sufficient to allow a stable water temperature to be reached.
- The flue gas must be at a sufficient temperature to prevent condensation inside the furnace.
- The burner is a critical part of a flow calorimeter.
- Cold flow modelling can be used for burner design.

7.1.2 NCV_P COAL ANALYSER DESIGN

The primary objective of this study was to develop an NCVp coal analyser based on the principle of a flow calorimeter on a laboratory scale. However, in order to achieve this, the main challenge was to design a PC burner and combustion chamber with supporting auxiliaries that could sustain a PC flame without flame support from a medium such as LPG, with a combustion efficiency that was as high as possible.

7.1.3 PROOF OF CONCEPT AND VALIDATION

The above was indeed achieved by accomplishing the following:

- Successful formulation of the required process for sustained combustion was done by applying burner and combustion principles in cold flow CFD modelling.
- Evidence is therefore provided in the comparison of the intended CFD cold flow streamlines, with the resulting actual flame profiles which validates the cold flow modelling.

- This intended burner was designed for a thermal heat rate of between 40 and 80 kW. However, in the proof of concept test, this burner was successfully fired at a heat rate of approximately 20 kW. Projections foreseen that if coal with a sufficient CV was received, the desired 40 – 80 kW could be achieved.
- Despite the low thermal rating during the test, low coal quality and an out -of -specification A: F (because the coal analyses were only available afterwards), a high combustion efficiency of 99.785% was attained.

This device displayed combustion characteristics similar to those of a full-scale burner used on power stations. Thus, the overall objective of developing a laboratory-scale device complying with the sustained coal combustion requirements (at relatively low cost, operating time and sample size) was achieved.

7.1.4 NCV_P DETERMINATION

After the attainment of the above mentioned device, the goal of determining the NCVp of coal could be pursued. By means of the mass-energy balance measurements during the test, an NCVp of coal of 13.013 MJ/kg was determined directly.

- This exercise proved a significant difference between:
  - Direct methods of GCVv (Bomb calorimeter) vs NCVp (NCVp coal analyser);
  - Direct NCVp (NCVp coal analyser) vs calculated NCVp (Dulong) and derived NCVp from the BS Bomb.
- Because of the above-mentioned discrepancies, a significant misjudgement of a power station unit efficiency is inevitable (a calculated error of > 1.75% overall plant efficiency, based on equation (6), Section 2.4 is possible).
- Likewise, a significant error in the planned procurement of coal may occur (> 6 million tons per annum for Eskom as a whole).

During the calibration of this device with the established value of LPG, the values of NCVp of coal that were determined can be regarded as trustworthy to a high degree. It is thus possible to construct a device for the direct NCVp determination for coal.

7.2 RECOMMENDATIONS

As mentioned previously, the PC burner was designed to be adjustable in thermal load, A: F, pre-heated air temperatures, and aerodynamics (amount of swirl, recirculation, etc.). However, the test was completed at the settings that enabled proof of concept: only one aerodynamic setting (swirlers at maximum), at one thermal load (≈ 20 kW), for one type of coal. Future studies can therefore be conducted to determine the conditions at which a specific type of coal achieves optimum combustion efficiency, flame temperature, flame stability and A: F.

The fact that the NCVp of the tested coal, determined by the NCVp coal analyser, differed by 16% from the calculated NCVp from the BS-Bomb calorimeter method is evidence of the need for future development and investigation in the direct determination of the NCVp of coal. The differences between the various methods used to calculate the NCVp, also show that a direct method must be standardised.

8 REFERENCES

Basu, P. 2000. Pulverized coal fired furnace. https://www.yumpu.com/en/document/read/11659333/pulverized-coal-fired-furnace Date of access: 16 Nov 2019. [PowerPoint presentation]

Basu, P. 2013. Biomass gasification, pyrolysis and torrefaction: Practical design and theory.2nd ed. San Diego, CA: Elsevier.

Basu, P., Kefa, C. & Jestin, L. 2012. Boilers and burners: Design and theory. New York, NY: Springer-Verlag New York Inc.

British Standards Institution. 2009. Solid biofuels – Determination of calorific value: 1-64.

Budapest University of Technology and Economics: Faculty of Mechanical Engineering. s.a. Determination of higher and lower heating values of natural gas and pb gas by calorimetry. file:///C:/Users/21468370/Downloads/CM_Calorimetry.pdf Date of access: 16 Nov 2019.

Cloke, M., Lester, E. & Gibb, W. 1997. Characterization of coal with respect to carbon burnout in p.f.-fired boilers. *Fuel,* 76(13):1257-1267.

Collins, F. 2016. Combustion and fuels: Aerodynamics of combustion. https://slidex.tips/download/aerodynamics-of-combustion-combustion-and-fuels Date of access: 21 Nov 2019.

Cushman-Roisin, B. 2015. Swirling flows. http://www.dartmouth.edu/~cushman/courses/engs250/Swirling-flows.pdf Date of access: 19 Nov 2019. [PowerPoint presentation].

Dryjanska, A., Węcel, D., Kotowicz, J. & Wiciak, G. 2006. Lower heating value: Laboratory of metrology. http://www.imiue.polsl.pl/dokumenty/106_M-8.ang.pdf Date of access: 16 Nov 2019.

El-Mahallaway, F. & Habik, S.E. 2002. Fundamentals and technology of combustion. Oxford, UK: Elsevier Science Ltd.

Falcon, R. 2013. Coal, coke and carbon in the metallurgical industry: Coal geology, types, ranks and grades. http://www.fossilfuel.co.za/conferences/2013/CoalCokeCarbon/Day-One/01-Rosemary-Falcon.pdf Date of access: 16 Nov 2019. [PowerPoint presentation].

Gu, M., Zhang. M., Fan, W., Wang, L. & Tian, F. 2005. The effect of the mixing characters of primary and secondary air on NO_x formation in a swirling pulverised coal flame. *Fuel,* 83:2093-2101.
Hall, B.F. & Povey, T. 2015. Experimental study of non-reacting low NO_x combustor simulator for scaled turbine experiments. Turbine Technical Conference and Exposition, ASME Turbo Expo 2015,

Heap, M.P., Lowes, T.M., Walmsley, R., Bartelds, H. & LeVaguerese, P. 1976. Burner criteria for NO_x Volume 1. Influence of burner variables on NO_x in pulverized coal flames. Washington, DC.

Howard, J.B. & Essenhigh, R.H. 1966. Pyrolysis of coal particles in pulverized fuel flames. Symposium on pyrolysis reactions of fossil fuels presented before the division pf petroleum chemistry, inc. https://web.anl.gov/PCS/acsfuel/preprint%20archive/Files/10_2_PITTSBURGH_03-66_0020.pdf Date of access: 29 Nov. 2015.

Khanafer, K. & Aithal, S. M. 2011. Fluid-dynamic and computation in swirl burners. *International journal of heat and mass transfer,* 54:5030-5038

Kim, R., Li, D. & Jeon, C. 2014. Experimental investigation of ignition behaviour for coal rank using a flat flame burner at the high heating rate. *Experimental thermal and fluid science,* 54:212-218.

Kitto, J.B. & Stulz, S.C. 2005. Steam: Its generation and use. Barberton, Ohio: The Babcock and Wilcox Company.

Langenhoven, H. 2019. The state of coal mining in South Africa. *2019 Coal industry day.* file:///C:/Users/21468370/Downloads/presentation-coal-industry-day-henk-langenhoven-24072019%20(1).pdf Date of access: 15 Nov 2019. [PowerPoint presentation].

Li, Z.Q., Chen, Z.C., Sun, R. & Wu, S.H. 2007. New low NOx, low grade coal fired swirl stabilized technology. *Journal of the energy institute,* 80(3):123-130.

Lieuwen, T. 2014. Unsteady Combustor Processes. *2014 CEFRC Summer school on combustion.*

Lowry, H. H. 1945. Chemistry of coal utilization: Volume 1. NY: John Wiley & Sons Inc.

Makino, A. & Law, C. K. 2009. An analysis of the transient combustion and burnout time of carbon particles. *Proceedings of the combustion institute,* 32:2067-2074.

Mason, D.M. & Gandhi, K. (1980, August). Formulas for calculating the heating value of coal and cola char: Development, tests and uses. Conference: 180. American Chemical Society meeting/2. Chemical congress of the North American Continent, San Francisco, CA, (pp. 1-11).

Miller, B.G. 2017. Clean coal engineering technology. Amsterdam, NL: Butterworth-Heinemann.

Nettleton, M.A. 2004. The influence of swirl angles on flame stability in pilot-scale plant. *Fuel,* 183:253-256.

Obert E.F. 1973. Internal combustion engines and air polution. New York: Harper & Row.

Priyadarshi, S. 2012. Calorific value of Coal. file:///C:/Users/21468370/Downloads/Calorific%20Value%20of%20Coal%20(2).pdf Date of access: 16 Nov 2019.

Rajoo, P. 2010. The application of pilot scale coal evaluation to full scale boilers. Johannesburg: University of Witwatersrand. (Dissertation – M.Sc.).

Ranade, V.V. & Gupta, D.F. 2015. Computational modelling of pulverized coal fired boilers. Boca Raton, FL: Taylor & Francis Group.

SGS. 2019. Mining coal calculations. https://www.sgs.co.za/en/mining/analytical-services/coal-and-coke/coal-calculations Date of access: 7 May 2019.

Sharifi, R. & Scaroni, A.W. 1996. Combustion aerodynamics of a pulverized-coal low NO_x swirl burner: Influence of flow types on NO_x emissions. Combustion in Industry – Status and needs into 21st Century, 1996 International Symposium, Amer. Flame research committee, Baltimore, Maryland.

Slezak, S.E., Buckius, R.O. & Krier, H. 1985. A model of flame propagation in rich mixtures of coal dust in air. *Combustion and flame,* 59:251-265.

Smoot, L. & Pratt, D.T. *eds.* 1979. Pulverized-coal combustion and gasification: Theory and applications for continuous flow processes. New York: Plenum Press.

Storm, C.P. 1998. A macroscopic determination of the impact of Lethabo coal quality upon the optimum combustion air quantity. Potchefstroom: NWU. (Thesis – PhD).

Storm, R.F & Reilly, T.J. 2009. Coal fired boiler performance improvement through combustion optimization. https://www.stormeng.com/pdf/Coal%20Fired%20Boiler%20Performance%20Improvement%20Through%20Combustion%20Optimization.pdf Date of access: 16 Nov 2019.

Van Der Merwe, S.W. 2014. Improving boiler combustion using computational fluid dynamics modelling. *Proceedings of the South African sugar technologists' association,* 8: 130-137.

Versteeg, H.K. & Malalasekera, W. 2007. An introduction to computational fluid dynamics: The finite volume method. 2nd ed. Upper Saddle River, NJ: Pearson education.

Wang, C., Liu, Y., Everson, R.M., Rahat, A. A. M. & Zheng, S. 2017. Applied Gaussian process in optimizing unburned carbon content in fly ash for boiler combustion. *Mathematical problems in engineering*: 2017:1-8. doi: 10.1155/2017/6138930.
Wang, C., Liu, Y., Zhang, X. & Che, D. 2011. A study on coal properties and combustion characteristics of blended coals in Northwestern China. *Energy fuels*, 25:3634–3645.

Worgas. 2011. Gas burner technology and gas burner design for application. A presentation brought to you by Worgas: Energy transformation technology. http://www.asge-national.org/Content/Files/Presentations/2011/7BurnerTechnology-ASGE2011-Worgas-G_Berthold.pdf Date of access: 28 Nov. 2015. [PowerPoint presentation].

World Energy Council. 2016. World energy resources. https://www.worldenergy.org/assets/images/imported/2016/10/World-Energy-Resources-Full-report-2016.10.03.pdf Date of access: 16 Nov 2019.

Wróblewska, V., Zelkowski, J. & Wójcicki, S. 1977. The optimum conditions for the combustion of low-calorific coal dust swirl burners. *Symposium (International) on combustion,* 16(1):401-410.

Wu, Y., Lu, Y., Al-Rahbi, I.S. & Kalghatgi, G.T. 2009. Prediction of the lift-off, blow-out and blow-off stability limit of pure hydrogen and hydrogen/hydrocarbon mixture jet flames. *International journal of hydrogen energy* 34(14):5940-5945.

Xiumin, J., Chuguang, Z., Jianrong, Q., Jubin, L. & Dechang, L. 2001. Combustion characteristics of super fine pulverized coal particles. *Energy fuels,* 15(5):1100-1102.

Xue, S. Hui, S., Zhou, Q. & Xu, T. 2009. Experimental study on NO_x emission and unburnt carbon of a radial biased swirl burner for coal combustion. *Energy and fuels,* 23:3558-3564.

Yang, J. C. 1993. Heterogenous combustion. (*In* Puri, I. K. Environmental implications of combustion processes. Florida: CRC Press).

9 BIBLIOGRAPHY

ANSYS FLUENT 12.0 Users guide – 6.2.2 Mesh quality. 2019. https://www.afs.enea.it/project/neptunius/docs/fluent/html/ug/node167.htm Date of access: 15 Nov 2019.

Arms, R.W. 1922. The ignition temperature of coal. Urbana, IL: University of Illinois.

Bakker, A. 2002. Lecture 15 – Discrete phase modelling: Applied computational fluid dynamics. http://www.bakker.org/dartmouth06/engs150/15-dpm.pdf Date of access: 17 Nov 2019. [PowerPoint presentation].

Baukal, C. *ed*. 2013. The John Zink Hamworthy combustion handbook: Fundamentals Volume 1. 2nd ed. Boca Raton, FL: CRC Press.

Baukal, C. *ed*. 2013. The John Zink Hamworthy combustion handbook: Application Volume 3. 2nd ed. Boca Raton, FL: CRC Press.

Baukal, C. *ed*. 2013. The John Zink Hamworthy combustion handbook: Design and operations Volume 2. 2nd ed. Boca Raton, FL: CRC Press.

Baukal, C. E. *ed.* 2003. Industrial burners handbook. Boca Raton, FL: CRC Press LLC.

Beér, J. 2000. Combustion technology developments in power generation in response to environmental challenges. *Progress in energy and combustion science,* 26:301-327.

Chattopadhyay, P. 2001. Boiler operation engineering: Questions and answers. 2nd ed. New York, NY: McGraw-Hill Education.

Eldrainy, Y.A., Saqr, K.M., Aly, H.S. & Jaafar, M.N.M. 2009. CFD insight of the flow dynamics in a novel swirler for gas turbine combustors. *International communications in heat and mass transfer,* 36:936-941.

Eskom. 2012. Fossil Fuel Firing Regulations. file:///C:/Users/Prof%20Chris%20Storm/Downloads/Fossil%20Fuel%20%20Firing%20Regulation%20Rev%200_Final%20(1).pdf Date of access: 29 Nov. 2015.

Forster, R. N. G. 1999. CFD modelling of vortex combustors. Guildford: University of Surrey. (Thesis – PhD).

Faculty of Engineering and Applied Science, Chemical Engineering, Queens University. 2014. *Heating values of hydrogen and fuels.* https://chemeng.queensu.ca/courses/CHEE332/files/ethanol_heating-values.pdf Date of access: 15 Nov 2019.

Glassman, I. & Yetter, R.A. 2008. Combustion. 4th ed. Oxford,UK: Elsevier Inc.

Grönwall, F. 2010. Optimization of burner kiln 7, Cementa Slite. http://www.diva-portal.se/smash/get/diva2:402796/FULLTEXT01.pdf Date of access: 20 Nov 2019.

Halpin, J.L. 1993. Swirl generation and recirculation using radial swirl vanes. Presented at the International gas turbine and aeroengine congress and exposition. Cincinnati, OH, 24-27 May 1993. https://asmedigitalcollection.asme.org/GT/proceedings/GT1993/78903/V03AT15A020/236271 Date of access: 20 Nov 2019.

Hattingh, B.B. 2012. Product evaluation and reaction modelling for the devolitization of large coal particles. Potchefstroom: NWU. (Thesis –PhD).

Ighodalo, O.A., Ajuwa, C.I. & Iredje, B.R. 2010. Development and performance evaluation of a high velocity burner for furnace operations. *American journal of scientific and industrial research,* 2(1): 49-53.

Incropera, F.P., Dewitt, D.P., Bergman, T.L. & Lavine, A.S. 2007. Fundamentals of heat and mass transfer. 6th ed. Danvers, MA: John Wiley & Sons.

Innovative Combustion Technologies Inc. 2018. Calculation of pulverized minimum primary airflow and proper air to fuel relationship. https://www.innovativecombustion.com/wp-content/uploads/2018/06/Calculation-of-Pulverizer-Minimum-Primary-Airflow-and-Proper-Air-to-Fuel-Relationship.pdf Date of access: 17 Nov 2019.

Italian section of the Combustion Institute. 2002. Combustion and sustainable development: XXV Event of the Italian section of the Combustion Institute.

Khan, S. & Khan, S. 2014. Boiler and its tangential fuel firing system. *International journal of automation and control engineering*, 3(3): 71-84.

Kirk, W. & Griffiths, J. 1958. Applying fundamental concepts to the engineering design of appliance burners. Chicago Illinois Meeting: 59-70.

LaFlesh, R.C., Rini, M.J. & McGowan, J.G. 1989. Development of an advanced efficiency coal combustor for boiler retrofit. Windsor, CT: Combustion Engineering, Inc.

Li, Z., Li, R. & Zhou, L. 2000. Cold gas particle flows in a new swirl pulverized coal burner by PDPA measurement. *Tsinghua science and technology,* 5(1): 100-104.

Lieuwen, T. & Zinn, B. 2007. Combustion instability and blowout characteristics of fuel flexible combustors: Final report. Atlanta,GA.

Lockwood, F.C. 2005. Prediction of combustion and NO_x emissions characteristics of flameless oxidation combustion. *IFRF combustion journal*: 2-28.

Macphee, J.E., Sellier, M., Jermy, M. & Tadulan, E. 2009. CFD modelling of pulverized coal combustion in a rotary lime kiln. *Seventh international conference on CFD in the minerals and process industries*: 1-6.

Milani, A. & Saponaro, A. 2001. Diluted combustion technologies. *IFRF combustion journal*: 1-32.

Noor, M.M., Wandel, A.P. & Yusaf, T. 2013. Detail guide for CFD on the simulation biogas combustion in bluff-body mild burner. *International conference mechanical engineering research*: 1-25.

Orfanoudakis, N.G., Hatziapostolou, A., Krallis, K., Mastorakos, E., Sardi, K., Pavlou, D.G. & Vlachakis, N. 2005. Design, evaluation measurements and modelling of a small swirl stabilised laboratory burner. *IFRF combustion journal*: 1-29.

Pradeep, K. 2013. Combustion techniques and coal flame for cement kiln. https://www.slideshare.net/pradeepdeepi/flame-for-cement-kilns-kppradeep-kumar Date of access: 20 Nov 2019. [PowerPoint presentation].

Rees-Gralton, T.M. 2007. The development of a prediction tool for utility boiler performance. Cardiff: Cardiff University. (Thesis – PhD).

Repic, B., Djurovic, A.E.D. & Zivkovic, G. 2012. Experimental determination of the swirl burner laboratory models hydraulic resistance. *Procedia engineering,* 42:672-682.

Ristic, D., Schuster, A. & Scheffknecht, G. 2010. On the potential of flameless oxidation to reduce NO_x emissions from pulverized coal combustion. *Journal of the international flame research foundation*: 1-16.

Rottner, B.L. 2006. Combustible dusts. https://www.scribd.com/document/204463817/Aiha-Combustable-Dusts Date of access: 17 Nov 2019. [PowerPoint presentation].

Saljinokov, A., Komatina, M. & Goričanec, D. 2006. Verification of the mathematical model of pulverized coal combustion in swirl burners. *FME Transactions,* 34(1): 45-52.

Shawabkeh, R. A. 2015. Handout: Steps for design of furnace & fired heater. https://www.researchgate.net/publication/281460206_Handout_Steps_for_design_of_Furnace_Fired_Heater Date of access: 20 Nov 2019.

Smit, D. 2016. Low NO_x coal burner temperature profile evaluation. Johannesburg: University of the Witwatersrand. (Dissertation – Masters).

Stern, F. 2013. Fluid kinematics. https://www.studocu.com/en/document/vellore-institute-of-technology/fluid-mechanics/tutorial-work/momentumtransfer/2604755/view Date of access: 17 Nov 2019.

Tamaru, M., Watanabe, S., Oone, E., Itokuzu, R. & Kozaki, T. 2011. Advanced development of pulverized coal firing technologies. *Engineering review,* 44(2):1-6.

Tamura, Y. .s.a. Lecture 4: Flow patterns and wind forces. http://www.wind.arch.t-kougei.ac.jp/info_center/ITcontent/tamura/4.pdf Date of access: 17 Nov 2019. [PowerPoint presentation].

Taniguchi, M. 2012. Fundamental experiments of coal ignition for engineering design of coal power plants. (*In* Rasul, M., *ed.* Thermal power plants. 65-88).

Taniguchi, M. 2013. Model to evaluate flame propagation velocity for pulverized coal particles. *Energy fuels,* 27:1662-2667.

Taniguchi, M. & Takeo, Y. 2013. Evaluation of flame stability for development of pulverized coal fired burners by using a Japanese industrial standard method (JIS Z8818; test method for minimum explosible concentration of combustible dusts). *Journal of the society of powder technology, Japan,* 50: 250-256.

Tharaniyil, R. 2013. Coal combustion products utilization handbook. 3rd ed. Wisconsin, WI: We Energies.

Vanierschot, M. 2007. Fluid mechanics and control of annular jets with and without swirl. Leuven: Katholieke Universiteit Leuven. (Proefskrif – PhD).

Viskanta, R. & Menguc, M.P. 1987. Radiation heat transfer in combustion systems. *Program of energy combustion and science.* 13: 97-160.

Watanabe, S., Tamura, M., Suko, T., Fujimori, T. & Suda, T. 2008. Development of low-volatile coal firing burner. *Engineering review,* 41(2): 68-73.

Weber, R. & Breusen, F. 1998. Scaling properties of swirling pulverized coal flames: From 180kW to 50MW thermal input. *Twenty-seventh symposium (International) on combustion/The combustion Institute*: 2957-2964.

Wuhan Global Metal Engineering Co., Ltd. (2016-2019). Handheld Thermocouple Temperature Sensor / Sheathed K Type Thermocouple. http://www.thermocoupleheater.com/sale-10029855-handheld-thermocouple-temperature-sensor-sheathed-k-type-thermocouple.html Date of access: 22 Nov 2019.

Wunning. J.G. & Milani, A. *eds.* 2009. Handbook of burner technology for industrial furnaces: Fundamentals burner applications. Essen, DE: Vulkan Verlag.

Yue, G. & Li, S., *eds*. 2016. Clean coal technologies and sustainable development: Proceedings of the 8th International symposium on coal combustion. Singapore, SG: Springer Nature.

Zalosh, B. 2010. Dust explosion fundamentals: Recognizing the dust hazard. https://pdfs.semanticscholar.org/ea44/6dbe8c0e91e3aeac6525fb9ede1874ff19ba.pdf Date of access: 20 Nov 2019. [PowerPoint presentation].

Zhang, Y., Li, Q. & Zhou, H. 2016. Theory and calculation in heat transfer in furnaces. London. UK: Elsevier: Academic Press.

Zhou, R. 2012. Swirl number for non-reacting and reacting conditions of Cambridge stratified swirl burner. https://www.repository.cam.ac.uk/bitstream/handle/1810/243259/DSpace_velocity_SwirlNumber_CSB_LDA.pdf?sequence=4&isAllowed=y Date of access: 19 Nov 2019.

Zlochower, I.A. & Green, G.M. 2009. The limiting oxygen concentration and flammability limits of gases and gas mixtures. *Journal of loss prevention in process industries,* 22(4):499-505.

10 APPENDICES

A. COAL ANALYSIS

A.1 INTERMEDIATE QUALITY COAL

TABLE A.1.1: PROXIMATE ANALYSIS FOR INTERMEDIATE QUALITY COAL

COAL QUALITY					
GRAVIMETRIC %	**SYMBOL**	**UNITS**	**AS RECEIVED**	**AIR DRIED**	**DRY BASIS**
PROXIMATE ANALYSIS					
Carbon $_{FIXED}$ (by difference)	C_{FIX}	%	43.300	44.410	46.162
Volatile matter	VM	%	22.035	22.600	23.491
Ash	Ash	%	28.465	29.195	30.347
Surface moisture	M_s	%	2.500	0.000	0.000
Inherent moisture	M_i	%	3.700	3.795	0.000
Total moisture	M_t	%	6.200	3.795	0.000
Gross calorific value	GCV_v	[MJ/kg]	20.524	21.050	21.880
Total		%	100.000	100.000	100.000

TABLE A.1.2: ELEMENTAL ANALYSIS FOR INTERMEDIATE QUALITY COAL

COAL QUALITY					
GRAVIMETRIC %	**SYMBOL**	**UNITS**	**AS RECEIVED**	**AIR DRIED**	**DRY BASIS**
ELEMENTAL ANALYSIS					
Nitrogen	N	%	1.151	1.180	1.227
Oxygen (by difference)	O	%	7.166	7.350	7.640
Carbon $_{TOTAL}$	C_{TOTAL}	%	53.021	54.380	56.525
Ash	A	%	28.465	29.195	30.347
Sulphur	S	%	0.878	0.900	0.936
Hydrogen	H	%	3.120	3.200	3.326
Surface Moisture	M_S	%	2.500	0.000	0.000
Inherent Moisture	M_i	%	3.700	3.795	0.000
Total moisture	M_T	%	6.200	3.795	0.000
Total		%	100.000	100.000	100.000

A.2 HIGH QUALITY COAL

TABLE A.2.1: PROXIMATE ANALYSIS FOR HIGH QUALITY COAL

COAL QUALITY					
GRAVIMETRIC %	SYMBOL	UNITS	AS RECEIVED	AIR DRIED	DRY BASIS
PROXIMATE ANALYSIS					
Carbon $_{FIXED}$ (by difference)	C_{FIX}	%	51.806	53.080	54.590
Volatile matter	VM	%	20.301	20.800	21.392
Ash	Ash	%	22.793	23.354	24.018
Surface moisture	M_s	%	2.400	0.000	0.000
Inherent moisture	M_i	%	2.700	2.766	0.000
Total moisture	M_t	%	5.100	2.766	0.000
Gross calorific value	GCV_v	[MJ/kg]	23.522	24.100	24.786
Total		%	100.000	100.000	100.000

TABLE A.2.2: ELEMENTAL ANALYSIS FOR HIGH QUALITY COAL

COAL QUALITY					
GRAVIMETRIC %	SYMBOL	UNITS	AS RECEIVED	AIR DRIED	DRY BASIS
ELEMENTAL ANALYSIS					
Nitrogen	N	%	1.405	1.440	1.481
Oxygen (by difference)	O	%	5.846	5.990	6.160
Carbon $_{TOTAL}$	C_{TOTAL}	%	60.941	62.440	64.216
Ash	A	%	22.793	23.354	24.018
Sulphur	S	%	0.595	0.610	0.627
Hydrogen	H	%	3.318	3.400	3.497
Surface Moisture	M_S	%	2.400	0.000	0.000
Inherent Moisture	M_i	%	2.700	2.766	0.000
Total moisture	M_T	%	5.100	2.766	0.000
Total		%	100.000	100.000	100.000

A.3 LOW QUALITY COAL

TABLE A.3.1: PROXIMATE ANALYSIS FOR LOW QUALITY COAL

COAL QUALITY					
GRAVIMETRIC %	SYMBOL	UNITS	AS RECEIVED	AIR DRIED	DRY BASIS
PROXIMATE ANALYSIS					
Carbon $_{FIXED}$ (by difference)	C_{FIX}	%	32.968	34.370	35.691
Volatile matter	VM	%	17.074	17.800	18.484
Ash	Ash	%	42.329	44.129	45.825
Surface moisture	M_s	%	4.080	0.000	0.000
Inherent moisture	M_i	%	3.550	3.701	0.000
Total moisture	M_t	%	7.630	3.701	0.000
Gross calorific value	GCV_v	[MJ/kg]	14.251	14.857	15.428
Total		%	100.000	100.000	100.000

TABLE A.3.2: ELEMENTAL ANALYSIS FOR LOW QUALITY COAL

COAL QUALITY					
GRAVIMETRIC %	SYMBOL	UNITS	AS RECEIVED	AIR DRIED	DRY BASIS
ELEMENTAL ANALYSIS					
Nitrogen	N	%	0.873	0.910	0.945
Oxygen (by difference)	O	%	7.184	7.490	7.778
Carbon $_{TOTAL}$	C_{TOTAL}	%	39.078	40.740	42.306
Ash	A	%	42.329	44.129	45.825
Sulphur	S	%	0.499	0.520	0.540
Hydrogen	H	%	2.408	2.510	2.606
Surface Moisture	M_S	%	4.080	0.000	0.000
Inherent Moisture	M_i	%	3.550	3.701	0.000
Total moisture	M_T	%	7.630	3.701	0.000
Total		%	100.000	100.000	100.000

B. HYPER-STOICHIOMETRIC COMBUSTION CHEMICAL EQUATIONS

B.1 HYPER-STOICHIOMETRIC COMBUSTION CHEMICAL EQUATIONS FOR INTERMEDIATE QUALITY COAL

TABLE B.1.1: HYPER-STOICHIOMETRIC COMBUSTION EQUATIONS FOR INETRMEDIATE QUALITY COAL

PRACTICAL INCOMPLETE COMBUSTION				
2C	+	O_2	=	2CO
24,022		31,999		56,021
1,000		1,332		2,332
52,693		70,191		122,884
2CO	+	O_2	=	$2CO_2$
56,021		31,999		88,020
1,000		0,571		1,571
122,884		70,191		193,074
122,805		70,146		192,951
S	+	O_2	=	SO_2
32,060		31,999		64,059
1,000		0,998		1,998
0,878		0,876		1,753
$2H_2$	+	O_2	=	$2H_2O$
4,032		31,999		36,030
1,000		7,937		8,937
3,120		24,763		27,883
$2N_2$	+	O_2	=	$2N_2O$
56,027		31,999		88,026
1,000		0,571		1,571
0,81880		0,468		1,286

B.2 HYPER-STOICHIOMETRIC COMBUSTION CHEMICAL EQUATIONS FOR HIGH QUALITY COAL

TABLE B.2.1: HYPER-STOICHIOMETRIC COMBUSTION EQUATIONS FOR HIGH QUALITY COAL

PRACTICAL INCOMPLETE COMBUSTION				
2C	+	O_2	=	2CO
24,022		31,999		56,021
1,000		1,332		2,332
60,679		80,829		141,508
2CO	+	O_2	=	$2CO_2$
56,021		31,999		88,020
1,000		0,571		1,571
141,508		80,829		222,337
141,418		80,777		222,195
S	+	O_2	=	SO_2
32,060		31,999		64,059
1,000		0,998		1,998
0,595		0,594		1,190
$2H_2$	+	O_2	=	$2H_2O$
4,032		31,999		36,030
1,000		7,937		8,937
3,318		26,338		29,657
$2N_2$	+	O_2	=	$2N_2O$
56,027		31,999		88,026
1,000		0,571		1,571
0,94178		0,538		1,480

B.3 HYPER-STOICHIOMETRIC COMBUSTION CHEMICAL EQUATIONS FOR LOW QUALITY COAL

TABLE B.3.1: HYPER-STOICHIOMETRIC COMBUSTION EQUATIONS FOR LOW QUALITY COAL

PRACTICAL INCOMPLETE COMBUSTION				
2C	+	O_2	=	2CO
24,022		31,999		56,021
1,000		1,332		2,332
38,591		51,406		89,997
2CO	+	O_2	=	$2CO_2$
56,021		31,999		88,020
1,000		0,571		1,571
89,997		51,406		141,402
89,940		51,373		141,313
S	+	O_2	=	SO_2
32,060		31,999		64,059
1,000		0,998		1,998
0,499		0,498		0,997
$2H_2$	+	O_2	=	$2H_2O$
4,032		31,999		36,030
1,000		7,937		8,937
2,408		19,109		21,517
$2N_2$	+	O_2	=	$2N_2O$
56,027		31,999		88,026
1,000		0,571		1,571
0,59494		0,340		0,935

C. FLUE GAS CALCULATIONS OF HYPER-STOICHIOMETRIC COMBUSTION

C.1 INTERMEDIATE QUALITY COAL

TABLE C.1.1: GRAVIMETRIC WET FLUE GAS ANALYSIS FOR INTERMEDIATE QUALITY COAL

GAS	[kg gas/100 kg coal]	[kg/s]	% Gravimetric
CO_2 (Ostwald CO_2^+)	192.951	3.761	21.377
CO	0.078	0.002	0.009
SO_2	1.753	0.034	0.194
NOx	1.286	0.025	0.143
O_2 (Ostwald $O2^+$)	31.318	0.610	3.470
H_2O from H_2	27.883	0.543	3.089
H_2O from coal	6.200	0.121	0.687
H_2O from air	9.671	0.188	1.071
N_2 from stoichiometric air	527.433	10.280	58.434
N_2 from excess air	103.708	2.021	11.490
N_2 from coal	0.332	0.006	0.037
Total Flue Gas	**902.615**	**17.592**	**100.000**
Total H_2O	43.754	0.853	4.847
Total N_2	631.473	12.307	69.960

TABLE C.1.2: VOLUMETRIC DRY FLUE GAS ANALYSIS FOR INTERMEDIATE QUALITY COAL

GAS	[kg gas/100kg gas]	[kg gas / kmole gas]	[kmole / 100kg]	% Volumetric
CO_2 (Ostwald CO_2^+)	21.377	44.010	0.486	15.679
CO	0.009	28.010	0.000	0.0100000
SO_2	0.194	64.059	0.003	0.0978815
NOx	0.143	46.006	0.003	0.1000000
O_2 (Ostwald $O2^+$)	3.470	31.999	0.108	3.500
H_2O from H_2	0.000	18.015	0.000	0.000
H_2O from coal	0.000	18.015	0.000	0.000
H_2O from air	0.000	18.015	0.000	0.000
N_2 from stoichiometric air	58.434	28.013	2.086	67.332
N_2 from excess air	11.490	28.013	0.410	13.239
N_2 from coal	0.037	28.013	0.001	0.042
Total Flue Gas	**95.153**	Molecular mass of Flue gas [kg/kmole]	**3.098**	**100.000**
Total H_2O	0.000		$R_{FLUE\ GAS}$ [kJ/kg-K]	0.000
Total N_2	69.960	**32.27894**	**0.25758**	80.613

C.2 HIGH QUALITY COAL

TABLE C.2.1: GRAVIMETRIC WET FLUE GAS ANALYSIS FOR HIGH QUALITY COAL

GAS	[kg gas/100kg coal]	[kg/s]	% Gravimetric
CO_2 (Ostwald CO_2^+)	222.195	3.771	21.502
CO	0.090	0.002	0.009
SO_2	1.190	0.020	0.115
NOx	1.480	0.025	0.143
O_2 (Ostwald $O2^+$)	36.024	0.611	3.486
H_2O from H_2	29.657	0.503	2.870
H_2O from coal	5.100	0.087	0.494
H_2O from air	11.125	0.189	1.077
N_2 from stoichiometric air	606.751	10.297	58.716
N_2 from excess air	119.289	2.024	11.544
N_2 from coal	0.464	0.008	0.045
Total Flue Gas	**1033.363**	**17.536**	**100.000**
Total H_2O	45.881	0.779	4.440
Total N_2	726.504	12.329	70.305

TABLE C.2.2: VOLUMETRIC DRY FLUE GAS ANALYSIS FOR HIGH QUALITY COAL

GAS	[kg gas/100kg gas]	[kg gas / kmole gas]	[kmole / 100kg]	% Volumetric
CO_2 (Ostwald CO_2^+)	21.502	44.010	0.489	15.698
CO	0.009	28.010	0.000	0.0100000
SO_2	0.115	64.059	0.002	0.0577384
NOx	0.143	46.006	0.003	0.1000000
O_2 (Ostwald $O2^+$)	3.486	31.999	0.109	3.500
H_2O from H_2	0.000	18.015	0.000	0.000
H_2O from coal	0.000	18.015	0.000	0.000
H_2O from air	0.000	18.015	0.000	0.000
N_2 from stoichiometric air	58.716	28.013	2.096	67.343
N_2 from excess air	11.544	28.013	0.412	13.240
N_2 from coal	0.045	28.013	0.002	0.051
Total Flue Gas	**95.560**	**Molecular mass of Flue gas [kg/kmole]**	**3.112**	**100.000**
Total H_2O	0.000		$R_{FLUE\ GAS}$ [kJ/kg-K]	0.000
Total N_2	70.305	**32.12930**	**0.25878**	80.634

C.3 LOW QUALITY COAL

TABLE C.3.1: GRAVIMETRIC WET FLUE GAS ANALYSIS FOR LOW QUALITY COAL

GAS	[kg gas/100kg coal]	[kg/s]	% Gravimetric
CO_2 (Ostwald CO_2^+)	141.313	3.775	21.396
CO	0.057	0.002	0.009
SO_2	0.997	0.027	0.151
NOx	0.935	0.025	0.142
O_2 (Ostwald $O2^+$)	22.755	0.608	3.445
H_2O from H_2	21.517	0.575	3.258
H_2O from coal	7.630	0.204	1.155
H_2O from air	7.017	0.187	1.062
N_2 from stoichiometric air	382.605	10.220	57.931
N_2 from excess air	75.351	2.013	11.409
N_2 from coal	0.278	0.007	0.042
Total Flue Gas	**660.454**	**17.641**	**100.000**
Total H_2O	36.164	0.966	5.476
Total N_2	458.234	12.240	69.382

TABLE C.3.2: VOLUMETRIC DRY FLUE GAS ANALYSIS FOR LOW QUALITY COAL

GAS	[kg gas/100kg gas]	[kg gas / kmole gas]	[kmole / 100kg]	% Volumetric
CO_2 (CO_2^+)	21.396	44.010	0.486	15.804
CO	0.009	28.010	0.000	0.0100000
SO_2	0.151	64.059	0.002	0.0765730
NOx	0.142	46.006	0.003	0.1000000
O_2 ($O2^+$)	3.445	31.999	0.108	3.500
H_2O from H_2	0.000	18.015	0.000	0.000
H_2O from coal	0.000	18.015	0.000	0.000
H_2O from air	0.000	18.015	0.000	0.000
N_2 from stoichiometric air	57.931	28.013	2.068	67.222
N_2 from excess air	11.409	28.013	0.407	13.239
N_2 from coal	0.042	28.013	0.002	0.049
Total Flue Gas	**94.524**	**Molecular mass of Flue gas [kg/kmole]**	**3.076**	**100.000**
Total H_2O	0.000		$R_{FLUE\ GAS}$ [kJ/kg-K]	0.000
Total N_2	69.382	**32.50642**	**0.25578**	80.510

D. ROSIN-RAMMLER COAL SIZE DISTRIBUTION

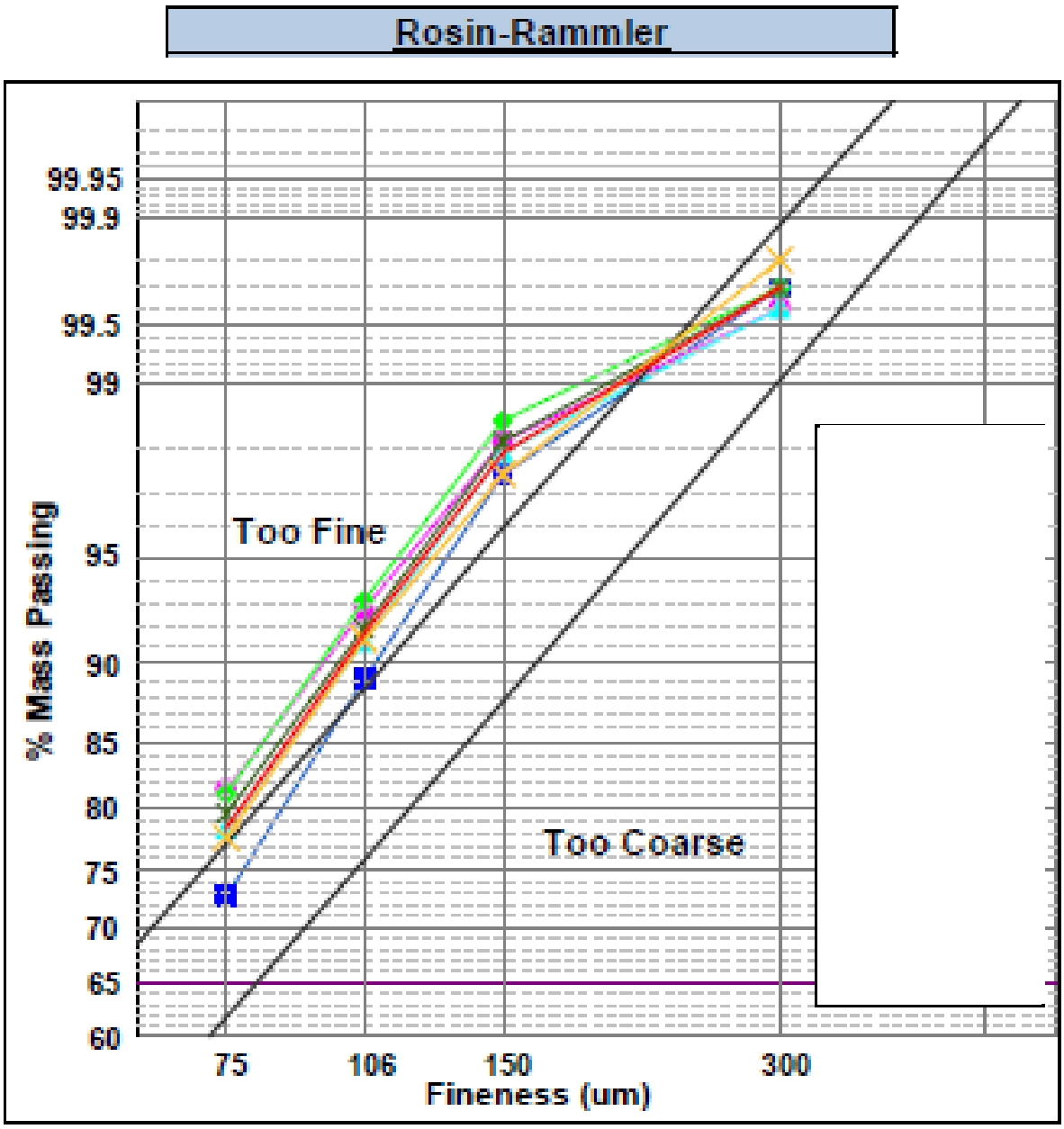

FIGURE D.1: ROSIN-RAMMLER SHOWING MILLING SIZE DISTRIBUTION FOR SOUTH AFRICAN COAL

E. DROP TUBE FURNACE DATA OF SOUTH AFRICAN COAL

TABLE E.1: DROP TUBE FURNACE DATA OF SOUTH AFRICAN COAL

Sample Name	IM	Ash-%	VM	FC	Total sulphur	Total CO2	CV	Carbon	Hydrogen	Nitrogen	Oxygen	SiO2	Al2O3	Fe2O3	TiO2	P2O5	CaO	MgO	Na2O
1	0,8	31,2	23,6	44,4	0,44	1,62	21,57	53,88	3,55	1,24	7,29	56,1	32,6	3,4	1,7	0,71	2,83	0,7	0,01
2	1	32,6	24,5	41,9	1,27	1,78	21,17	51,8	3,42	1,46	6,97	53,4	30,1	5,2	1,5	0,84	4,4	1,3	0,01
3	1	34,4	22,5	42,1	0,96	1,91	20,37	50,55	3,15	1,18	6,85	51,5	33,4	5	1,8	0,73	4,2	1,3	0,01
4	2,6	17	24,8	55,6	2	0,77	25,5	64,52	3,7	1,53	7,88	50,1	25,8	15,2	1,1	0,12	2,8	1,6	0,01
5	2	18,4	27	52,6	2,14	0,84	24,62	63,08	3,66	1,49	8,39	36,6	20	31,3	0,9	0,11	5,3	1	0,01
6	2	24,8	20,6	52,6	1,13	1,33	22,53	59,54	3,13	1,37	6,7	57,8	26,5	5,9	1,5	0,11	5	1,1	0,01
7	3	23,1	21,6	52,3	1,22	1,94	22,42	58,55	2,99	1,34	7,89	54,2	25,2	7	1,4	0,1	7,6	1,9	0,01
8	6,9	23,6	16,4	53,1	0,7	1,97	22,41	55,51	2,19	1,35	7,78	41,8	40,3	1,5	1,6	0,64	6,7	1,7	0
9	6,5	28,2	15,2	50,1	1,28	3,96	20,32	53,38	2,16	1,32	3,2	30,3	38,4	4,2	1,1	0,5	13,2	3,4	0
10	6,6	30,6	15,4	47,4	0,55	2,2	19,17	49,39	2,12	1,32	7,22	43,4	39,8	0,7	1,5	0,65	5,8	1,6	0
11	4,5	28,8	18,7	48	1,07	0,77	21,18	55,67	2,95	1,31	1,12	46,4	39,4	3,7	1,9	0,3	4,6	1,1	0,5
12	5,1	23,2	22,6	49,1	2,37	1,86	22,44	58,14	2,31	1,39	5,63	48,4	24,5	11,1	1,2	0,61	7,3	3,1	0,01
13	2,2	25,2	24,2	48,4	0,76	0,57	23,57	59,29	3,27	1,22	6,86	50,1	31,5	3,9	1,6	0,7	4,8	1,8	0,01
14	5,2	20,8	22,8	51,5	0,79	1,36	19,98	61,25	3,63	1,48	5,49	62	28,7	3,86	2,24	0,49	0,2	0,1	0,05
15	6,6	14,8	27,6	51	1,08	0	24,23	59,97	2,69	1,75	13,11	59,3	27	7,8	1,4	0,14	1,8	0,4	0,01
16	4,2	32,8	21,7	41,3	1,25	2,99	18,63	49,01	2,39	1,31	6,05	53,3	24	5,5	1,3	0,16	6,1	2,3	0,01
17	4,2	25	22,1	48,7	0,6	1,07	22,27	56,73	2,75	1,26	8,39	54,7	27,3	3,4	1,3	0,56	4,4	1,7	0,01
18	4,5	27,2	21,8	46,5	0,73	1,86	20,76	55,1	2,84	1,44	6,33	53,7	25,5	3	1,4	0,73	6,8	2,4	0,01
19	4,9	22,3	22,6	50,2	0,56	2,06	22	58,78	3,01	1,54	6,85	44,4	28,2	2,1	1,6	1,11	10,9	3,3	0,8
20	4,3	25,8	20,1	49,8	0,49	0,59	21,95	58,4	2,36	1,36	6,66	64,4	26,4	3,2	1,3	0,2	1,8	1	0,01
21	3,7	23,2	22,2	50,9	1,36	0,24	22,92	59,61	3,12	1,55	7,22	54,4	33,4	5,4	1,8	0,36	1,2	0,8	0,01
22	6,2	39,6	19,2	35	1,07		15,15	41,62	2,2	0,65	8,36	54,2	28,4	4,9	1,3	0,44	4,4	1,5	0,01
23	1,8	33,7	25	39,5	0,96	0,46	20,3	51,31	3,24	1,02	7,51	60	29,8	4,2	1,2	0,56	1,8	0,8	0,01
24	2,8	35,7	21,4	40,1	1,42	2,17	18,58	47,9	2,87	1,23	5,91	52,6	30,4	5,51	1,37	0,66	4,63	1,56	0,27
25	5,4	25,5	24,2	44,9	1,06		21,21	56,04	3,1	1,47	6,11	44,66	26,81	7,74	1,66	1,75	8,37	1,65	0,14
26	2,3	34,2	19	44,5	0,61	1,84	19,98	52,98	2,15	1,1	4,86	52,7	30,1	4,1	2	1,15	6,2	1,6	0,01
27	2,8	29	20,4	47,8	0,8	2,98	21,22	53,45	2,63	1,16	7,18	42,7	26,5	5,4	1,4	2,96	11,2	2	0,01
28	2,6	35,6	20,8	41	1,24	2,32	19,24	49,25	2,73	1,14	5,12	51,9	26,1	6,4	1,4	0,57	5,1	1,3	0,01
29	2	34	19,1	44,9	1,16	1,28	23,96	50,9	2,3	1,12	7,24	48,2	31,8	4,72	1,42	1,73	7,68	0,9	0,09
30	5,4	23,2	26,1	45,3	1,51	2,37	22,7	56,9	2,9	1,3	6,47	38,6	32,8	5,2	1,4	1	8,5	2,8	0,01
31	2,8	25	21,3	50,9	1,18	2,12	22,95	59,8	3,12	1,32	4,66	45,7	30,4	5,6	1,8	1,04	6,7	0,8	0,01
32	7,3	24,6	19,2	46,5	0,75	1,43	21,29	56,8	3,3	1,4	4,43	41,6	38,2	2,91	1,79	0,51	6,2	1,5	0,33
33	5,7	24,1	17,7	47,1	0,58	0,91	22,75	58,54	2,49	1,4	6,28	60,7	21,6	7	1,1	0,15	3	1,3	0,01
34	4,3	27,9	20,7	47,1	0,53	1,86	20,62	54,89	2,38	1,41	6,73	60,9	19,5	4,86	1,42	0,36	7,03	1,98	0,12
35	1,5	19,9	21,3	54,3	0,69	1,85	23,87	62,19	2,31	1,55	10,01	48,9	28,8	3,3	1,4	0,68	7,9	3,3	0,05
36	4,4	22,6	23,8	49,2	0,92	2,04	22,4	58,42	2,66	1,3	7,66	42,9	31,2	6,6	1,3	1,28	8,1	2,5	0
37	3,6	37,3	20,8	38,3	0,83	1,57	17,1	45,85	2,24	1	7,61	53,6	30,1	2,6	1,5	0,6	4,3	1,9	0,2
38	3,4	31,2	19,3	46,6	1,11	0,01	20,77	54,24	2,9	1,31	6,33	53,6	37,2	4,2	2,3	0,4	0,3	0,5	0,01
39	1,2	34,3	17,4	47,1	1,74	0,14	20,49	51,35	2,68	1,16	7,43	61,4	27,9	4,9	1,6	0,34	0,3	0,6	0,01
40	2,2	30	18,7	49,1	0,58	1,03	21,43	57,38	2,61	1,21	4,99	58,6	32,1	2,79	1,72	0,55	1,34	0,6	0,14
41	3,4	29,4	22,4	44,9	0,93	1,74	20,79	55,2	2,76	1,22	5,35	60,6	24,4	3,7	1,5	0,25	3,1	1,3	0,01
42	5,2	22,4	20,3	52,1	1,05	0,87	22,14	57,61	2,74	1,5	8,63	45,4	35,6	7,8	2	1,16	3,1	1,5	0,01
43	4,31	24,1	22,7	48,5	0,78	2,09	21,87	58,16	2,32	1,44	7,91	52,73	29,91	4,42	1,77	1,08	5,31	1,31	0,31
44	2,2	38,5	18,4	40,9	0,5	1,34	17,43	47,95	2,42	1	6,09	49,5	33,8	2,8	1,5	0,75	4,5	1,7	0,01
45	1,7	26,4	20,2	51,7	0,74	2,62	23,35					44,1	36,1	4,2	1,6	1,28	7,7	2	0,01
46	2,4	32	19,8	45,8	0,97	1,76	21,24	54,89	2,99	1,22	3,77	56,2	27,7	5,7	1,6	0,17	4,1	1,8	0,01
47	4,1	30,8	19,7	45,4	1,24	0,63	19,91	53,43	2,52	1,16	6,12	49,2	30	4,07	1,61	1,34	8,12	2,53	0,24
48	6,4	27	22,2	44,4	0,6	2,61	19,46	51,1	2,61	1,34	7,86	46	32,4	8,04	1,74	0,32	6,66	1,99	0,13
49	4,8	22,4	23	49,8	0,79	2,16	22,74	59,1	2,44	1,71	6,6	41,4	31,3	2,4	1,5	1,76	9,4	3,2	0,01
50	4,9	32,2	18,4	44,5	0,8	1,41	18,91	49,5	2,46	1,14	7,59	45,6	38,9	5,2	2,2	0,38	1,3	0,8	0,01
51	4,5	29,2	20,4	45,9	1,01	1,49	20,79	53,13	2,98	1,33	6,36	43,8	40,2	5,08	2,32	0,4	4,52	0,91	0,18
52	2,2	30,7	20,6	46,5	1,14	1,9	21,31	55,1	2,69	1,12	5,15	60,3	23,6	4,3	1,6	0,12	5	1,4	0,01
53	2,6	34	20,4	43	1,34	3,32	19,63	50,71	2,56	0,99	4,48	54,7	23,4	6,2	1,6	0,11	5,5	2,4	0,01
54	5,2	26,8	22,6	45,4	1,06	1,06	19,9	53,57	2,68	1,32	8,31	44,2	30,1	4,2	1,7	1,04	8,1	1,3	0,01
55	3,9	20	25,6	50,5	1,58	0,55	24,08	62,38	3,33	1,56	6,7	50,1	28	7	1,2	0,26	6	1,8	0,01
56	6,6	15,8	29,6	54,6	1,08	0	24,34	59,97	2,69	1,75	13,1	59,3	27	7,8	1,4	0,14	1,8	0,4	0,01
57	3,9	17,4	28,4	54,2	0,96	0,28	26,7	64,16	3,19	1,79	9,02	56,9	28,7	4,8	1,4	0,026	5,4	0,8	0
58	2,4	34,6	22,2	40,8	1,12	0,91	19,26	49,81	2,82	0,98	7,36	59,7	24,7	3,5	1,2	0,52	2,6	0,7	0,01

Sample Name	K2O	SO3	Mn	Def (ºC)	Hem (ºC)	Flo (ºC)	Abrasive index (mmFe)	HGI	Volatiles by DTF, VMDTF%	CV of volatiles, CVvm	Heat in volatiles (HIV)%	Activation Energy	Energy Ratio	Burnout time in seconds
1	0,5	2,7	0,04	1550	1550	1550	224	48	28,1	29	37,5	91,7	1,5	2,3
2	0,6	3,9	0,04	1400	1480	1500	200	40	28,6	28,9	38,6	82,7	1,7	1,7
3	0,4	3,2	0,05	1480	1530	1550	161	49	28,1	29,5	40,4	82,7	1,7	1,7
4	0,2	4,5	0,09	1370	1390	1400	275	47	32,6	28,7	35,7	61,4	2,7	1,3
5	0,1	4,5	0,34	1280	1300	1320	361	44	37,2	26,4	39	56,4	3,3	1,5
6	0,2	4,5	0,09	1450	1480	1500	243	54	28,7	25,9	32,3	61,7	2	1,5
7	0,1	3,8	0,15	1290	1320	1330	238	55	32,1	24,6	34,2	62,2	2,2	1,3
8	0,7	4,9	0,03	1490	1550	1550	20		27,8	30,3	35	53,4	2,6	1,4
9	0,5	4,8	0,04	1410	1430	1440	30		26,6	25,8	31,6	56,6	2	1,5
10	0,8	3,4	0,03	1550	1550	1550	82		28,1	29,6	40,6	57,3	2,4	1,3
11	0,7	2,9	0,02	0	0	0	0		17	23,8	25,2	97,2	0,8	2,9
12	0,3	7					424	50	32,9	27,3	38	72,9	2,2	1,4
13	0,5	2					284	56	29,5	30,1	36,8	53,8	2,8	2,5
14	0,48	0,16		1300	1330	1350	380	69	28,8	15,6	21,4	63,4	1,2	2,4
15	0,7	1,3							34,9	26,36	35,3	42,6	4	0,99
16	0,1	4	0,04	1300	1320	1340	154		23,7	24,7	30	67,4	1,4	1,3
17	0,6	2,7					284	56	31,3	28,5	28,4	58,5	2,7	2,2
18	0,5	4,5					272	49,17	33,6	25,5	39,5	78,8	2	1,7
19	0,5	4,9					166	57,85	33,2	23,3	33,4	72,1	1,9	1,9
20	0,4	1,7					400	61	36,7	30,2	46,4	75,6	2,8	1,6
21	0,4	1,3					68	61,87	27,3	25,5	29,2	84,7	1,4	2,3
22	0,6	4,4					832	58	29,5	24,1	44,1	83,7	1,4	1,9
23	0,8	1,3					225	47	29,7	29,9	43	64,8	2,3	1,6
24	0,97	2,02	0				295	48	29,7	27	40,3	68,7	2	1,5
25	0,8	8,15	0,01				179,3	56	36,2	26,2	42,3	85,9	2,1	1,5
26	0,3	2,3							19,2	25,2	23,7	83,6	0,9	2,3
27	0,4	4	0,04	1330	1370	1400	0		18,4	27,5	23,2	46,4	1,6	2,3
28	0,5	4,3	0,05	1430	1480	1500	0		19,3	32,4	31,7	53,9	1,7	1,4
29	0,6	3,39	0,05						27,8	41,5	47,2	39,4	4,9	1,2
30	1	7,6		1350	1390	1410	155	47	34	26,1	37,7	69,8	2,3	1,6
31	0,6	4,4	0,06	1380	1400	1420	260		38,5	30,4	49,7	50,9	4,5	1,5
32	1,17	5,38	0	1429	1487	1500			29	26,7	33,8	71,4	1,8	2,2
33	1,5	3,5	0,03	1430	1490	1530			22,1	25,7	24,2	74,3	1,2	2,3
34	0,4	1,88	0	1300	1320	1340	244		27,9	24,3	31,5	35,8	3,2	1,3
35	0,5	2,2							31,7	24,8	32,5	59,5	2,3	1,3
36	0,3	5,8							27,6	24,4	28,9	95,8	1,2	1,9
37	0,6	3,2							26,9	24,1	36,5	131,9	0,8	1,7
38	1,2	0,3	0,01	NM	NM	NM	115	NM	23,2	32,9	36,8	88,6	1,3	1,6
39	1,2	0,2	0,01	1550	1550	1550			23,2	32,9	36,8	88,6	1,3	1,6
40	0,44	2,22	0	1450	1490	1540	276	55	22,5	25,8	26,6	37,8	2,4	
41	0,6	3,1	0,02	1470	1510	1530	551		28,8	30,9	41,2	67,4	2,2	1,3
42	0,3	3,1	0,08	1390	1440	1480		68	31,7	27,4	37,2	62,4	2,4	1,2
43	0,57	3,18		1262	1344	1363		50	27,3	28,7	33	88,3	1,5	1,8
44	0,8	1,3	0,03						15,2	18,3	15,6	66,2	0,6	2,5
45	0,5	2,8	0,05						27,3	28,7	33			1,8
46	0,3	3	0,05	1310	1370	1410			25,6	30,2	35,5	76	1,6	1,5
47	0,65	1,03							26,9	24,4	31,6	56,9	1,9	1,4
48	0,48	2,98		1360	1390	1420	83	59	29,2	20,7	29,1	65,2	1,6	1,5
49	0,7	5	0,03	1310	1350	1380			30,5	26,3	33,6	77,9	1,8	1,6
50	0,3	1,5	0,03	1600	1530	1580	0		33,2	35,1	58,7	68,2	3,1	1,3
51	1	2,62					105	54	24,7	24,9	29,1	88,8	1,1	1,7
52	0,1	3,6	0,02	1250	1300	1340	0		24,9	33,3	38,1	68,8	1,9	1,3
53	0,1	3,1	0,03	1250	1300	1340	0		21,4	32,4	34,8	57,6	1,8	1,4
54	0,4	7,1	0,04	1370	1430	1480	238	64	29,6	21,3	29,9	88,6	1,3	1,6
55	0,9	5,8	0,04	1300	1330	1344			43,3	30	51,8	51,8	5,3	2,2
56	0,7	1,3	0,03				600		34,9	26,3	35,3	42,6	4	0,99
57	0,6	3,1	0,04									55,2		1
58	0,8	2,5	0,01	0	0	0	410		34,5	27	47,2	58,4	2,9	1,3

F. AL-30 PROPERTIES

Zircar CERAMICS

Alumina Type AL-30

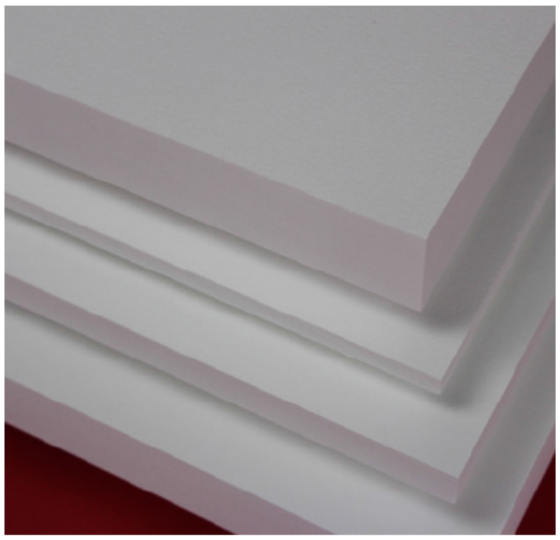

General Information

ZIRCAR Ceramics' Alumina Type AL-30 is a medium-density, high-strength, uniformly rigid refractory structure composed of high-alpha polycrystalline alumina fibers and high-purity inorganic binders. AL-30 exhibits a fine, open-pore structure and is made to an optimum bulk density of 0.48 g/cc (30 pcf) which gives it very low thermal conductivity at elevated temperatures. AL-30 has very good hot strength and dimensional stability to 1600°C (2822°F) and withstands intermittent use to 1700°C (3192°F).

AL-30 is manufactured with a high fiber-to-binder ratio making it highly machinable to precise dimensional tolerances. It exhibits high electrical resistivity with low losses in microwave and RF transparency at elevated temperatures. AL-30 is pure white and exhibits high reflectance.

AL-30 is pre-fired, contains no organic binders and will produce no smoke or odors when heated. AL-30 shows excellent resistance to chemical attack and is not affected by oil or water. It is, however, affected by hydrofluoric acid, phosphoric acid and strong alkalis.

Characteristics & Properties

Color	White
Typical Composition, %	
Al_2O_3	85
SiO_2	15
Organic Content	0
Density, g/cc (pcf)	0.48 (30)
Melting Point, °C(°F)	1870 (3392)
Open Porosity, %	85
Specific Heat, J/kg°K (BTU/lb °F)	1047 (0.25)
Maximum Use Temperature*, °C (°F)	
Continuous	1600 (2822)
Intermittent	1700 (3092)
Linear Shrinkage‡, %	
24 hrs. at 1500°(2730°F)	1
24 hrs. At 1650°(3002°F)	3
Thermal Expansion Coefficient, Room Temperature to 1000°C (1832°F)	5.0 x 10^{-6}/°C (2.8 x 10^{-6}/°F)
Compressive Strength**, MPa (psi) at 10% Compression	2.8 (400)

ZIRCAR Ceramics, Inc.
PO Box 519
100 N. Main St., Florida, NY 10921-0519
Telephone: (845) 651-6600
E-mail: sales@zircarceramics.com

Alumina Type AL-30

Characteristics & Properties Continued

Flexural Strength**, MPa (psi) at 30% Strain	3.1 (450)
Thermal Conductivity**, (ASTM C177-76) W/m°K (BTU/hr ft² °F/in)	
250°C (482°F)	0.09 (0.65)
525°C (977°F)	0.12 (0.85)
800°C (1472°F)	0.16 (1.10)
1075°C (1967°F)	0.19 (1.30)
1350°C (2462°F)	0.23 (1.60)
1650°C (3002°F)	0.27 (1.86)

The data presented herein is intended to help the user to determine the appropriateness of this material for their application.
This data is a nominal representation of this product's properties and characteristics and therefore should not be used in preparing specifications.
* Maximum use temperature is dependent on variables such as stresses, both thermal and mechanical, and the chemical environment that the material experiences. ** Properties expressed parallel to thickness. ‡ Properties expressed perpendicular to thickness.

Suggested Applications

Primary thermal insulation in low-mass furnaces and thermal process systems operating to 1650°C (3002°F).
Backup thermal insulation in furnaces and thermal process systems operating to temperatures exceeding 2000°C (3632°F).
Precision-machined thermal insulation in scientific analytical instruments.
High-temperature setters, supports and process fixtures.
Electrical insulation in high-temperature systems operating to 1650°C (3002°F).

Availability of Standard Boards

ITEM #	DESCRIPTION
A11013	AL-30, 24"W x 48"L x 0.50"T
A11014	AL-30, 24"W x 48"L x 0.75"T
A11015	AL-30, 24"W x 48"L x 1.00"T
A11016	AL-30, 24"W x 48"L x 1.50"T

To Order

Standard boards: order online or specify quantity, item # and description.
Standard boards are available for immediate shipment from stock.

Standard tolerances for boards are +/- 1/8" on length and width and +/- 1/16" on thickness.

Custom boards as thick as 3"T have been manufactured.

Custom shapes: our state-of-the-art tight-tolerance machining techniques allow a wide variety of sizes and shapes to be made.

Cylinders can be manufactured with IDs from 1in. to 18" with ½" to 2" wall thickness and length up to 36".

Surface treatments including rigidization with colloidal alumina (AL-R/H) or colloidal silica (SI-RIG) or coating with alumina cement (AL-CEM) are all available.

Zircar® CERAMICS

ZIRCAR Ceramics, Inc.
PO Box 519
100 N. Main St., Florida, NY 10921-0519
Telephone: (845) 651-6600
E-mail: sales@zircarceramics.com
www.zircarceramics.com
Revision Date Dec 3, 2016

G. CFD ANALYSIS SHOWING AIR HEATERS AND BURNER PRESSURE DISTRIBUTION

G.1. CA HEATER PRESSURE

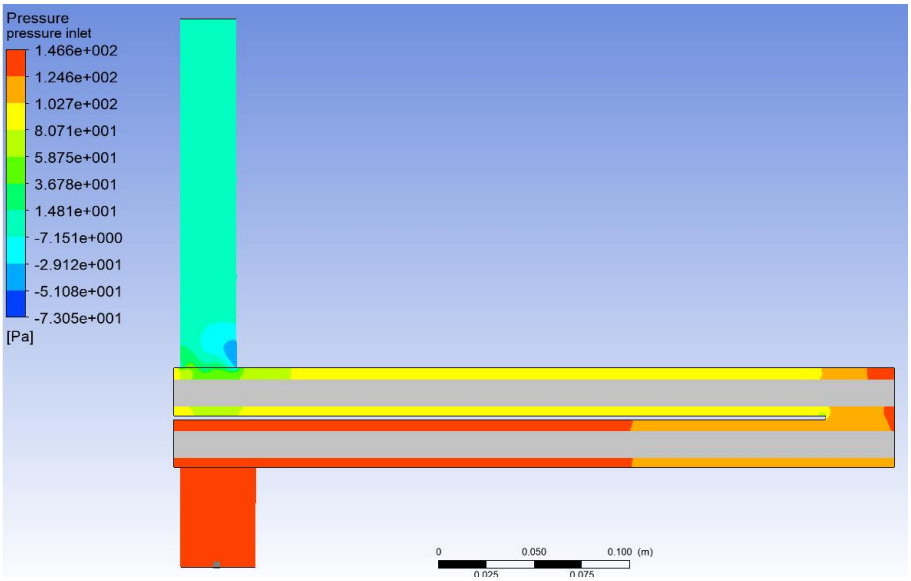

FIGURE G.1.1: CFD SHOWING PRESSURE DISTRIBUTION INSIDE CA HEATER

G.2. PA HEATER PRESSURE

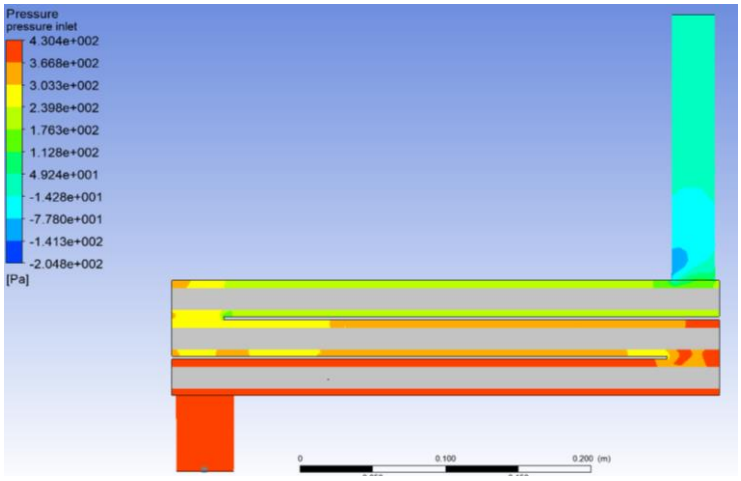

FIGURE G.2.1: CFD SHOWING PRESSURE DISTRIBUTION INSIDE PA HEATER

G.3. SA HEATER PRESSURE

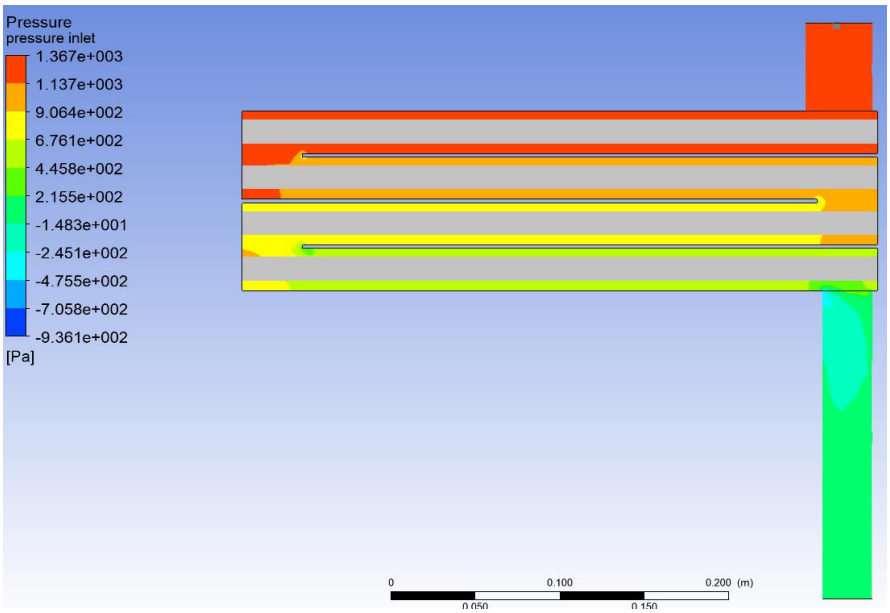

FIGURE G.3.1: CFD SHOWING PRESSURE DISTRIBUTION INSIDE SA HEATER

G.4. TA HEATER PRESSURE

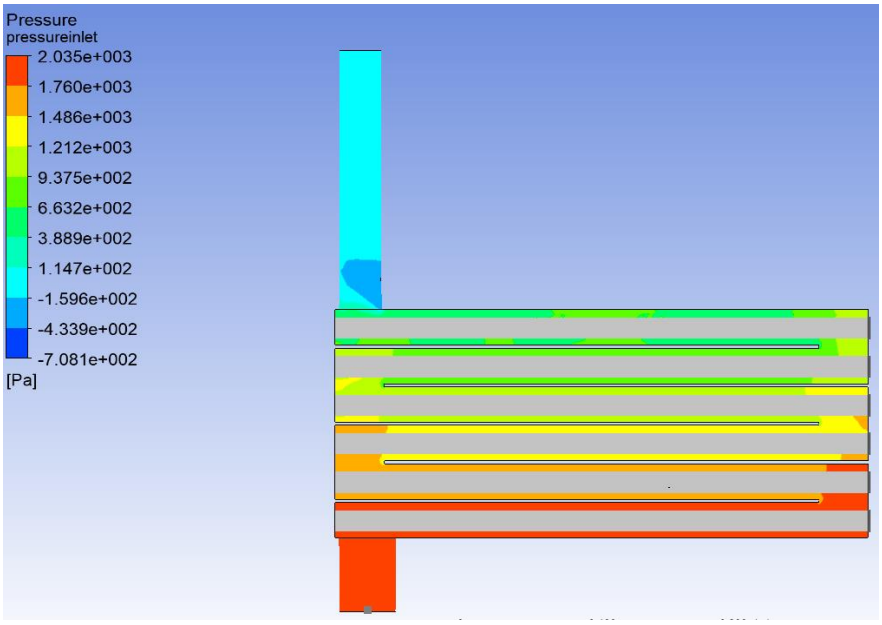

FIGURE G.4.1: CFD SHOWING PRESSURE DISTRIBUTION INSIDE TA HEATER

G.5. BURNER TUBES PRESSURE DISTRIBUTION

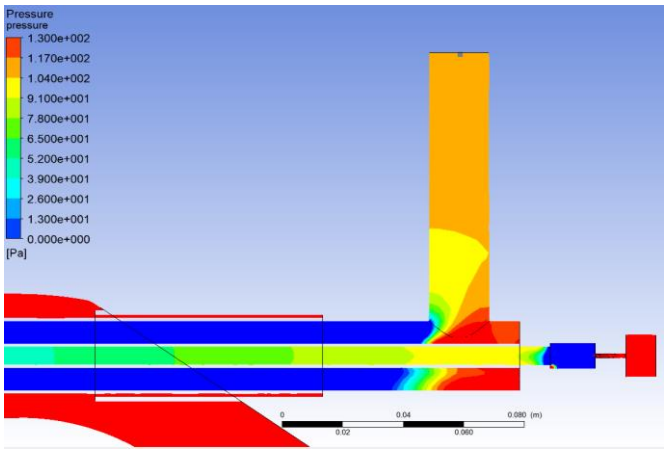

FIGURE G.5.1: CFD SHOWING PRESSURE DISTRIBUTION INSIDE CA AND LPG TUBE

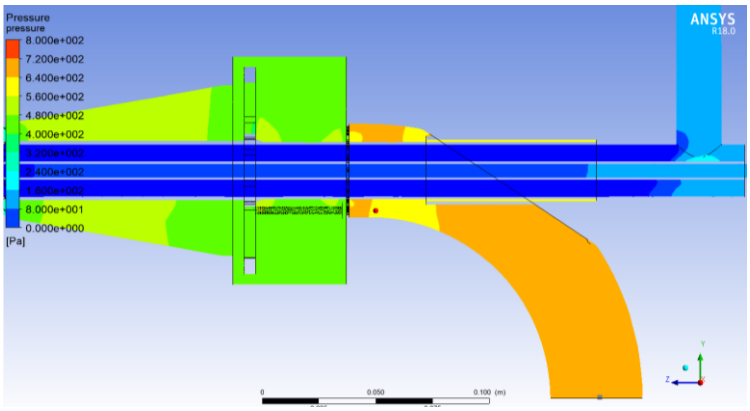

FIGURE G.5.2: CFD SHOWING PRESSURE DISTRIBUTION INSIDE PA/PC TUBE

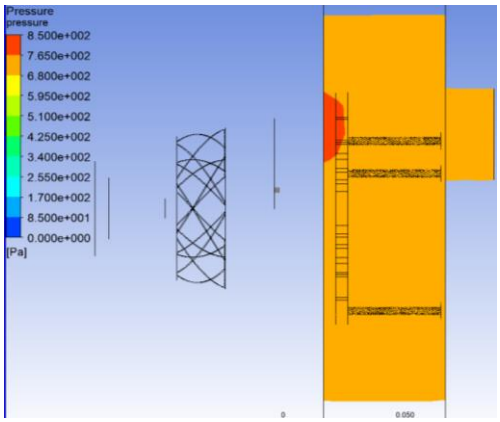

FIGURE G.5.3: CFD SHOWING PRESSURE DISTRIBUTION INSIDE SA WIND BOX

H. SPECIFICATIONS OF BLOWER USED TO PROVIDE COMBUSTION AIR

ZXB Series Selection Diagram: 50Hz 1 phase

The performance curves are valid for pumping air at 15°C at the inlet flanges with an air pressure of 1.013 mbar and a tolerance of ±10%.The total pressure differences are valid up to an intake and ambient temperature of 25°C.

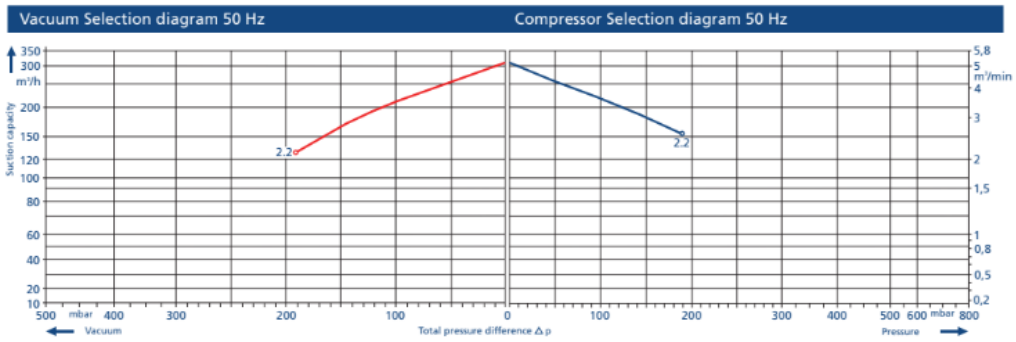

Selection and ordering data

ZXB 710 SERIES - 1 phase

ORDER NO.	MOTOR				Weight approx.	Sound pressure level	Maximum airflow	Maximum vacuum	Maximum pressure
	Frequency	rated							
		output	voltage	current					
	Hz	KW	V	A	kg	dB(A)	m³/h	mbar	mbar
ZXB 710-7AA11	50	2,2	230	12,8	30	72	318	-190	190

Dimensions for installation

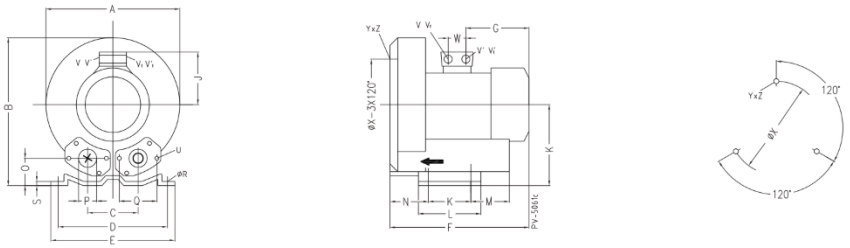

MODEL	PHASE	A	B	C	D	E	F	G	H	J	K	L	M	N	O	øP	Q	øR	S	U	V(1)	V'(1)	V1(3)	V'1(3)	YxZ	X-Holes	øX	W
ZXB 710-7AA11	1ph	382	384	125	290	325	377	191	197	128	140	180	84	109	54	55	83	15	4.5	M8 x 17	M25x1.5	M16x1.5	–	–	M10x20	0°/120°/240°	240	29

FIGURE H.1: SPECIFICATIONS OF BLOWER

I. PRESSURE DISTRIBUTION AND AIR FLOW INSIDE COOLING JACKET

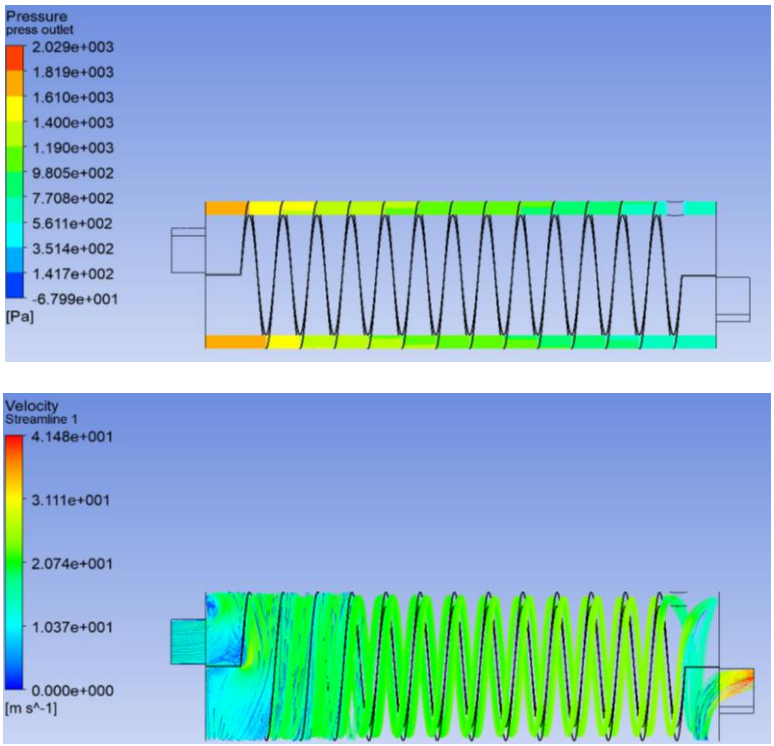

FIGURE I.1: CFD PRESSURE DISTRIBUTION SECTION VIEW (TOP) AND VELOCITY STREAMLINES (BOTTOM) INSIDE COOLING JACKET

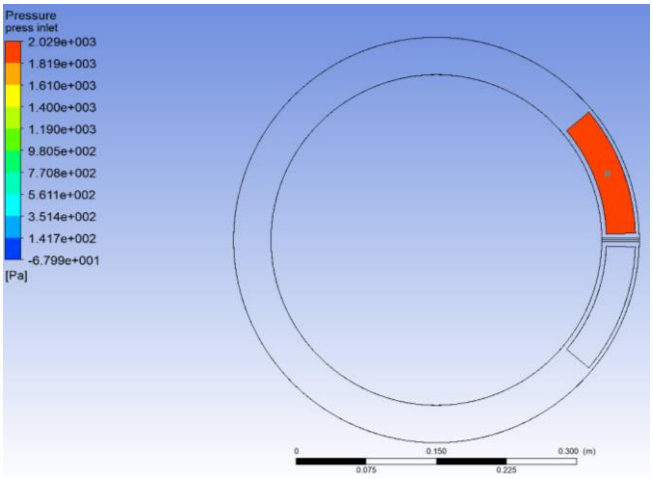

FIGURE I.2: CFD SHOWING COOLING JACKET INLET PRESSURE

J. PERFORMANCE CURVE OF CENTRIFUGAL FAN - COOLING JACKET

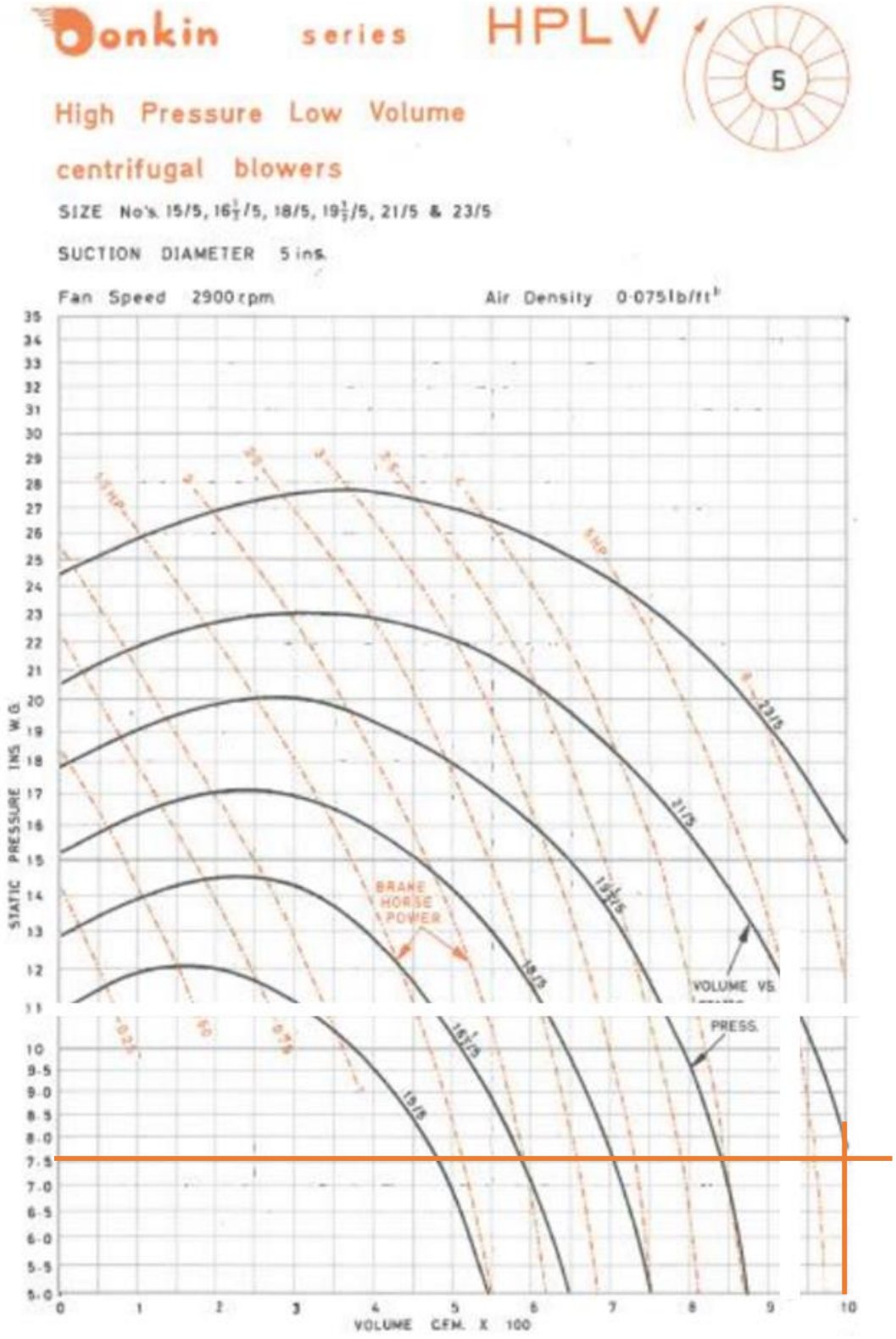

FIGURE J.1: PERFORMANCE CURVE OF CENTRIFUGAL FAN

K. ROTAMETERS CALIBRATION CERTIFICATE

TECFLUID s.a.
Instrumentación para fluidos
Narcís Monturiol, 33
E - 08960 SANT JUST DESVERN (Barcelona)
Tel. +34 93 372 45 11 - Fax +34 93 473 44 49
E-Mail: tecfluid@tecfluid.com
Internet: www.tecfluid.com

pàg. nº 1 / 1
pág. nº
page nº

DECLARATION OF CONFORMITY WITH THE CALIBRATION

SANT JUST DESVERN: November 15, 2012

CERTIFICATE NO.: 5015119

CUSTOMER:: C & F TECHNOLOGIES

1. CALIBRATED INSTRUMENT

FLOW METER

MANUFACTURER: TECFLUID
MODEL: SC250 / AISI-316
DN: 50
SERIAL NUMBER: 12/5015119
FLUID: H2O 20 ºC
FLOW RATE: 1,5 - 15 m³/h

2. CALIBRATING PROCEDURE

The calibration has been done as per the internal Procedure C-PR-07.

Reference Instrument: DCCBC007 , DCCBC008
Reference Fluid: H_2O

3. INCERTITUDE OF MEASURE

The uncertainty associated to the calibration has been estimated with a degree of reliability of k=2 in ± 1% F.S.

4. RESULTS

TECFLUID, S.A. certifies that the results got in the calibration agree with the maximum tolerances of accuracy according to VDI/VDE 3513 Norm Class 2,5 (± 2,5 % F.S.D.).

5. TRACEBILITY

The Reference Instrument has been calibrated according to the internal Procedure C-PR-13, with our reference instrument DPSBD003, with Calibration Certificate number BT 8 6076 of METTLER-TOLEDO and that it is traceable to their standards codes MS 800394, MS 80506, which tracebility to National Standards is accredited by ENAC (Entidad Nacional de Acreditación).

6. NEXT CALIBRATION

When one observes that the measuring components (float, calibrated orifice, flow tube) shows some wear and/or they are dirty it will be necessary to recalibrate the flow meter.

FLOW CALIBRATING DEPT.

Daniel Perea Estrany
Flow Calibrating Chief

TECFLUID s.a.
c/. Narcís Monturiol, 33
SANT JUST DESVERN
(Barcelona)

QUALITY DEPT
(FOR DELEGATION)

Ivan Brugalla Bosch
Technical Engineer in Chemical Process

Tecfluid manufactures its products according to a Quality Assurance System ISO 9001:2008
Certificated by the Centro de Certificación LGAI.

L. CALIBRATION OVEN - CALIBRATION CERTIFICATE

Repcal Services cc
Reg No: 2002/087115/23

sanas Calibration Laboratory

146
208
308
846
1446
1546

CERTIFICATE OF CALIBRATION

CERTIFICATE NUMBER: 308-61602

Calibration of a	:	Dry Block
Manufacturer	:	Isotech
Model No	:	Pegasus
Serial No	:	241273-1
Calibrated for	:	North West University
Address	:	Main Campus Potchefstroom
Issue Date	:	04 October 2019
Calibration Date	:	03 October 2019
Technical Signatory	:	J.W Ysel
Calibrated by	:	J.W Ysel

Digitally signed by Johannes willem Ysel

The South African National Accreditation System (SANAS) is a member of the International Laboratory Accreditation Co-Operation (ILAC) for the Mutual Recognition Agreement (MRA). The MRA allows for the mutual recognition of technical test and calibration data by the member accreditation bodies worldwide. For more information on the MRA please refer to www.ilac.org

The calibration values in the certificate were correct at the time of calibration. The continuous accuracy of the instrument will depend on such factors as the care exercised in handling and use of the instrument and the frequency of use. Re-calibration should be performed after a period which has been chosen to ensure that the item's accuracy remains within the desired limits.

508 Nupen Crescent
Halfway House
Midrand

P.O. Box 6093
Halfway House
1685

Phone (011) 315 3134
Fax (011) 315 8726
e-mail : service@repcal.co.za

Page 1 of 4 pages

REPCAL SERVICES
SANAS ACCREDITED CALIBRATION LABORATORY

1. LABORATORY STANDARDS AND EQUIPMENT USED FOR MEASUREMENTS

Standards or Equipment	Serial Number	Certificate Number	Due Date
Type R Thermocouple	13G0912/01	308-54246	2020/01
Fluke 8842A Digital Multimeter	5386263	146-58329	2020/06

2. PROCEDURE

2.1 Procedure used: - TEMP 15

3. REMARKS

3.1. Traceability

The accuracy of the equipment used during calibration is traceable to the National Measuring Standards as maintained in Republic of South Africa or International Measuring Standards.

3.2. Calibration Environment

The calibration was performed in an environmentally controlled laboratory.
The Temperature were maintained at: 23°C ±5°C. The temperature did not vary more than 2°C per hour at the time of calibration.

3.3. Results

The UUT was calibrated to Customers' requirements. These results only apply to the Unit Under Test (UUT) calibrated.

3.4. Condition of the Unit Under Test

The UUT is in a good condition and fully functional.

3.5. Uncertainties of Measurement

The reported uncertainty of measurement are based on a standard uncertainty multiplied by a coverage factor of k = 2, which unless specifically stated otherwise, provide a level of confidence of approximately 95 %.

Certificate No : 308-61602

REPCAL SERVICES
SANAS ACCREDITED CALIBRATION LABORATORY

4. METHOD

The Dry Block Calibrator was calibrated from 100 °C to 1200 °C. The true temperature of the calibrator was measured with a standard Thermocouple.

5. RESULTS

Actual Temperature ITS-90 (°C)	UUT Set Point (°C)	UUT Indicated Temperature (°C)	UUT Correction (°C)
101.2	100.0	100.0	+1.2
302.0	300.0	300.0	+2.0
602.9	600.0	600.0	+2.9
904.9	900.0	900.0	+4.9
1210	1200	1200	+10

The uncertainty of measurement was: ±2 °C

Actual Temperature ITS-90 (°C)	UUT Set Point (°C)	UUT Indicated Temperature (°C)	UUT Correction (°C)
Axial Uniformity:			
Full Immersion			
602.9	600.0	600.0	+2.9
20 mm Withdrawn:			
600.9	600.0	600.0	+0.9

The uncertainty of measurement was: ±2 °C

Actual Temperature ITS-90 (°C)	At Set Point (°C)	+10 min (°C)	+20 min (°C)	+30 min (°C)
Temperature Stability At 600	602.9	602.7	602.8	602.9

The uncertainty of measurement was: ±2 °C

Certificate No : 308-61602

REPCAL SERVICES
SANAS ACCREDITED CALIBRATION LABORATORY

5. RESULTS (Cont)

Actual Temperature ITS-90 (°C)	6mm Hole A (°C)	6mm Hole B (°C)
Hole to Hole Uniformity: At 600	602.9	602.6

The uncertainty of measurement was: ±2 °C

6. NOTES

6.1 Calibrated from: 100 °C to 1200 °C.

6.2 All measurements performed in 6 mm boring marked A.

6.3 Hole to hole uniformity test was performed in the 6 mm boring marked A & B.

6.4 Immersion depth: 110 mm.

6.5 Laboratory standard diameter: 6 mm.

6.6 The top of the dry block was packed with isolation material to prevent loss of heat.

6.7 No Probe supplied for the UUT indicator.

6.8 The UUT correction was calculated from the UUT indicated temperature on the controller.

6.9 No loading effect was performed.

6.10 The Dry Block Calibrator was allowed to stabilize at each set point before measurements was recorded.

End of Certificate

Certificate No : 308-61602

Page 4 of 4 pages

M. TESTED COAL ANALYSIS AND COMBUSTION CALCULATIONS

M.1 TESTED COAL ANALYSIS

Eskom

sanas
Laboratory Number T0055

Central Coal Laboratory

TEST REPORT

Final Task Report

Attention	C van Alphen	Report Reference	
Client Name	FUELS SECTION	COA2019-010315	
Address	Eskom RT&D Fuels Section	Date	2019-07-24
	Private Bag 40175	Tel. No.	+27 11 629 5254
	Cleveland	Fax. No.	+27 86 66 28380
	2022		
Fax	011 629 5542		
Telephone	082 856 3372		

Report Title WMC COAL
Burner A and B JULY 2019
These results are reported on an air dried basis.

Number of Samples 2
Description of Samples
Date Received 23/07/2019
Date Reported 24/07/2019
Task Comments

Approved By : _____
Patrick Musie
Senior Technician (Coal & X-Ray)

Date : _____

Lower Germiston Road Cleveland 2022 Private Bag 40175 Cleveland 2022 SA
Tel +27 11 629 5254 Fax +27 86 66 28380 patrick.musie@eskom.co.za
Eskom Holdings Reg No 2002/015527/06

Page 1 of 3

Central Coal Laboratory Test Report		Report Reference COA2019-010315	
Sample ID	**9878966**	**WMCC-2019-07-19/4044**	
Burner A			
Component		**Unit**	**Value**
Analytical Moisture		%	3.3
Ash		%	41.3
Volatile Matter		%	20.5
Fixed Carbon (by difference)		%	34.9
Carbon		%	40.35
Hydrogen		%	1.84
Nitrogen		%	1.16
Total Sulphur		%	0.84
Carbonate		%	2.02
Oxygen (by difference)		%	9.19
Gross Calorific Value		MJ/kg	15.18

Sample ID	**9878967**	**WMCC-2019-07-19/4045**	
Burner B			
Component		**Unit**	**Value**
Analytical Moisture		%	3.4
Ash		%	41.2
Volatile Matter		%	20.7
Fixed Carbon (by difference)		%	34.7
Carbon		%	40.52
Hydrogen		%	1.90
Nitrogen		%	0.98
Total Sulphur		%	0.82
Carbonate		%	2.03
Oxygen (by difference)		%	9.15
Gross Calorific Value		MJ/kg	15.18

The analysis was performed using the following methods:

Analytical Moisture	**LABORATORY METHOD No 103**	**Accredited**
Ash	**LABORATORY METHOD No 101**	**Accredited**
Volatile Matter	**LABORATORY METHOD No 102**	**Accredited**
Fixed Carbon	**LABORATORY METHOD No 128**	**Accredited**
Carbon, Nitrogen, Hydrogen	**LABORATORY METHOD No 118**	**Not Accredited**
Carbon, Nitrogen, Hydrogen	**ESKOM METHOD No 118 REV 1**	**Not Accredited**
Carbonate	**LABORATORY METHOD No 100**	**Not Accredited**

Page 2 of 3

The analysis was performed using the following methods:

Total Sulphur	LABORATORY METHOD No 104	Accredited
Oxygen (Difference)	LABORATORY METHOD No 132	Not Accredited
Gross Calorific Value	LABORATORY METHOD No 105	Accredited

Tests marked "Not SANAS accredited" in this report are not included in the SANAS Schedule of Accreditation for this laboratory.

Opinions and interpretations expressed herein are outside the scope of SANAS accredition.
The results contained in this report only pertain to the sample submitted. If you rely on the information and data contained in this report you are responsible for ensuring by independent verification the accuracy or completeness of the sample submitted.

End of Report

Page 3 of 3

M.2 TESTED COAL ANALYSIS CONVERTED TO AN AS RECIEVED, AIR DRIED AND DRY BASIS

TABLE M.2.1: CONVERTED ANALYSIS OF TESTED COAL

COAL QUALITY					
GRAVIMETRIC %	**SYMBOL**	**UNITS**	**AS RECEIVED**	**AIR DRIED**	**DRY BASIS**
PROXIMATE ANALYSIS					
Carbon $_{FIXED}$ (by difference)	C_{FIX}	%	34,900	34,900	36,091
Volatile matter	VM	%	20,500	20,500	21,200
Ash	Ash	%	41,300	41,300	42,709
Surface moisture	M_s	%	0,000	0,000	0,000
Inherent moisture	M_i	%	3,300	3,300	0,000
Total moisture	M_t	%	3,300	3,300	0,000
Gross calorific value (Bomb)	NCV_P	[MJ/kg]	15,180	15,180	15,698
Total		%	100,000	100,000	100,000
ELEMENTAL ANALYSIS					
Nitrogen	N	%	1,160	1,160	1,200
Oxygen (by difference)	O	%	9,190	9,190	9,504
Carbon $_{TOTAL}$	C_{TOTAL}	%	40,350	40,350	41,727
Ash	A	%	41,300	41,300	42,709
Sulphur	S	%	0,840	0,840	0,869
Hydrogen	H	%	1,840	1,840	1,903
Carbonates	CO_2	%	2,020	2,020	2,089
Other	Cl, F	%	0,000	0,000	0,000
Surface Moisture	M_S	%	0,000	0,000	0,000
Inherent Moisture	M_i	%	3,300	3,300	0,000
Total moisture	M_T	%	3,300	3,300	0,000
Total		%	100,000	100,000	100,000

M.3 HYPER-STOICHIOMETRIC COMBUSTION CHEMICAL EQUATIONS FOR TESTED COAL

TABLE M.3.1: HYPER-STOICHIOMETRIC COMBUSTION CALCULATIONS FOR TESTED COAL

PRACTICAL INCOMPLETE COMBUSTION				
2C	+	O_2	=	2CO
24,022		31,999		56,021
1,000		1,332		2,332
40,142		53,472		93,614
2CO	+	O_2	=	$2CO_2$
56,021		31,999		88,020
1,000		0,571		1,571
93,614		53,472		147,086
93,525		53,421		146,945
S	+	O_2	=	SO_2
32,060		31,999		64,059
1,000		0,998		1,998
0,840		0,838		1,678
$2H_2$	+	O_2	=	$2H_2O$
4,032		31,999		36,030
1,000		7,937		8,937
1,840		14,604		16,444
N_2	+	O_2	=	2NO
28,013		31,999		60,012
1,000		1,142		2,142
0,687040		0,785		1,472

M.4 FLUE GAS CALCULATIONS FOR HYPER STOICHIOMETRIC COMBUSTION OF TESTED COAL

TABLE M.4.1: WET FLUE GAS CALCULATIONS FOR HYPER-STOICHIOMETRIC COMBUSTION OF TESTED COAL

PRACTICAL				
GAS	[kg gas/100kg coal]	[g/s]	% Gravimetric	c_P [kJ/kg-K]
CO_2 (Ostwald CO_2^+)	146,945	2,091	14,808	1,259026
CO	0,090	0,001	0,009	1,051872
SO_2	1,678	0,024	0,169	0,738767
NOx	1,472	0,021	0,148	1,058726
O_2 (Ostwald $O2^+$)	100,933	1,436	10,171	1,095070
H_2O from H_2	16,444	0,234	1,657	2,361384
H_2O from coal	3,300	0,047	0,333	2,361384
H_2O from air	7,324	0,104	0,738	2,361384
N_2 from stoïchiometric air	378,421	5,384	38,134	1,186677
N_2 from excess air	335,253	4,770	33,784	1,186677
N_2 from coal	0,473	0,007	0,048	1,186677
Total Flue Gas	**992,333**	**14,118**	**100,000**	1,219156
Total H_2O	27,068	0,385	2,728	2,361384
Total N_2	714,146	10,161	71,966	1,186677

TABLE M.4.2: DRY FLUE GAS CALCULATIONS FOR HYPER-STOICHIOMETRIC COMBUSTION OF TESTED COAL

PRACTICAL				
GAS	[kg gas/100kg gas]	[kg gas / kmole gas]	[kmole / 100kg]	% Volumetric
CO_2 (Ostwald CO_2^+)	14,808	44,010	0,336	10,419
CO	0,009	28,010	0,000	0,0099846
SO_2	0,169	64,059	0,003	0,0817560
NOx	0,148	46,006	0,003	0,0998274
O_2 (Ostwald $O2^+$)	10,171	31,999	0,318	9,843
H_2O from H_2	0,000	18,015	0,000	0,000
H_2O from coal	0,000	18,015	0,000	0,000
H_2O from air	0,000	18,015	0,000	0,000
N_2 from stoïchiometric air	38,134	28,013	1,361	42,152
N_2 from excess air	33,784	28,013	1,206	37,343
N_2 from coal	0,048	28,013	0,002	0,053
Total Flue Gas	**97,272**	Molecular mass of	**3,230**	**100,000**
Total H_2O	0,000	Fluegas [kg/kmole]	$R_{FLUEGAS}$ [kJ/kg-K]	0,000
Total N_2	71,966	**30,96432**	**0,26852**	79,547